TITLE: SINGLE AND TWO-PHASE FRICTIONAL

PRESSURE DROP IN HELICALLY COILED TUBES

BY: MARK J. ROBBIE

THIS THESIS IS SUBMITTED AS PART OF THE REQUIREMENT FOR THE DEGREE OF MSc BY RESEARCH AT THE UNIVERSITY OF GLASGOW.

DEPARTMENT OF MECHANICAL ENGINEERING

THE UNIVERSITY OF GLASGOW

GLASGOW

STRATHCLYDE REGION

SCOTLAND

JANUARY 1987

ProQuest LLC.
789 East Eisenhower Parkway
P.O. Box 1346
Ann Arbor, MI 48106 – 1346

ACKNOWLEDGEMENTS

I would like to thank:-

The Directors, N.E.L. and Dr. Brain for the use of the facilities for this thesis.

John Henry for guidance, patience and support in test, analysis and supervision.

Dr. N. R. L. McCallum for help in adminstration, guidance and supervision.

Dr. I. Grant for help on aspects of Two-Phase Technology.

R. Fuggle and D. Young who helped in many small ways during my short stay at the National Engineering Laboratory, J. Henry on shifters and C. Cotchin on keyboards.

ABSTRACT

Correlations for pressure drop, in terms of mass flux and tube diameter, have been obtained for two-phase flow in tubes, both straight and coiled. The two-phase correlation for straight test sections is presented in Equations 5.1 and 5.2.

$$\phi_l^{2}_{new} = \phi_l^{2} \cdot C3 \qquad (5.1)$$

The parameter ϕ_l, used above, is a two-phase multiplier of a type used by Chisholm (34) and a standard correlation for this has been developed by HTFS*. In the present work a revised parameter "ϕ_l new" is introduced, related to ϕ_l by coefficient C3. This coefficient is given by:-

$$C3 = 0.5 + (G/(d \cdot 10^5)^{1.115})^{0.5} \qquad (5.2)$$

where $G/(d \cdot 10^5)^{1.1554} > 1.0$ and

$C3 = 1.0$ for $G/(d \cdot 10^5)^{1.1554} < 1.0$ where G, the mass flux, is in $kg/m^2.s$ and d is the tube bore in metres. The range of this correlation is 1152 $kg/m^2.s < G < 6257$ $kg/m^2.s$ and 0.0077 m < d < 0.0124 m.

The above correlation, and also the subsequent one for two-phase flow in coils, are effective at mass fluxes up to 6500 $kg/m^2.s$ and in small bore tubes (d < 13 mm). The earlier correlations of Baroczy and Chisholm Sutherland have been restricted to mass fluxes less than 4000 $kg/m^2.s$.

A correlation for single-phase friction factor in the coils tested, is presented (Equation 6.3) and is shown to agree well with other well established correlations.

$$f_c(D/d)^{0.5} = 0.081 \cdot (Re\ (d/D)^2)^{-0.225} \qquad (6.3)$$

where D and d are the coil diameter and tube bore respectively, in metres.

* HTFS - Heat Transfer and Fluid Flow Service, National Engineering Laboratory, East Kilbride, Scotland.

An improved correlation for two-phase frictional pressure loss in helically coiled tubes is also presented (Equations 5.1 and 5.3).

$$C3 = 0.1 + (G/(10^5 \cdot d)^{1.0671})^{0.35} \qquad (5.3)$$

where $G/(d \cdot 10^5)^{1.0671} > 1.0$ and

$C3 = 1.0$ where $G/(d \cdot 10^5)^{1.0671} < 1.0$ where G again is the mass flux in $kg/m^2.s$ and d the tube bore is in metres. The range of this correlation is 1063 $kg/m^2.s < G < 4735$ $kg/m^2.s$ and 0.0077 m < d < 0.0124 m.

Another aspect of this research was the discovery of flow pattern induced vibration in the test coils.

It was noted that when the mass flux of the two-phase mixture was greater than approximately 1000 $kg/m^2.s$ and the quality greater than 0.005 (mass flow of air/total mass flow), then vibration started in the coils. The frequency appeared to increase with air mass flowrate. The vibrations became severe, shaking the whole test bench and apparatus. The test coils were replaced with clear plastic tubes of similar dimensions to enable flow visualisation tests to take place. These tests showed that the flow regime known in straight tube, two-phase flow, terminology as churn flow was seen to rotate within the tube.

While the test apparatus did not allow conclusive tests to be carried out, some high speed photographs were taken which showed that the rotation could switch in either direction and that there was no evidence of a time related pattern.

Suggestions are presented for possible flow patterns that might be occurring under these vibrating conditions.

CONTENTS

CONTENTS (Cont'd)

CONTENTS (Cont'd)

LIST OF APPENDICES

NOTATION			UNITS
A	-	Blasius Equation Numerator	-
a	-	Section Area	m
C	-	C - Coefficient in two-phase multiplier	-
C2	-	Chisholm-Sutherland Mass Flux Dependant Coefficient	-
C3	-	Test Correlation, Mass Velocity and Diameter Dependant, Coefficient	-
D	-	Coil Diameter	m
Dn	-	Dean Number	-
Dp	-	Pressure gradient	N/m^3
d	-	Tube Inside Diameter	m
f	-	Friction factor	-
G	-	Mass Velocity or Flux	kg/m^2s
K	-	Slip Ratio	-
M	-	Mass Flowrate	kg/s
m	-	Test Correlation Indice	-
n	-	Blasius Equation Indice	-
P	-	Coil Pitch	m
p	-	Pressure	N/m^2
Re	-	Reynolds Number	-
r	-	Section Radius	m
S	-	Force Per Unit Length of Interface Between Tube Wall and Fluid Phase or Between Fluid Phases	N/m
U	-	Velocity	m/s
X	-	Lockart-Martinelli Parameter	-
x	-	Circumferential Dimension	m
Z	-	Dimensionless Group Defined In Equation 2.26	-
z	-	Axial Dimension	m
δ	-	Helix Angle	-
ε	-	Surface Roughness	-
ρ	-	Phase Density	Kg/m^3

NOTATION (Cont'd) UNITS

$\mathcal{P}$	-	Phase Perimeter	m
$\mathcal{C}$	-	Shear Stress	N/m^2
Λ	-	Baroczy Property Index	-
Θ	-	Chisholm Model Phase Angle	
ϕ	-	Two-Phase Multiplier	
μ	-	Dynamic Viscosity	Ns/m^2

SUFFIXES

a	-	Accelerational
c	-	Coil
f	-	Friction
g	-	Gravity
r	-	Ratio
T	-	Total
TRANS	-	Transition
tp	-	Two-Phase
x	-	Circumferential
z	-	Axial
ϕ_c	- c -	Calculated
ϕ_m	- m -	Measured

ABBREVIATIONS

HTFS - Heat Transfer and Fluid Flow Service, National Engineering Laboratory, East Kilbride, Scotland

ESDU - Engineering Science Data Unit

1.0.0 INTRODUCTION

The aim of this project is to determine a suitable correlation to predict pressure drop for single and two-phase flow along a given set of helical coils. The need for this information has arisen from development work being carried out on a new type of compact Rankine-cycle power plant in which boiling of the working fluid is carried out, not in a bank of tubes, but along a single-pass pair of coils in contact with the heat source. The coils lie one inside the other. The inner, a stainless steel tube of approximately 7.7 mm diameter heats the fluid from the subcooled state to the saturation temperature. The working fluid is then passed to the outer coil, 12.4 mm inside diameter, on the outside of the heat source where it is boiled to produce steam which emerges considerably superheated.

During tests on the power package it was found that measured pressure losses in the boiler coils differed greatly from the values calculated by the most accepted methods. There are many possible reasons for this discrepancy in value. There is, for instance, a possibility of the fluid starting to boil before leaving the inner, small bore, coil. If this were the case an appropriate two - rather than single-phase, correlation would have to be applied to the unit design. The resulting two-phase flow in the restricted channel would greatly increase the observed pressure drop - an effect not taken into account in the presently used calculations.

As will be seen in a later section, the accelerational pressure drop is also important during boiling and can greatly increase the total pressure drop. These effects are not considered in this report but may require to be the object of future investigation.

In the present tests it is proposed to use air and water to examine the frictional pressure drop through the coils. In order to be confident of the results it is also proposed to test straight samples of the same tubing in order to obtain an accurate correlation to verify whether it can be considered smooth. The sequence of tests will therefore be carried out in

order of increasing uncertainty:-

a) Single-phase (air and water) flow through straight tubes.

b) Single-phase flow through coils.

c) Two-phase flow through straight tubes.

d) Two-phase flow through coils.

At each stage, comparisons will be made with existing theory and data, but it is not the object of this work to produce a correlation which predicts all geometries of coil. What is required is an accurate correlation which applies only to the coils under test or limited extrapolations of them.

2.0.0 THEORY

When there is flow through a tube or other channel pressure drop occurs for various reasons:

1) A frictional component which can be attributed to the irreversible conversion of mechanical energy to thermal energy by the mechanism of viscous damping.

2) An accelerational component which can occur either by density change in the vapour (or gaseous) phase or by phase change where the flow is accompanied by heat transfer.

3) A gravitational component where the flow rises or falls in the gravitational field.

These components can be added to give the total pressure gradient

$$(dp/dz)_T = (dp/dz)_f + (dp/dz)_a + (dp/dz)_g \qquad (2.1)$$

In the present studies the prime interest is going to be in the frictional component since in the boiler the high pressure prevailing will tend to make the accelerational component of secondary importance. However in the tests, carried out as they are at lower pressure, the accelerational component will have to be taken into consideration. The straight tubes are tested in the horizontal position and so there is no gravitational component to allow for. The mass velocity of the flows tested in the coils are such that the fluids are subjected to centrifugal forces which have a far greater effect on flow patterns than does the force of gravity. Additionally, the first and last tappings are mounted on the same horizontal plane. The gravitational component will therefore be ignored.

2.1.0 Single-phase frictional pressure gradient

2.1.1 Straight Tubes

When flow of either gas or liquid occurs through a tube of circular section the pressure falls in the direction of flow due to shear forces occurring within the flow. Carrying out a force balance on the element of fluid shown in figure 2.1 gives the equation

$$a\ dp = \quad . \quad . d\ .\ dz \tag{2.2}$$

The Fanning friction factor for turbulent flow is defined in terms of the shear stress and the mean kinetic head to give

$$f = \frac{\tau}{1/2\ .\rho.\ U^2} \tag{2.3}$$

This can be substituted into equation 2.2 to give the well known relationship

$$dp/dz = \frac{4\ .\ f\ .\ U^2.\rho}{2\ .\ d} \tag{2.4}$$

For flow through a straight tube research has been carried out over many years and shows that

$$f = f\ (Re.\ \varepsilon) \tag{2.5}$$

where describes the roughness of the wall of the tube.

The form of the relationship in eq (2.5) is, in its simplest form, for a smooth tube

$$f = \frac{A}{Re^n}\ , \tag{2.6}$$

for turbulent flow through an hydraulically smooth tube. The constants A and n often take the values 0.046 and 0.2 respectively. This is known as the Blasius equation,

$$f = \frac{0.046}{Re^{0.2}} \tag{2.7}$$

A modified form of the equation which applies over a wider range of Reynolds Number is that of White (39) and is

$$f = 0.0014 + \frac{0.125}{Re^{0.32}} \tag{2.8}$$

For laminar flow, where the Reynolds Number is less than 2100, the friction factor is given by

$$f = \frac{16}{Re} \tag{2.9}$$

2.1.2 Coiled Tubes

It has been shown that for a straight tube a friction factor is defined as $f = \frac{\tau}{1/2 \cdot \rho \cdot U^2}$. This was for the case of one-dimensional flow. For flow in a coil the equation will be more complicated due to the presence of secondary flow. A suitable model might be,

$$f_c = \frac{\tau}{1/2 \cdot \rho \cdot (u_z^2 + u_x^2)} \qquad (2.10)$$

where u_z and u_x are the axial and circumferential velocities respectively, their relative sizes, it might be expected, being a function of the coil geometry d, D, and the helix angle. Various workers (2,3,5) have reported that the helix angle is of minor importance and it is usually not necessary in correlating data.

A dimensionless number often used to characterise the laminar flow is the Dean (22) Number,

$$Dn = Re\left(\frac{d}{D}\right)^{0.5} \qquad (2.11)$$

It should be noted that there are other similar numbers which can be mistaken for this value but which are used for different purposes. For turbulent flow a common plot used to non-dimensionalise data for coils with different diameters is one which has $Re\left(\frac{d}{D}\right)^2$ and $fc\left(\frac{D}{d}\right)^{0.5}$ as the axes (see fig 3.5).

Existing correlations will be considered in the literature survey in section 3.

The transition from laminar to turbulent flow occurs at a greater Reynolds Number than for a straight tube. In the literature survey the correlations for friction factor put forward by Srinivasan(2) have been selected as the most reliable and his correlation for the transition point is

$$Re_{TRANS} = 2100\ [1 + 12\left(\frac{d}{D}\right)^{0.5}] \qquad (2.12)$$

This has the advantage over the other correlations (3,10,12,36) of reducing

to the straight tube value for a coil of infinite diameter and/or exceptionally small bore where secondary flow ceases.

2.2.0 Two-Phase Frictional Pressure Gradient

2.2.1 Straight Tubes

Two-phase pressure drop is not so well defined as for single phase flow. This is because of the existence of various flow patterns depending on the phase flowrates and properties which make the understanding of the physics of the flow very difficult. The simplest of these models is probably a homogenous model, where the phases move with the same velocity and the specific volume can be calculated by a simple sum of the mass ratios and specific volumes of each phase. The viscosity can be either the liquid viscosity or one of several effective viscosities averaged by equations proposed, for example by McAdams(38) or Cicchitti(37). The homogenous model is found to be reasonably accurate for vertical tubes at low velocities (u = approx. 2 m/s) but in many other applications has been found to be grossly in error. The homogenous model will be returned to later in this section. The next stage of complexity is to allow the phases to have differing velocity, known as the 'slip flow' model.

Consider a tube with the cross section occupied partly by liquid and partly by gas (see fig 2.2) and for a case where the friction factor is independent of the phase Reynolds Number (i.e. $f_l = f_g = f$). If we balance the forces in the axial direction we have equations similar to the one for single phase friction drop (equ 2.2) but with an extra variable S representing the shear force per unit length acting between the phases, then

$$a_l . Dp_{tp} - \tau_l . \phi_l + S = 0 \qquad (2.13)$$

$$a_g . Dp_{tp} - \tau_g . \phi_g - S = 0 \qquad (2.14)$$

(where it is assumed the gas flows faster than the liquid). As is the case for the single phase equation (2.3)

$$\tau = \frac{f . u^2 . \rho}{2} \qquad (2.15)$$

for each phase. For convenience a shear force ratio is defined

$$S_r = \frac{S}{(a_g \cdot Dp_{tp})} \tag{2.16}$$

Combining eqs 2.13, 2.15 for the liquid and 2.16, for the shear force ratio, we get

$$Dp_{tp}\left(1 + S_r\left(\frac{a_g}{a_l}\right)\right) = \frac{f_l \cdot u_l^2 \cdot \phi_l \cdot \rho_l}{2 \cdot a_l} \tag{2.17}$$

also eqs 2.14, 2.15 for the gas phase and 2.16 combine to give

$$Dp_{tp}\left(1 - S_r\right) = \frac{f_g \cdot u_g^2 \cdot \phi_g \cdot \rho_g}{2 \cdot a_g} \tag{2.18}$$

In fig 2.2 the assumed phase area geometry is shown and in fig 2.3 it is seen how the shape of the area can be changed without grossly changing the length of the phase interfaces or the surface area. From a consideration of the geometry involved

$$\frac{\phi_g}{a_g} = \frac{4 \cdot \theta \cdot d}{\theta \cdot d^2} = \frac{4}{d}\ , \tag{2.19}$$

similarly

$$\frac{\phi_l}{a_l} = \frac{4}{d}\ , \tag{2.20}$$

recalling that

$$a = a_g + a_l \tag{2.21}$$

Combining equations 2.17 and 2.20 together with 2.18 and 2.19 yields

$$Dp_{tp}\left(1 + S_r\left(\frac{a_g}{a_l}\right)\right) = \frac{4 \cdot f_l \cdot u_l^2 \cdot \rho_l}{2 \cdot d} \tag{2.22}$$

$$Dp_{tp}\left(1 - S_r\right) = \frac{4 \cdot f_g \cdot u_g^2 \cdot \rho_g}{2 \cdot d} \tag{2.23}$$

respectively.

Using these equations to describe the two-phase pressure drop in terms of each fluid we can equate one with the other to give

$$K = \frac{u_g}{u_l} \tag{2.24}$$

Recalling that since $f_g = f_l = f$ then $\frac{f_g}{f_l}$ or $\frac{f_l}{f_g} = 1$

$$K = \frac{1}{Z} \cdot \left(\frac{\rho_l}{\rho_g}\right)^{0.5} \tag{2.25}$$

; where $Z = \dfrac{\left(1 + S_r\left(\dfrac{a_g}{a_l}\right)\right)^{0.5}}{1 - S_r}$; (2.26)

and from the phase continuity equations

$$M_l = a_l \cdot \rho_l \cdot u_l \quad , \tag{2.27}$$

$$M_g = a_g \cdot \rho_g \cdot u_g \quad , \tag{2.28}$$

and equ 2.25 we can derive,

$$\frac{a_l}{a_g} = \frac{1}{Z}\frac{M_l}{M_g}\left(\frac{\rho_l}{\rho_g}\right)^{0.5} \tag{2.29}$$

If the phases were to flow alone, the pressure drop per unit length would be

$$Dp_l = \frac{2 \cdot f_l \cdot M_l^2}{d \cdot a^2 \cdot \rho_l} \tag{2.30}$$

and

$$Dp_g = \frac{2 \cdot f_g \cdot M_g^2}{d \cdot a^2 \cdot \rho_g} \quad , \tag{2.30}$$

Combining 2.29 and 2.30 gives

$$\frac{a_l}{a_g} = \frac{1}{Z}\left(\frac{Dp_l}{Dp_g}\right)^{0.5} \quad . \tag{2.31}$$

Recalling equ 2.21, then from equations 2.22, 2.27, 2.30

$$\frac{Dp_{tp}}{Dp_l} = \frac{\left(1 + \dfrac{a_g}{a_l}\right)^2}{\left(1 + S_r \cdot \dfrac{a_g}{a_l}\right)} \tag{2.32}$$

Substituting equations 2.26 and 2.31 into 2.32 gives

$$\frac{Dp_{tp}}{Dp_l} = 1 + C\left(\frac{Dp_g}{Dp_l}\right)^{0.5} + \left(\frac{Dp_g}{Dp_l}\right) \tag{2.33}$$

$$= 1 + \frac{C}{X} + \frac{1}{X^2} \tag{2.34}$$

where $C = Z + \dfrac{1}{Z}$ (2.35)

and the parameter $X = \left(\frac{Dp_l}{Dp_g} \right)^{0.5}$ (2.36)

where the general forms

$$\phi_l^2 = 1 + \frac{C}{X} + \frac{1}{X^2} \quad (2.37)$$

and $$\phi_g^2 = 1 + CX + X^2 \quad (2.38)$$

are used it is possible to fit these equations to data simply by modifying the factor C. Since the value of S is not known, equation 2.26 cannot be used to evaluate the value of Z. However if the slip ratio K is known then equation 2.25 can be used. Consider the case for homogenous flow. The value of K is 1, i.e. the two phases have the same velocity and by equation 2.25

$$Z = \left(\frac{\rho_l}{\rho_g} \right)^{0.5} \quad (2.39)$$

which using equation 2.35 gives

$$C = \left(\frac{\rho_l}{\rho_g} \right)^{0.5} + \left(\frac{\rho_g}{\rho_l} \right)^{0.5} \quad (2.40)$$

For the case of no shear between the phases S = 0, Z = 1 and therefore

$$K = \left(\frac{\rho_l}{\rho_g} \right)^{0.5} \quad (2.41)$$

and C = 2.

Homogenous flow results in a C value which is dependent on the density ratio of the two phases. We might therefore expect that as the critical point is reached, where $\rho_l = \rho_g$, that K would approach unity and C approach to a value of two. In practice Chisholm has found this to be the case (34).

Such correlations will be set aside in favour of correlations of the type of Baroczy(33), and his work subsequently adapted and revised by Chisholm and Sutherland(45). These correlations are dependent on mass flux and this is considered important since it is intended to attempt to raise

mass flux values to an excess of 2000 kg/m^2.s in the tests for this work. The Baroczy(33) method is graphical and quite unsuitable for use in a computer program for handling and processing data. Chisholm and Sutherland(35) transformed the Baroczy(33) method to provide a set of simple curves. In addition they proposed their own correlation.

$$C = C2\left(\left(\frac{\rho_l}{\rho_g}\right)^{0.5} + \left(\frac{\rho_g}{\rho_l}\right)^{0.5}\right) \qquad (2.42)$$

where C2 is dependent on the density ratio as well as the mass flux (35).

These correlations have brought the calculating of two-phase pressure drop extensively forward. However, correlations are required which will provide accurate values for pressure drop under a wide range of conditions. The HTFS* have, using the Chisholm and Sutherland work (35) as a basis, correlated the C - coefficient based on their very large database. This correlation is available only to members of HTFS but it can be said that C is a function of mass flux and Λ, the Baroczy property index.

2.2.2 Coiled Tubes

A model for two phase flow in coils could be built in a similar fashion to the method used for straight tubes but with consideration of the factors raised in the section on coiled tube single phase flow (2.1.2).

Basing such a model on stratified flow we could carry through the concept of there being a secondary flow within each flow stratum (see fig 2.4). This concept of stratified flow is further justified in its use by the work of Banerjee et al (10) describing the effects of centrifugal forces in a coiled tube flow stream. The mathematics for a solution would be difficult to resolve without making assumptions. Wattendorf(24) showed that the degree of secondary flow is dependent on the flow section shape. If we assume the two phases are flowing in separate but continuous strata the degree of secondary flow in each phase will also change with flow quality.

There will be a situation where the circumferential flow is so strong in

* Heat Transfer and Fluid Flow Service, at NEL, East Kilbride, Scotland.

one phase that it impinges on the other strata.

Various models have been proposed but there is none which can claim to be in general use. What is of interest is that it has been found by many workers that the use of Lockart-Martinelli type (2.37 and 2.38) equations proved adequate (5) after having replaced the equations used for the single phase pressure gradients with ones for pressure loss in coiled tubes.

It is proposed that this work will examine the accuracy of the HTFS correlation used in this way and comment and/or revise this correlation to provide a suitable correlation for the tubes under scrutiny.

3.0.0 LITERATURE SURVEY

3.1.0 Single Phase Flow

3.1.1 Straight Tubes

The relationship between Reynolds Number and friction factor for a case with laminar flow is well established by analytical study. Such analysis can be found in many standard textbooks, for example Kays(41) or Rogers and Mayhew(42). The reliability of the relationship

$$f = \frac{16}{Re} \tag{2.9}$$

has been proved by experiment and is accurate and consistent due to the predictability of the laminar flow stream.

Because of the random motion in turbulent flow no completely satisfactory mathematical relationship has been found. There are however a number of forms which have subsequently been 'tuned' by the alteration of coefficients to fit experimental data. One such equation, the Blasius equation, is found to be a good approximation to the Karman-Nikuradse equation (from 41) and as will be shown in 3.1.2 the simplicity of the Blasius equation, 2.6 and 2.7, and a modified Blasius equation, 2.8, make this form a powerful foundation for making comparisons with single phase flow in coils.

3.1.2 Coiled Tubes

In the 1920's Dean (22,31) wrote two papers wherein the motion of a single phase liquid flowing through a coiled tube is considered. The first product of his analysis of the similarity laws, as applied to the flow in curved bends was to show that for a given shear, the ratio of the mean velocities in two tubes of the same dimensions, one straight and one curved, depended on a parameter given by the product

$$\left(\frac{(\tau/\rho) \cdot d)}{\nu}\right)^2 \left(\frac{d}{D}\right)^{0.5} \tag{3.1}$$

His theoretical ground-work established his position as the researcher who first presented the prime flow patterns for single phase flow in coils and

the parameters on which these depended. He introduced the concept that, through centrifugal forces, a secondary flow would be set up (see figs 3.1 and 3.2) and at the time his ideas were corroberated by the experiments of Eustice(23). Eustice had carried out flow visualisation work nearly twenty years earlier, having carried out tests himself comparing the effects of varying coil diameter using flexible, rubber covered, canvas tubing.

White(32) found it easier to apply the converse of Deans statement and this can be expressed thus; for a given velocity in two tubes of the same dimensions, one straight and the other curved, the ratio of the resistances depends on a parameter given by the product of the Reynolds Numbers and the root of the curvature ratio,

$$Re \left(\frac{d}{D}\right)^{0.5} . \qquad (3.2)$$

White(32) carried out a substantial programme of tests on coiled tubes and used equ. 3.2 to help correlate the data. The increased resistance of flow with the increase of curvature was held to be a function of the Dean number but only as long as the flow remained laminar. White(32) discovered that the onset of turbulence occurs at a higher Reynolds Number than for a straight tube. He suggested that this was probably due to the centrifugal force which would dampen eddy current movements in the radial direction relative to the coil central axis.

Taylor (30), like Eustice(23), carried out flow visualisation tests. Dye was introduced through an orifice in the wall of the tube through which the liquid was running, a method far more revealing than the method employed by Eustice(23) who had simply introduced dye at the entrance to the coil section, (stream movement due to settling probably dispersing the dye before the settled patterns could be examined properly). The tests confirmed the conclusion reached by White (32) with respect to the late onset of turbulence with Taylor(30) noting that with a d/D ratio of 0.055 turbulence did not become established until the Reynolds number reached 5800. Taylor

(30) also noted that the secondary flow streamline (fig 3.2) persisted despite high turbulence.

Experiments were carried out by Wattendorf(24) to try to determine the effect that flow section shape would have on friction losses. The experiments involved measuring the losses through rectangular sections with a very small width-to-depth ratio. The experiments showed that the resistance to flow for these sections when coiled was only slightly more than for a straight tube of the same section. In conclusion it was proposed that the virtual elimination of a third dimension of the flow pattern had also had a dampening effect on the second dimension. The movement of flow outward from the inner wall is inhibited by the flow moving in the opposite direction around the tube wall (see fig 3.3). This being the case, the flow pattern approached that of flow in a straight tube, it is almost one dimensional.

Keulegan and Beij (1937) (14) carried out a study of flow in curved pipes which was to set a post-war trend with their presentation of laminar, transitional and turbulent flows as separate areas for investigation. This was most appropriate since it had already been shown that the plot of friction factor against Reynolds Number for a coil consisted of a continuous line with three distinct sections. This is unlike the case for a straight tube where there are two lines, one for each of laminar and turbulent flow joined by a 'broken leg' transitional line. While curved tubes were used instead of coils, care was taken to allow settled flow to establish itself and thereafter tappings through the tube wall were used for pressure measurement. Unfortunately correlations for laminar and transitional flow only were presented since the authors felt that a further study would be required to cover the field of turbulent flow adequately.

With the various post Second-World War nuclear power generation projects there has been renewed interest in the use of coils for fluid transport in heat transfer roles. While two-phase experiments are more

common in the post 1945 literature, a number of investigators have sought to complete the study of single-phase flow in coils. Questions asked with respect to previous work include:-

a) Had workers considered the change in section areas and ovality which would result from bending the tubes into coils?.

b) How would accuracy be affected given the relatively crude experimental arrangements (pressure readings were previously taken before and after test sections instead of at intermediate tappings placed after a settling length and before fittings at the outlet)?

c) Could flow visualisation be improved with the aid of modern high speed photographic techniques?

Rogers and Mayhew(22) used the correlation proposed by White(32) and found that while the equation for laminar flow was accurate, the equation for turbulent flow was considerably adrift of their data. Ito(43) had a correlation which performed better and was accurate to within 3% for Roger and Mayhew's data. A later comparison between White(32) and later researchers (of which there are many) can be seen in fig 3.5.

While there were workers who carried out conventional studies on flow in coiled tubes, progress had presented new fields which could add to the understanding of methods of analysis which might be used. Patankar, Pratap and Spalding(15) used a finite difference method to predict the development of laminar and turbulent flow in curved pipes. The use of such methods had only been made possible by the arrival of computers to carry out the mass of calculations. However, while there were improvements over previous results the outcome was the same as it had been for many previous theoreticians. While the results for laminar flow were acceptable the results for turbulent flow required further development. Tarbull and Samuels(13) used the alternating direction-implicit method to solve the equations of motion and energy. The correlation given is for a very low Dean number (laminar flow range), which was not new, but their plots of velocity and temperature are

common in the post 1945 literature, a number of investigators have sought to complete the study of single-phase flow in coils. Questions asked with respect to previous work include:-

a) Had workers considered the change in section areas and ovality which would result from bending the tubes into coils?.

b) How would accuracy be affected given the relatively crude experimental arrangements (pressure readings were previously taken before and after test sections instead of at intermediate tappings placed after a settling length and before fittings at the outlet)?

c) Could flow visualisation be improved with the aid of modern high speed photographic techniques?

Rogers and Mayhew(22) used the correlation proposed by White(32) and found that while the equation for laminar flow was accurate, the equation for turbulent flow was considerably adrift of their data. Ito(43) had a correlation which performed better and was accurate to within 3% for Roger and Mayhew's data. A later comparison between White(32) and later researchers (of which there are many) can be seen in fig 3.5).

While there were workers who carried out conventional studies on flow in coiled tubes, progress had presented new fields which could add to the understanding of methods of analysis which might be used. Patankar, Pratap and Spalding(15) used a finite difference method to predict the development of laminar and turbulent flow in curved pipes. The use of such methods had only been made possible by the arrival of computers to carry out the mass of calculations. However, while there were improvements over previous results the outcome was the same as it had been for many previous theoretitians. While the results for laminar flow were acceptable the results for turbulent flow required further development. Tarbull and Samuels(13) used the alternating direction-implicit method to solve the equations of motion and energy. The correlation given is for a very low Dean number (laminar flow range), which was not new, but their plots of velocity and temperature are

interesting (see fig 3.7).

Mishra and Gupta(12) set out to look at the effect of coil pitch on flow resistance. Sixty different coils were tested and correlations of their own were presented. They stated that since the data collected could be expressed by

$$fc - fst = A\ (D/d)^{-0.5} \qquad (3.3)$$

where A is a constant, coil pitch has no direct effect on the flow resistance. Other workers were more cautious. Srinivasan(2), used coils with pitch-to-coil diameter ratios from 0.029 to 0.749 and noted that the effect of pitch was "insignificant" given that the maximum variation in friction factors over his test range of P/D ratios was $\pm$4%. Sadasivudu(3) tested coils with P/D <1 and confirmed the insignificant effect of pitch stated by Srinivasan(2). This may be the case for 'normal coils' but if a coil of infinite pitch and very small coil diameter is considered the tube losses should approach those of a straight tube. In such a case we might consider at what point the radius of curvature of the tube is affected by the coil pitch (see fig 3.6). The ESDU(6) paper on coiled tube flow suggests that for P/D ratios greater than 0.5, an equivalent diameter for the coil should be used which makes allowance for pitch dominating the true radius of curvature.

In 1970 Srinivasan, Nandapurkar and Holland(2) presented a paper 'Friction Factors for Coils'. The paper dealt with both helical coils and Archimedean spirals and provides equations to predict friction factors in the laminar, transition and turbulent regions of the flow spectrum as well as providing equations to predict critical Reynolds numbers where there are changes in the flow regime.

Comparing various equations for the critical Reynolds numbers

a) Fastovskii and Rovinskii (1957)

$$Rec = 18500\ (d/D)^{0.28} \text{ for } d/D > 0.0004 \qquad (3.4)$$

b) Ito (1959)

$$Rec = 20000\ (d/D)^{0.32} \quad \text{for } 0.00116 > d/D > 0.0667 \tag{3.5}$$

c) Aronov (1960)

$$Rec = 18500\ (d/D)^{0.3} \tag{3.6}$$

d) Schmidt (1967)

$$Rec = 2300\ [1 + 8.6\ (d/D)^{0.45}] \tag{3.7}$$

e) Srinivasan(2), (1968)

$$Rec = 2100\ [1 + 12\ (d/D)^{0.5}] \tag{3.8}$$

The equations by Schmidt, and Srinivasan(2) in particular, approximate to the equation for a straight tube for small d/D ratios. Additionally the paper presenting Srinivasan's equation contains details of both tube geometries used (12 in all) and graphs displaying data. For these reasons the use of Srinivasan's(2) equation for the critical Reynolds number is recommended.

For the case of laminar flow the following equations are presented.

a) White(32) (1932)

$$fc/fs = 1 \,/\, 1 - [1 - (11.6/Dn)^{0.45}]^{2.2} \tag{3.9}$$

$$\text{for } 11.6 < Dn < 2000$$

b) Srinivasan et al(2) (1970)

$$fc/fs = 1 \qquad \text{for } Dn < 30 \tag{3.10}$$

$$fc/fs = 0.418\ Dn^{0.275} \qquad \text{for } 30 < Dn < 300 \tag{3.11}$$

$$fc/fs = 0.1125\ Dn^{0.5} \qquad \text{for } Dn > 300 \tag{3.12}$$

c) Schmidt (1967)

$$fc/fs = 1 + [0.14\ (d/D)^{0.97}\ Re\ (1 - 0.644\ (d/D)^{0.314})] \tag{3.13}$$

$$\text{for } Re > 100 \text{ and } 0.012 < d/D < 0.2$$

d) Ramana Rao and Sadasivudu(3) (1974)

$$fc = 1.55 \exp (14.12\ (d/D)\ Re^{-0.64} \tag{3.14}$$

$$\text{for } Re > 1200 \text{ and } 0.0159 < d/D < 0.0566$$

As was the case for laminar flow in a straight tube, the relatively good order in a laminar flow stream has led to close agreement between theoretical and experimental results. For this reason the first workers to

publish papers on the theory of laminar flow and subsequent experimental results, Dean(22) and White(32) respectively, have provided answers that have stood the test of time. White's(32) correlation covers a good range of Dean numbers and has been plotted for comparison by many authors and has been found to give good agreement. Outside the range of Dean numbers given for this correlation, Srinivasan has two equations, 3.10 and 3.12, which can be used with accuracy.

For the case of turbulent flow most of the tests carried out are using plastic or smooth drawn metal tubes so that the effects of roughness are not known. A number of correlations have been presented to date and these include,

a) White(32) (1932)

$$fc\ (D/d)^{0.5} = 0.08\ [Re\ (d/D)^2]^{-0.25} + 0.012 \qquad (3.15)$$

$$\text{for } 1.5 \times 10^4 < Re < 10^5$$

b) Ito(43) (1959)

$$fc\ (D/d)^{0.5} = 0.076\ [Re\ (d/D)^2]^{-0.25} + 0.00725 \qquad (3.16)$$

$$\text{for } 0.034 < Re\ (d/D)^2 < 300$$

c) Srinivasan(2) (1970)

$$fc\ (D/d)^{0.5} = 0.084\ [Re\ (d/D)^2]^{-0.2} \qquad (3.17)$$

$$\text{for } Re\ (d/D)^2 < 700 \text{ and } 0.0097 < (d/D) < 0.135$$

d) Ramana Rao and Sadasivudu(3) (1974)

$$fc\ (D/d)^{0.5} = 0.382\ [\exp\ (11.7\ (d/D))]\ Re^{-0.2} \qquad (3.18)$$

$$\text{for } Rec < Re < 2.7 \times 10^4 \text{ and } 0.0159 < d/D < 0.0556$$

The line given by equ 3.15 by White(32) is adrift of the other correlations but b), c) and d) all agree within 15%. The form given by Srinivasan(2) can also be broken down for any ratio of diameters to give a Blasius type equation

$$fc = 0.084\ (d/D)^{0.1} / Re^{0.2} \qquad (3.19)$$

making it suitable for comparison with straight line data without sacrificing accuracy.

Finally, a paper by Constantine, Vytoyannis and Hsien-wen hsu(18) discusses the effects of vibration on friction factor. The results of their tests are largely in graphical form where the increase in friction factor for a coil with vibration of various fixed types is given by a ratio of the friction factor of the coil with vibration to the friction factor without. From the summary graph it can be seen that vibration can have a massive effect in increasing the friction factor. An ESDU paper (6) quotes an example based on the information given in (18). For a situation where Re = 1400, the fluid water, D/d = 23.25, D = 0.59 m, vibrations are at 125 Hz and with an amplitude of 5.1×10^{-4} m: the friction factor is doubled. Additionally it was noted that the transition to turbulence could occur at a Reynolds number as low as 800 depending on the magnitude and frequency of vibration.

3.2.0 Two-Phase Flow

The field of two-phase flow has received a lot of attention particularly over the span of this century. Chisholm(34) opens his book with a brief historical review of earlier work. He states that a worker by the name of Gouse published an extensive Bibliography of two-phase data in 1966 which contained about 8000 references. It was observed that up to 1948 the number of papers doubled every 9.66 years ; after that the number of publications doubled every 5.12 years. Chisholm believed this was due to the post war interest in water cooled reactors because both USA and USSR have extensive nuclear power programmes based on this type of reactor.

Given the mass of literature available it was decided to reduce the data search areas to those directly related to the project in hand. The purpose of the project was to investigate friction losses in coiled boiler tubes; it was decided therefore to carry out a survey limited to this field. Additionally there were other factors which were unique to the system under investigation. The mass flux of the system was expected to be very high and a number of references were found which were found to be of interest in this

respect. The fact that the boiler tubes were in the form of a helical coil was expected to have a significant effect on the losses. Finally, in the later stages of the test programme it was found that the test sections developed a strong vibration in certain flow conditions and given the implications with respect to friction factors suggested by Hsien-wen hsu(18) it is intended to return to this paper in section 6.0.

3.2.1 Straight Tubes

Lockart and Martinelli(20) made one of the earliest attempts to produce a general correlation for two-phase frictional pressure gradient. They showed that their data could be correlated by plotting the two-phase multiplier for liquid or gas against the Lockart Martinelli two-phase flow modulus $X = ((Dpfl/Dpfg)^{0.5})$. They separated the data into four sets dependent on whether the phases would be laminar or turbulent when flowing alone in the same tube. The curves in fig 3.8 show the relations between the multipliers and modulus as shown in their paper.

$$\Lambda = \left(\frac{\rho_G}{\rho_L}\right)\left(\frac{\mu_L}{\mu_G}\right)^{0.2} \qquad (3.20)$$

Baroczy(33) used a property index, in his correlation of data (see fig 3.9). The relationship between the index and multiplier was also dependent on quality since,

$$X^2 = \frac{1}{\Lambda^2}\left(\frac{1-x}{x}\right)^{2-n} \qquad (3.21)$$

Many workers had noted that there was often an effect on the two-phase pressure gradient related to flowrate. While the curve in fig 3.9 is restricted to one mass flux (1356 kg/m^2.s), Baroczy(33) provided a set of correction curves (fig 3.10) which allowed for correction for mass flux rates of up to 4068 kg/m^2.s. While this method of prediction was graphical it provided the best correlation of the time for high mass flux flows.

Chisholm and Sutherland(28) approximated the Baroczy(33) correlation by the family of curves for the coefficient C as can be seen in fig 3.10 where C is used in equ 2.37. In addition, Chisholm and Sutherland (28) presented

their own correlation (equ 2.42) which had the advantage of not being graphical but set in the form of an equation, thereby making calculations using computer a more straight forward process. This correlation was also sensitive to mass flux and as such might suit the requirements of this investigation.

3.2.2 Coiled Tubes

Lacey(25) carried out a survey (1970) of what was known at the time of two-phase flow in bends and helices. A number of factors affecting flow patterns are explained and backed by experimental data where possible. It is worth noting some of these since they will clarify the understanding of the flow mechanisms in section 6.3.0.

It was thought that the water rivulets seen through the clear tube wall during visualisation tests with high quality mixtures indicated a highly helical flow on the part of the gas core. Closer examination showed that the rivulets were waves with a bulge at one end which was simply the most upstream part of the wave. The gas secondary flow has, it appears, a very strong axial flow aspect with less circumferential flow evident than had been expected. Another phenomenon occurs when the gas core in a high quality flow is travelling so fast that the vortices can whip droplets from the top of the waves at the inner wall and deposit them on the outer wall where they are pulled back along the wall, by the force of the gas core secondary flow, to the inner wall, see fig 3.12.

Another paper to which Lacey contributed (25) was that by Maddock, Lacey and Patrick(27). Again the main theme of the work is the structure of two-phase flow in helical coils. However, this paper is not a survey of literature but an experimental investigation carried out on annular film flow. Pictures are shown which have been taken from within the flow passage and velocity profiles have been constructed using pitot tubes.

Bannerjee, Rhodes and Scott(10) carried out tests on a number of coils. They found that their data agreed well with the Baker plot (see fig 3.13)

for straight tubes. This was something that a number of workers had reported : Stepanek and Kasturi(8), Lacey(25), Reddy and Satyanarayan(4) and Boyce, Collier and Levy(5), Akagawa(1) and Kozeki(16) carried out experiments and showed where the small differences between straight tube flow and coiled tube flow occurred. Essentially however all the references obtained come to the same conclusion with respect to the similarity in flow patterns between straight and coiled tube flow. For this reason all of these workers attempted to correlate their data using the Lockart-Martinelli(20) correlation.

It is generally agreed that the modified Lockart-Martinelli method gives a good approximation to the correlation. The modification consists of replacing straight tube single-phase pressure loss gradients by coiled tube single-phase pressure loss gradients in the calculation of the two-phase multiplier and Lockart-Martinelli parameter.

Papers by Stepanek and Kasturi(8), and Puri et al(11) have noted that the correlation starts to lose accuracy at higher liquid mass flow rates as well as higher total mass flow rates. This is not surprising since the same tendency was noted in straight tube flow, hence the Baroczy(33) and Chisholm and Sutherland(28) correlations specialising for high mass flowrates in staight tube flow. Rippel, Eidt and Jordan(44) discussing the flow patterns in two-phase flow in a coil, correlate their data using Lockart-Martinelli and suggest alternative methods of correlating coil two-phase flow data where higher mass flow effects are apparent. It is interesting to note their reasoning as to why Lockart-Martinelli and other straight tube correlations can be used for low but not high mass flux flows. They point out that up to a point (slug flow), and depending on the two-phase quality, the nature of the flow patterns are such that they make it very difficult, if not impossible, for the Dean effect (secondary flow brought about by centrifugal forces) to establish itself, and until this happens there is no reason why the coiled tube flow should be any different from straight tube

flow. It is also interesting to note that in this paper an attempt is being made to deal with increasing flowrate effects where the maximum flow being dealt with is less than 100 $Kg/m^2.s$. It is intended to run the tests for this investigation up to mass flux values in excess of 4000 $Kg/m^2.s$.

Since the Lockart-Martinelli method could be modified for use with coiled flow by the replacement of straight tube single-phase pressure gradients by coiled tube single-phase pressure gradients it may be possible to do the same with the Chisholm and Sutherland(28) and other mass flux and quality dependent correlations. It is intended that this approach be adopted in the data analysis for this report.

4.1.0 Test Loop

An open circuit test loop was constructed using light gauge copper pipework, as shown in fig 4.1.

The pipework immediately before and after the test section was made from 1/2" bore tube and had couplings fitted which enabled the test sections to be changed without disturbing the remaining pipework. The couplings consisted of T-pieces which were fitted with pressure gauge lines and thermocouple glands. After the test section outlet coupling a short length of straight tube led to the main flow control valve. From this valve a length of large bore rubber tubing led the test fluids into a separator tank. The separator allows air to exhaust to atmosphere and the water to drain to a sump tank in the laboratory basement. A pump recirculates the water to a constant head tank on the laboratory roof.

The test loop supply pump draws water from the constant head tank. A short bypass loop was installed between the pump discharge and inlet, and was fitted with a hand operated valve. This arrangement would provide better control and more flexibility over water supply flowrates and pressures. At the pump outlet a T-piece was fitted to house a thermocouple and a high pressure purging water supply which allowed de-aeration of the pressure tapping lines. A water cooler was installed to prevent an excessive rise in temperature. The cooling element was supplied with water from a main supplied by the site cooling tower.

Since the cooler had been installed at floor level, advantage was taken of a long straight vertical section running to the test bench level to install a turbine flowmeter.

At bench level the tubing was turned to the horizontal before being coupled to a flow mixer. From here the test fluid mixture entered a straight section of tube leading to the test section.

Air is supplied to the mixer from the main air line via a bank of

rotameters. Immediately before the mixer, the air line is fitted with a pressure regulator and flow control valve. Finally each test section is installed with the coil axis horizontal and in line with the supply tubing as shown in figure 4.1.

4.2.0 Equipment

4.2.1 Drive Pump

The loop drive pump used was a 5WMV20 Worthington Simpson multistage pump. This model is capable of supplying 19 bar pressure at a flowrate of 0.5 kg/sec.

4.2.2 Cooler

A Bowmans shell and tube heat exchanger with disc and doughnut baffling was used as a cooling unit. The exchange heat rating was 4.5 kW.

4.2.3 Mixer

A sintered tube flow mixer was used to mix the air and water phases. This unit consisted of a body-shell made from 2.5" bore pipe fitted with an internal sleeve made from porous sintered tube. Water enters the pipe through the side wall and occupies the annular space between the sintered tube and the pipe inner wall. Under pressure the water passes through the sintered tube wall and mixes with the air which is moving through the central passage. The combined phases then move together down the central passage of the sintered tube and out to the test section.

4.2.4 Flow Separator

At the discharge from the test section the two-phase mix passes into a separator consisting of a tank which allows the water to separate under gravity while exhausting the separated air to atmosphere (see fig 4.1). The unit is made from a simple steel casing with ports for the two-phase inlet, water and air emission and a water level indicator. This last item was installed to avoid accidental flooding.

4.3.0 Instrumentation

4.3.1 Flowmeters

Air

A bank of four rotameters were used to monitor the air flowrate through the test section. Due to the large quantities of air which it was anticipated would be used it was decided to measure the air at the inlet to the test section where the pressure would be highest and hence the volume lowest. These rotatmeters had a scale indicating the volume of air corrected to a standard atmosphere of 1.013 bars and 15 degrees Celsius. Although the rig was run with the air supply considerably in excess of these pressures there is a standard method by which higher or lower supply pressures can be corrected without undue loss to the accuracy of the units.

Water

A Bestobell type M9 turbine flowmeter was used to measure the water volumetric flowrate. This flowmeter gives an electromagnetically generated signal which has a frequency proportional to volumetric flow. Calibration was carried out at the test bench and with the flowmeter in it's intended working location. The accuracy of this unit is $\pm$0.05% of its maximum rating within the calibration range. A copy of the calibration graph is found in Appendix 1.

4.3.2 Pressure Gauges

Four Bourdon-type pressure gauges were used. Two were used as safety measures to protect the pressure transducer and the manometer tubing network. Two more were of test instrument standard and were used to measure the rotameter and test section inlet pressures. In conjunction with the barometric reading these values provided absolute pressures. Calibration was carried out by the gauge company and a test certificate issued.

4.3.3 Pressure Transducer

The main function of the experimental rig is to measure pressure drops over designated lengths of pipework. To this end a system of valves and hypodermic pressure tappings were used in conjunction with a pressure transducer to measure pressure drop through the system. The majority of the

pressure measurements made were those involving water and air. The complex system of tappings shown in fig 4.2 is used with a differential pressure transducer to provide pressure drop measurements along the test section. The pressure transducers used were Rosemount E1151DP differential transducers. Three were used depending on the range required. They were calibrated for 1, 3 and 7 bar FSD respectively. This type of unit can be calibrated in situ to cover a wide range of pressure differentials up to 2000 KN/M^2 and have an accuracy of 0.1% FSD. A typical calibration graph is included in Appendix 2.

4.3.4 Thermometers and Thermocouples

Three thermocouples were used in the test loop. One was used to monitor the loop temperature at the multistage pump discharge to ensure that liquid in recirculation did not build up too great a temperature. Two thermocouples were also used, one each at the inlet and outlet of the test section. A thermometer was also used to read the air stagnation temperature at the exit from the separator.

Thermocouples

Three K-type thermocouples were used to obtain stage temperatures in the test loop. Manufactured to B.S. 4937, these are of the Chromel/Alumel type and have a generated EMF of 41 microvolts per degree Celsius. Calibration was carried out at the National Engineering Laboratory over the range +50C to -5C. Overall accuracy when used with the Solartron Multimeter 71520 is estimated to be $\pm 0.1^{o}K$. Calibration graphs for the thermocouples are in Appendices 3, 4 and 5.

Thermometer

A mercury filled glass thermometer was used at the separator to determine the stagnation temperature of the air. This was mounted above and behind the two-phase inlet to the separator thus reducing the water pick-up to a minimum by immersing the mercury bulb in the air while the air is at a suitably low velocity. The accuracy was taken to be approximately $\pm 0.25^{o}K$.

4.3.5 Voltmeter

Voltage readings from the pressure transducers and thermocouples were taken from a Solartron Digital Multimeter, via channelling through an instrument-standard multiway switchbox.

4.3.6 Digital Counter

An Orbital B-115M digital counter was used to read the signal from the turbine meter. Readings from both the voltmeter and the counter were taken directly, the various programmes used to calculate the results being equipped with the required constants and linear equations supplied by calibration.

4.3.7 Hypodermic Tapping Circuit

The ten tappings on the test section were connected to the pressure transducer via a bank of valves and a Schrader manifold. The various components were all interconnected using 1/8" bore nylon, used for its flexibility and small effect on the response time. A clean water purging supply was taken direct from the pump to the manifold to provide a means of removing air bubbles from the hypodermic tubing. The circuit used can be seen in fig 4.2.

4.4.0 Test Sections

There were four test sections in all, the details for which are as given below:-

COIL DIMENSIONS

COILED TUBES:	LARGE BORE	SMALL BORE
TUBE ID	0.0124 m	0.007 m
COIL MEAN DIAMETER	0.274 m	0.0745 m
TAPPING BORE	1.6 mm	1.6mm
NO. OF TAPPINGS	10	9
NO. OF TURNS	4	5
ANGULAR DISPLACEMENT OF TAPPINGS	160^{o}	270^{o}

FIRST TAPPINGS AT	0°	0°
TAPPING TYPE	1/8" BSP	1/8" BSP
END FITTINGS	1/2" BSP	1/2" BSP
MATERIAL	STAINLESS STEEL (ADMIRALTY SPEC)	
STRAIGHT TUBES:	LARGE BORE	SMALL BORE
TUBE ID	0.0124 m	0.007
LENGTH	1 m	1 m
NO. OF TAPPINGS	10	10
TAPPING TYPE	1/8" BSP	1/8" BSP
END FITTINGS	1/2" BSP	1/2" BSP
MATERIAL	STAINLESS STEEL (ADMIRALTY SPEC)	

5.0.0 METHODOLOGY

5.1.0 General

There are a number of aspects of this work, which do not appear to have been met with and studied by other investigators, which form this thesis and these were arranged into three different sections.

First, the experimental methods, commonly used in assessing fluid pressure drop in a tubular length of test section, were modified to suit the test section orientation and conditions of test. A single-phase correlation was also developed at this point for use during the two-phase analysis. While many investigators have tested coils with the coil central axis running vertically, conditions of service of the boiler being modelled required that these tests be carried out with the central axis lying horizontally. The test method development was carried out during the single-phase test work and while collecting single phase data.

In the second section, straight tubes were tested and the changes in test method, required for carrying out two-phase tests, developed while comparing the test section data with readily available correlations.

Finally, tests are carried out for two-phase flow in the coiled test sections and compared with correlations where possible. At this stage improved correlations for all the two-phase test data were developed.

5.2.0 Single Phase Tests

5.2.1 Experimental Method

The single-phase water tests with straight tubes were run first. The use of water made leak detection a simple matter and due to the incompressible nature of the fluid at the test conditions the analysis procedure was the simplest of the fluids under test. Having established that the test rig was functioning properly, single-phase air tests were also carried out with minor changes to the test method to enable the fluid volume to be assessed.

The test method involved the following stages:-

1) For water tests, the water supply to the rig was turned on and the multistage pump was primed. For air tests, the pressure regulator on the air supply to the rotameter bank was set, before opening first the butterfly valve on the chosen rotameter and then the supply valve to the flow mixer. This routine was adoped to make sure that any water which might have leaked back through the air supply route during water tests did not find its way into the rotameters.

2) All pressure gauge and transducer tapping and supply lines were purged, for water or two-phase tests. For air tests the rig would be left to run dry at a nominal flow with bleed points open to dry all tappings and instrumentation.

3) For water tests the multistage pump was switched on and the supply pressure to the test section raised to a maximum safe level to check all connections for leakage. For air tests, having turned on the air supply at the required pressure, a special soap solution could be sprayed onto couplings to assist in leak detection.

4) Having assessed the maximum and minimum flow which could pass through the section fitted and be measured, the range obtained was divided into ten subdivisions, (a set of test readings would be taken at each of the ten calculated flows).

5) Starting at the highest flowrate, the pressure gauge reading was taken from the first tapping (number 1) and, by the use of the tapping isolation valves, a sequence of pressure differential voltage values were taken from the pressure transducer/voltmeter. The readings were taken between the tapping furthest down the section and tapping number one, first, and then between tapping number one and each preceding tapping towards tapping number one. By following this method it is possible to reduce the ingress of air bubbles to the tapping lines, during two-phase tests, to a minimum and so this method of purging was adopted generally.

6) Having taken all relevant pressure readings, the signal value from the

flowmeter/counter was taken (having been given time to settle while the pressure readings had been taken) and the thermocouple voltages read.

7) After all readings had been taken, and before reducing the flowrate to the next selected value, the tapping lines would be purged or dried again.

As a rule, whether required or not, the ambient temperature and barometer reading were taken before all tests, single-phase water, air and all two-phase tests. Typical raw data can be found in Figure 5-25.

5.2.2 Data Analysis

For single-phase tests on either test fluid, air or water, equation 2.4 can be used to determine the friction factor where there is no gravitational or accelerational pressure drop to take into account. A computer progam was written which read test data files, converting voltage and frequency values as required, and determined friction factors based on frictional, as well as accelerational pressure losses where air is the test fluid. The results obtained can be seen in figure 5.1, 5.2, 5,3 and 5.4 It should be noted that separate programs were written for coils and straight sections as well as for each fluid. While the flow in the straight tubes did not require additional settling length other than that which was provided up to the first tapping, the literature survey had produced papers which suggested that up to 270^{o} of rotation should be allowed as settling length before pressure differentials are read from coils. The early water tests on the coiled test sections confirmed this as being the case. Hence the computer programs handling coil test data did not include pressure readings for tapping numbers one and two in their calculation of the frictional pressure drop. From figure 5.5 it can be seen that the air data does not follow the expected trend. Estimates showed that the air tests were producing stream velocities in excess of 80% of the critical velocity. At these velocities it is necessary to use a Fanno line method used in gas dynamics(40) to assess the value of the friction factor. A computer program was written which produced the required Mach Numbers, but since the method employed

is graphical it was decided to carry out the finishing calculations by hand since the work involved in producing the software for the whole solution was not justified. From figure 5.6 it can be seen that this method succeeded in producing the expected results for the straight tubes. While improvement resulted, a satisfactory solution was not found for the high velocity gas flow in the case of the coiled tube. On comparing the data (figures 5.7 and 5.8) it was suggested that the reason for the disparity between the compressible and incompressible results was almost certainly due to the failure of the Fanno line method to allow for secondary flow in the flow stream of the coil, the analysis of which is outwith the remit of the report. Fortunately this air data was unlikely to be needed in the analysis of the two-phase data,in Chapter 6.0 the case is discussed further.

The water test results for flow in a coiled tube showed good agreement with the correlation proposed by Srinivasan(2) (figures 5.9 and 5.10).

5.3.0 Two-Phase Results for Straight Tubes

5.3.1 Experimental Method

The experimental method employed was essentially the same as for the single-phase tests. Regular checks had to be made of the pressure tapping lines to ensure that they remained free of air bubbles and as an additional precaution the test sections were inserted with the tappings to the bottom. Due to the presence of finely dispersed air bubbles in the test mixture, the procedure had to be ordered in such a way that pressures in the tapping lines always erred on the positive side to make sure that there was no induction of the bubbles into the lines. Where checks had to be made on data points, the whole system was purged with clean water before retaking data.

5.3.2 Data Analysis

The values of the density, velocity, mass flow, viscosity, measured two-phase multiplier and Lockart-Martinelli parameter were calculated by computer program and comparison made with the Lockart-Martinelli correlation

(figure 5.11).

From the graph it can be seen that the smaller tube data with higher mass flux values lies closer to the Lockart-Martinelli line. Chisholm(34) presented a graph showing this tendency for particular mass velocities (up to 2078 $kg/m^2.s$) to show better agreement with the Lockart-Martinelli correlation. Brief comparisons were made with the Baroczy(33) and the Chisholm and Sutherland(35) correlations and there was a reasonable (within 20%) agreement at the lower mass flux values achieved on test. This was, perhaps to be expected since the limit to the Baroczy(33) data was in the region of 4000 $kg/m^2.s$ with Chisholm and Sutherland(35) using the same data as a base for their correlation. Finally the correlation presented by HTFS* was used in a computer program. This correlation was developed using computer software to provide a fit to the HTFS adiabatic two-phase flow data. Based on the Lockart-Martinelli method (equation 2.37), the C coefficient is 'tuned' to provide a fit to the HTFS data and is mass flux and property index (density and viscosity) dependent. Figures 5.12 and 5.14 show the two-phase multipliers obtained by the HTFS correlation compared to the two-phase multipliers measured and using equation 2.8 for the single-phase friction factor. The computer output supplying other information for this data can be found in tables 5.1 and 5.3. An alternative equation for the friction factor, obtained from the single-phase test data, was employed and the resultant graphs and data are found in figures 5.13 and 5.15, tables 5.2 and 5.4. It was found however that the difference in values of the two-phase multipliers obtained was insignificant. The two-phase correlation used here provides the best fit for the test data to date but the tendency for even this correlation to become less accurate at higher mass velocities can still be seen. This is not surprising if the mass velocities are examined. The best correlations available have been dependent on data with a mass velocity upper limit of

* Heat Transfer and Fluid Flow Service, NEL, East Kilbride, Scotland.

approximately 4000 kg/m^2.s but the test data obtained has an upper limit of 6400 kg/m^2.s. Also it can be seen that there is a difference between the multipliers for the respective tube diameters even after allowing for the high mass flux values. It was noted that the HTFS correlation had been fitted to data which had thousands of points above, but practically no data for tubes below, 18 mm in diameter. Other data for small tubes was extracted and compared with the test data and the resultant graph can be found in figure 5.16. The 8 mm data shown has mass flux values of up to 9000 kg/m^2.s and displays some data confirming the test results. Some data points appear to be adrift but it is worth noting that this data is for boiling flow. The 2.6 mm data also show fair agreement. It was decided to collect the coil two-phase data to confirm the trends shown in the straight tube data before attempting to find a suitable correlation which would add tube diameter and further mass velocity dependence.

5.4.0 Two-Phase Results for Coiled Tubes

5.4.1 Experimental Method

During all of the coil two-phase tests and over almost the entire range of qualities tested the test section vibrated with substantial force. This vibration persisted despite the rotation of the coil so that the central axis was in the vertical position. The resultant fluctuations in the various instrument readings may have reduced the consistency of the data obtained so far. To minimise the effects of the vibration the instrumentation was mounted on a separate bench. The procedure for collecting readings was as described in section 5.2.1., forces acting on the liquid phase producing a fairly consistent water cover over the tapping entrances, reducing the amount of purging required.

5.4.2 Data Analysis

The literature survey had not produced any reference to research work for two-phase flow in coils at high mass velocities of the magnitude covered in these tests. Those references which had dealt with two-phase flow in

coils had only dealt with low velocity flows, and found flow patterns to be similar to those found in straight tube horizontal flow. Additionally the replacement of the straight tube single-phase friction factor with that of the coiled tube single-phase friction factor had produced a calculated two-phase multiplier with a good agreement with measured multipliers. This approach was adopted in writing the software to handle the coiled tube two-phase flow test data. Versions were written utilizing both the equation proposed for the single-phase friction factor by Srinivasan(2) and the equation obtained from the test data. The resultant graphs and output are found in figures 5.17 to 5.20 and tables 5.5 to 5.8. Again it was found that the change in single-phase friction factor had very little effect on the ratio of the calculated - to measured - multipliers. With reference to the multiplier ratios it should be noted however that the correlation is in fact better than the case for straight tubes. Typical raw data can be found in Figure 5-25.

5.5.0 Two-Phase Data Correlation

Both the straight and coiled tube data suggest a relationship exists between the HTFS two-phase multiplier and the tube diameter. It has also been established that the mass velocities achieved during test are greatly in excess of the limits of the data for which existing mass velocity-dependent correlations have been produced. Therefore it is proposed that a correlation developed for the test data be further dependent on both these parameters. In addition it is proposed that there is a limit up to which the flow patterns for two-phase flow in a coiled tube can be predicted as being similar to those for a straight tube. Lacey(25) did not provide test data but did present such evidence from flow visualisation tests. He showed that at low mass velocities, bubble and slug flow are much the same in each type of tube geometry, with the phase breakages preventing secondary flow from establishing a difference. It is suggested however that there will come a point, with the increase in velocities and at certain

qualities, where the secondary flow will establish itself in the coil. At this point there will be differences between the flows in straight tubes and coils for which different correlations must be provided.

5.5.1 Straight Tube Correlation

The new correlation was only required to come into effect at a certain level of mass flux for each tube. Accordingly a ratio of the chosen mass flux to the tube diameter was chosen. The new two-phase multiplier would be of the form,

$$\phi_1^2 new = \phi_1^2 \cdot C3 \qquad (5.1)$$

where C3 contains the mass flux/tube diameter ratio and ϕ_1^2 is as found in equation 2.37. Having examined both the large and small bore data and after trying a number of different values, a suitable computer subroutine was written which achieved good results for both tubes. It was decided to adopt the methods of Chisholm and Sutherland who presented different values of the coefficient C2 depending on certain ratios of mass flux. For the test data, each tube diameter had a suitable value of mass flux chosen, after which the new correlation was required to have an effect. This value was 3750 $kg/m^2.s$ for the large bore tube and 2162 $kg/m^2.s$ for the small bore tube.

The group $(G/(const \cdot d)^m)$ was used as a ratio which should equal 1 when the required mass flux was reached. This same group was in turn used, being diameter and mass flux dependent, as the base for the modifying C3 coefficient as described in equation 5.1

The value for the constant was taken as 1×10^5 for both the cut-off point ratio and the modification factor. The index was taken as 1.554 for the cut-off ratio and 1.115 for the correlation. The final form of the straight tube correlation coefficient C3 for equation 5.1 is,

$$C3 = 0.5 + (G/(d \cdot 10^5)^{1.115})^{0.5} \qquad (5.2)$$

where $G/(d \cdot 10^5)^{1.1554} > 1.0$ and

$C3 = 1.0$ for $G/(d \cdot 10^5)^{1.1554} < 1.0$

The graphs of the modified multipliers compared to the test measured

multipliers can be seen in figures 5.21 and 5.22 together with the actual data in tables 5.9 and 5.10.

5.5.2 Coiled Tube Correlation

As was the case for the straight tube correlation, the coiled tube correlation is not required to come into effect until certain levels of mass flux are reached for a particular diameter of tube. The levels of mass velocity at which the correlation is needed for the coiled tube flow can be seen to be considerably lower than those for straight tube flow as can be seen if figures 5.12 and table 5.1 are compared with figure 5.18 and table 5.5.

The format of the correlation is the same as for the straight tube data, based on equation 5.1. A significant difference achieved was that of retaining the same index m for both the cut-off ratio and the correlation. The final form of the coiled tube two-phase flow correlation coefficient C3 is,

$$C3 = 0.1 + (G/(10^5 \cdot d)^{1.0671})^{0.35} \qquad (5.3)$$

where $G/(d \cdot 10^5)^{1.0671} > 1.0$ and

$C3 = 1.0$ where $G/(d \cdot 10^5)^{1.0671} < 1.0$.

The graphs and specific data for this correlation can be found in figures 5.23 and 5.24, tables 5.11 and 5.12.

5.5.3 Correlation Development

As can be seen from Figures 5.14 and 5.12, the HTFS correlation could be improved for high mass flux values and low diameters. The first stage in improving the mass flux and diameter dependency was to include a term involving these parameters. Examining the data from Tables 5.5 and 5.6 it was decided that the new correlation should take effect from approximately 2000 $kg/m^2.s$ for the 12.4 mm tube data and 1200 $kg/m^2.s$ for the 7.7 mm tube data.

Since at this point the new term in the correlation should equal 1.0 for each set of data the term can be solved to provide a suitable index.

$$\frac{2000\ kg/m^2.s}{(0.0124\ m \times 10^5)^N} = 1.0 = \frac{1200\ kg/m^2.s}{(0.0077\ m \times 10^5)^N}$$

$$\Rightarrow \quad \frac{2000\ kg/m^2.s}{1200\ kg/m^2.s} = \left(\frac{0.0124 \times 10^5}{0.0077 \times 10^5}\right)^N$$

$$1.667 = 1.614^N$$

$$N = 1.0671$$

A computer program was written which calculated the mean, standard deviation and percentage of data within 10% of the correlation in use. The original HTFS correlation was then compared with the same correlation multiplied by the new term $G/(d \times 10^5)^{1.0671}$, term succeeds in realigning the two diameter data sets, as can be seen in Tables 5.13 and 5.14 respectively. The intention of introducing a diameter term had been to bring the line of data for each diameter together (Figures 5.5 and 5.6) by bringing in a mass flux factor "lifting" the high mass end of the data group. It was recognised that in bringing the groups together and then "lifting" both sets of data together that a considerable proportion of low mass flux data would exceed the 10% limits on the correlation. However there can be seen to be a very large improvement in the total group (both diameter sets) as well as a substantial improvement in the smaller diameter set standard deviation.

Having brought the data sets into alignment the next stage was to reset the lower mass flux data to the HTFS correlation line. A constant would be added to achieve this and the effects of adding valves of 0.1, 0.11 and 0.09 can be seen in Tables 5.15, 5.16 and 5.17 respectively. The lower mass flux data in the large bore results were examined but it was found that the effects of the constants could not be assessed easily.

The differences in standard deviation and mean for the large bore data were very small. It was decided that the best measure was a 3% increase in

data within the 10% limit when a constant of 0.1 was added.

The new term now read

$$0.1 + G/(d \times 10^5)^{1.0671}$$

The data at this stage will lie on a single line, agreement with the measured values of pressure drop varying from good at lower mass flux values to poor at higher values.

The final stage of development involves "bending" the correlation to remove the mass flux effect variance. To achieve this an index is applied to the mass flux/diameter ratio to give an equation, of the form

$$0.1 + (G/(d \times 10^5)^{1.0671})^m$$

Values of index of 0.5, 0.35 and 0.2 were tried and the results can be seen in Tables 5.18, 5.19 and 5.20. Where m = 0.35. It can be seen that the correlation shows a maximum of data within 10% of the measured values, and has a greater consistency of standard deviation and mean for both large and small bore data. before deciding on 0.35 as an index value the sensitivity of the index was examined by trying values of 0.36 and 0.34 for m, (see Tables 5.21 and 5.22). The correlation with m = 0.35 has a mid-value for both total mean and standard deviation but the variation between the three sets of values can be seen to occur in the third significant figure. Additionally with m = 0.35 the correlation has the greatest amount of data within the 10% limits.

6.0.0 DISCUSSION

This discussion will be divided into four parts. The pressure drop in straight tubes will be discussed firstly for the single and two-phase results. The second section will essentially repeat this for coiled tubes. The third section will deal with the usefulness of these tests in modelling boiling flow. Finally a brief discussion with respect to the flow visualisation tests will relate the findings of the high mass flux tests carried out using clear plastic tube.

Compressibility effects were experienced with single-phase air flow which resulted in a significant accelerational pressure gradient as discussed in connection with equ (2.1). Gas dynamic methods were employed in order to compare the single phase air results with the existing correlations for incompressible single-phase flow. While the Fanno method employed produced satisfactory results for the straight tubes, the results for flow in coiled tubes did not compare so well with the Srinivasan correlation. Possible reasons for this apparent discrepancy will be discussed.

6.1.0 Straight Tubes

The relationship between friction factor and Reynolds Number for straight tubes has been thoroughly investigated by other researchers and a number of correlations are in common use covering various ranges of Reynolds Number.

Two of the simplest of these, covering a relatively limited range of Reynolds Number are given in equ (2.7) and (2.8). These, particularly equ (2.7), have the advantage of simplicity of form which makes them useful for substitution into other equations. The widest range of Reynolds Number is found in a correlation found in the ESDU(45) papers on frictional pressure drop. Good agreement was obtained when comparing these correlations with the test data obtained.

As has been discussed in section 2, the prediction of two-phase

pressure drop is much less certain owing to the greater complexity of the flow. The best available correlation for the prediction of two-phase frictional pressure drop is of a proprietary nature, being the property of the Heat Transfer and Fluid Flow Service (HTFS) and is based on a large data bank covering a range of fluid properties : mass flux, quality, tube diameter and orientation. There are however in the data bank relatively few data for tubes less than 12 mm in diameter and it might therefore be expected that this might be an area of weakness.

6.1.1 Single-Phase

Tests carried out using air and also water in the straight tubes are to provide confirmation that the rig instrumentation is functioning accurately, that the experimental technique is adequate and to establish whether the tube can be regarded as smooth. This area of study is particularly well covered and results are compared with the friction characteristic equations chart and showed good agreement.

Looking at fig 6.1 showing pressure loss against distance it can be seen that there are a number of small deviations from the straight line. These are also discussed in the chapter on experimental methods and were, it is believed, due to small burrs on the inside of the tappings (see figs 6.2 and 6.3). The depth of these irregularities is uncertain but they were positively identified by the use of a flexible fibrescope. There were distinct grinding marks around the inside of the tappings. There were also considerable amounts of weld burn - through where the tappings had been welded to the tube, and large areas of rust. This rust was present despite the use of stainless steel for the tube construction.

Despite the presence of these surface irregularities in the tube bore, the data, when plotted on the friction characteristic, agreed with the line for an hydraulically smooth tube.

Whilst the results for air flow through the large bore tube showed a good agreement with the Blasius line, the small bore results did not. It

was decided to use a method from John(40) where, having calculated the Mach numbers at two different points a known distance apart, the difference between the results of a standard integral give a term:

$$C \text{ (the difference)} = \frac{f \cdot z}{d} \qquad (6.1)$$

Tests were run and differences calculated for a range of Mach Numbers. In calculating Mach Numbers for both large and small bore tubes with single-phase air flow it was found that the method originally used was adequate until Mach Numbers exceeded approximately 0.2. Thereafter it became necessary to apply the Fanno method, employing the equation shown (6.1) and respective method based on gas dynamic theory. It should be noted that the Mach Numbers were estimated to have reached values as high as 0.83 in the small tube. It was believed that at the point where accelerational and frictional terms became insufficient, local changes in the temperature would have started to affect the true volume of the fluid. Additionally while Mach Numbers reached 0.83 at the tapping with the lowest pressure value, the changes of section and still lower pressures at the downstream coupling gave rise to the possibility of there being choked flow conditions affecting the through flow of fluid.

However, the Fanno flow method used succeeded in bringing the data to the expected position on the Reynolds Number/friction factor plot. Where the Mach Numbers were less than 0.2 - 0.3 the two methods employed provided very similar results, confirming the suitability of the Fanno flow method for use in this application.

The single phase water tests provided good agreement with the line for an hydraulically smooth tube. For the purposes of calculating two-phase pressure drop, an equation for the friction factor was derived from this data,

$$f = 0.0016 + 0.106/Re^{0.32} \qquad (6.2)$$

6.1.2 Two-Phase

The method used to assess the accuracy of two-phase correlations is to compare a calculated multiplier ratio with the actual two-phase multipliers measured in the tests. Calculations are based both on a recognized equation for the single-phase gradient and for an improved equation based on single phase data from this test work (equ 6.1). The difference between the equations and the resultant multiplier comparisons was minimal as can be seen comparing figures 5.12 with 5.13 and 5.14 with 5.15. Comparing these graphs it was decided that there was no difference, with respect to single-phase friction factors, worth investigating.

The measured multipliers for the large-bore data can be seen to agree quite closely with the calculated multipliers. Tables 5.1 and 5.2 show a grouping of the ratio $\pm$ approximately 30%. However the small-bore data shows a different trend. The values of measured multipliers were between two and three times the calculated value (tables 5.3, 5.4 and figures 5.13 and 5.14). Noting the tendency of the ratio of calculated-to-measured multiplier to decrease as the mass flux increases, we may also note that this same trend is visible in the large-bore data (tables 5.1, 5.2 and figures 5.11 and 5.12) but the movement here is less noticeable. There is no direct link since from the data we can see that a mass flux value for say 4500 $kg/m^2.s$ has a very different multiplier ratio value for the large and small-bore tubes respectively. However it may be the case that a relationship may exist which entails factors related to tube diameter. Graphs displaying both large and small-bore results for mass quality and mass flux against calculated and measured multipliers (figs 6.4, 6.5, 6.6 and 6.7) show that while there is a small difference between the calculated and measured values of mass flux there is a marked difference in the values of measured mass quality from that expected. Only when mass flux and quality were shown against individual multipliers instead of their ratio did this trend become apparent. In order to check the truth of the small-bore test data a comparison was made with data from the HTFS (fig 5.16) data

bank. Referring to fig 5.16 it can be seen that while there are some data points which are askew of the main trend (High mass flux boiling data) it can be seen that there are points which confirm the trend found for the measured two-phase multiplier to increase with mass flux at a greater rate than calculated values.

Summarising the assessment of the data, while it was found that the values for the large bore two-phase flow data is fairly accurately predicted by the combined Baroczy-Chisholm-Sutherland method it was found that the small bore data is not. Plots of mass quality against measured and calculated multipliers indicate that the relationship between these factors changes for two-phase flow in smaller diameter tubes (less than 10 mm).

In section 5.0, as part of the data analysis an attempt was made to provide a correlation for the data which, in addition to providing a better estimation of the characteristics of these particular test sections, would have a base on which later work could develop.

First, the effect of mass flux. It has been shown that the general limit of data, on which mass flux dependent correlations have been based, is approximately 4000 $kg/m^2.s$. Since the data collected rises to values in excess of 6500 $kg/m^2.s$ it was decided that the new correlation would present an additional mass flux dependent term. Secondly, it is suggested, that for a given combination of phases, there is a lower limit of diameter under which this parameter has been correlated to date. Up to this point in time investigators may only have noted a trend in data for small tubes tested to 10 mm diameter. However, when viewed from the point where evidence of a diameter effect is sought, data for quite large tubes may show signs displaying such an effect. It was therefore proposed that the correlation should include a tube diameter dependent term. Finally, the design of the test rig was such that the spectrum of mass qualities which could be investigated was limited. For this reason it would not be appropriate, despite the evidence of figs 6.6 and 6.7, to include a term dependent on

mass quality. The range of mass qualities tested was narrow and so the visible effects on these tests are small.

6.2.0 Coiled Tubes

Single-phase flow in coiled tubes has not been investigated to the same extent as flow in straight tubes but there are a number of sound correlations in use. These tend to break down to the same forms as those for straight tubes but with the addition of ratios related to the Dean Number. Both Blasius and modified Blasius forms are found to be in reasonable agreement with the data taken; but the line proposed by Srinivasan(2), taking the Blasius form with $Re^{0.2}\ (d/D)^{0.1}$ replacing $Re^{0.32}$ was found to be the best from those available. While this correlation was found to be good it was decided to fit a line through the test data for the specific coils under test and to compare these with values obtained using Srinivasan's correlation. This is important since the best method to date of predicting two-phase flow in coiled tubes involves replacing the straight tube single-phase gradient by an equation for single-phase flow in coiled tubes.

The coiled tube two-phase test results were analysed in exactly the same way as those for the straight tube tests but with the replacement of the straight tube friction correlation by the coiled tube correlations, both Srinivasan(2) and a correlation based on the single-phase test data were used.

6.2.1 Single-Phase

The single-phase data were closely predicted by a number of the existing correlations available with Srinivasan(2), Akagawa(1) and White(32) all within an acceptable range. In addition to these a line was fitted through the data to provide a correlation for this specific data.

$$fc(D/d)^{0.5} = 0.081 \ . \ (Re(d/D)^2)^{-0.225} \qquad (6.3)$$

In discussing the straight tube data it was shown that compressibility effects had to be dealt with by using a method normally employed in gas

dynamic work. While this method worked well for the straight tube it can be seen from fig 6.8 that it did not work when used with the coil data. Tests were carried out to check both straight and coiled tube data but no reason was found for the apparent drop in friction factor values. There may be, however, given the differences in flow regime between flow in the straight and coiled tubes, an explanation available.

In the literature survey it was shown that a number of papers agree that the maximum velocity of a fluid flowing round a bend is greater than would expected to be the case (see figure 6.9) due to the secondary flow pattern which develops. A simple vector diagram will show that the true velocity of the fluid would involve adding a vector of circumferential velocity. Extending this concept it is possible to imagine that local Mach Numbers can rise above estimated values rendering the method for straight tubes (dependent on one-dimensional flow) inadequate.

6.2.2 Two-Phase

The two-phase data for coils were better predicted by the methods adopted than the straight tube data. This appears at first to be an odd situation. There are, however, a number of important features of the coil flow which should be considered before conclusions are drawn.

Firstly it was noted that during the two-phase coil tests there was a constant vibration from the coil. Fig 6.10 gives some idea of the magnitude involved, surprising if only because the coil is firmly fixed at one end and suppressed at the other. While the frequency of this vibration changed with flow rate it was of an intensity such that the whole test bench shook and it became necessary to remove the instrumentation and other loose equipment to a separate table. The vibration was steady and powerful and it is feasible that this phenomena had a regulating effect on the two-phase mix which is not normally present in straight tube flow. The orientation of the coil was moved from having the central axis horizontal to vertical, but did not have any effect on the vibration. (It is worth noting that none of the papers

dealing with two-phase flow in coils made any reference to such vibrations. This may have also been due to the generally low limit of mass velocities tested).

It has been stated that these tests have been run to new, higher limits of mass flux. It is suggested that a point had been reached where rather than the flow moved in a generally single dimension, secondary flow patterns have established themselves and it is no longer valid to apply the single-phase friction factor as previously used.

6.3.0 Limitations of Modelling Boiling Flow with an Air/Water Mixture

For the purpose of this research water and air have been used to model boiling flow in a coiled boiler tube. It was recognized at the outset that there would be a limit to which the comparison could be taken and this section will deal with areas where it is expected that differences would be met.

First it is important to know how the flow patterns in boiling and two component two-phase flow differ.

With air and water it has been shown how various types of flow pattern evolve as the volumes of the two phases change. Starting with bubble flow with a relatively small amount of gas dispersed as bubbles in a continuous liquid phase, as the quantity of gas increases plug flow will develop with coalescing gas bubbles forming plugs of gas. With greater gas volume stratified flow may form and as the gas phase increases in quantity, and hence velocity, the liquid phase may be whipped up to form wavy flow and then slug flow as the waves cover the tube section and are pushed along as slugs of liquid. If the gas phase flows with a high enough velocity relative to the liquid phase the gas may push the liquid to the wall to form an annulus and the gas itself run along the tube centre as a core to give annular flow perhaps with liquid entrainment as small waves on the liquid surface are broken off and carried in the gas flowstream. With the flow in

a coiled tube there may well be other patterns which develop. The secondary flow and the centrifugal effects will both act to alter the liquid and gas distribution in the tube section. While for low velocities it has been shown that the liquid phase will tend to dominate the outer areas of the tube section, if the gas phase velocity is high enough film inversions will occur (Lacey(25)) with the gas occupying the outer regions but with secondary flow within the gas phase causing entrainment of liquid from the inner liquid strata.

In the case of boiling flow there are a number of differences in the way in which the flow patterns develop.

At the tube wall the presence of nucleate boiling will have the effect of increasing the friction losses between the phases and the tube wall. Indeed it is not altogether impossible that if the rate of heat flux were great enough dryout could occur whilst there is still a liquid core, forming an annular flow with vapour to the tube wall. The point is made that for a given quality, the boiling flow situation will have a dry wall before the two-component adiabatic flow and this will have an effect on the accuracy of the friction pressure drop prediction.

The boiler being modelled in this study consists of two coils, one forming the inner wall and the other forming the outer wall with the heat source placed between the coils, (see fig 6.11). The effect of this arrangement is to limit the heat transfer almost exclusively to the outer side of the inner coil and the inner surface of the outer coil. This presents a situation which is an opposite to the ideal.

It is intended that the inner coil be used to heat the liquid from a subcooled state to a saturated condition. If indeed it is the case that the liquid in this coil remains liquid then there will be no problem in predicting the pressure drop in this coil. However if there is any boiling of the liquid, the surface on which nucleate boiling will occur will be the outer surface (see fig 6.12). As has been discussed earlier, where there is

a small amount of gas or vapour present in the coil travelling at a low velocity relative to the liquid, it will move to the inner surface due to the centrifugal forces acting on both phases. These phase flow phenomena present a situation where the highest part of the liquid velocity profile is moving along the surface with the highest local friction factor caused by the nucleate boiling. Additionally the interphase shear will be at a maximum since the vapour bubbles will traverse the whole tube diameter before arriving at the inner surface where they may recondense.

The situation is similarly far from ideal at the outer coil.

In this coil the saturated liquid is to be heated to a point where at the coil exit the steam is superheated. During the boiling process the heat transfer is through the inner wall but due to the mass of vapour being generated the increasing vapour phase velocity will quickly bring about film inversion (see fig 6.13). This will occur at a point where the centrifugal forces acting on the vapour are greater than those acting on the liquid due to the higher velocity outweighing the effects of the greater liquid mass. Again there is a situation where the vapour bubbles will be formed at the wetted surface, maximising the interphase shear and if the entrainment model by Lacey(25, 27) is considered, liquid at the boiling surface may be entrained in between the secondary flow vortices and thrown onto the cool outer wall surface.

These circumstances may not be the worst imaginable and indeed the resultant effects on the pressure drop may be negligible. However it can be seen that the effects and circumstances described above could not happen in the air/water tests and consideration should be given before applying the results of this research directly to the intended boiler design.

6.4.0 Flow Visualisation Tests

Clear plastic tube of 12.4 mm internal diameter was wound onto a mandrel to give an arrangement exactly the same as that of the larger bore coil.

The primary goal of these tests was to ascertain the flow patterns which were responsible for the coil vibration. At the same time general observations were made of the flow patterns at lower mass flowrates.

With the air content at a minimum the mixed flowstream quickly moved to form a stratified flow as the section became curved and the centrifugal forces separated the phases.

When the operating conditions were reached which had been present at the onset of vibration the stratified flow pattern was seen to break up. The use of a high speed polaroid photograph allowed the examination of the flow pattern but it was felt that high speed cine or video film would be required for a thorough examination.

It appears that secondary flows impart a rotational motion to the whole mixed fluid body in bursts. Sections of low quality flow could be seen swirling along the tube broken up by sections of high quality flow.

It is suggested that the secondary flows present were rotating slugs of liquid with forces which exceeded the centrifugal forces created by the flow about the heli central axis. These slugs of liquid, rotating about the secondary flow axis amount to eccentric masses causing out-of-balance forces, subsequently causing vibrations. As the velocity increases the vibrational frequency will increase, with increased secondary flow. Additionally however the increased secondary flow will lead to homogenisation, less slugging and hence the reduction of the out-of-balance forces. It is expected therefore that the vibration would reduce in power at sufficiently high mass velocities.

7.0.0 CONCLUSIONS

Frictional pressure drop for two particular coil geometries has been examined with air and water adiabatic, both single and two-phase flows.

For the single-phase friction factor, the correlation by Srinivasan (equ 3.17) is confirmed by experiment and is recommended for general use. A correlation is also presented for the specific coils under test (equ 6.3).

For frictional pressure drop with two-phase flow either the Chisholm-Sutherland(31) or HTFS coefficient is confirmed by experiment as suitable for use up to certain mass velocity and tube diameter conditions. Thereafter a correlation is provided which allows for the correction of the two-phase multiplier by equation 2.37 for the coils under test and for general use at high mass flux.

Straight tubes of similar bore were also tested at the same wide range of flow conditions. A suitable correlation for small tube diameters and high mass flux flows is also provided (equ 5.2).

The possible use of this study with respect to using the results for modelling the changing quality flow in a boiler is discussed as are the results of a short series of flow visualisation tests carried out with the large bore coiled tube.

Finally, strong vibrations were produced in the coils over most of the two-phase flow conditions. These were at a high mass velocity and the flow visualisation tests indicated that secondary flow was causing a rotational slugging which produced the vibrations. While data was not collected for these flow visualisation tests it was noted that the frequency of vibration increased with mass flux. A paper by Hsien-wen hsu(18) on vibration effects on single-phase flow suggests that such vibration could cause massive increases in frictional losses.

8.0.0 RECOMMENDATIONS FOR FUTURE WORK

The area of study concerning single-phase flow in helical coils has been adequately covered for the purposes of this work.

It may be that the case for study of near critical flow in a coil would be one of interest to users of gas dynamic studies. It is understood by the author that some work is being carried out at the time of writing this thesis whereby a two-phase flow is being treated as a single compressible fluid and the laws applicable to compressible flows used to provide a correlation for high velocity two-phase flow.

From the literature survey and the work carried out for this study it is felt that the subject of high mass velocity two-phase flow is one which could be expanded considerably together with the effect of tube diameter on two-phase flows. It is likely that the applications and hence the justification of such study would be limited. If a use for such information has not arisen to date for such conditions what likelihood in the future? However, the ever present need for the compaction of plant gives constant life to studies which might apply to coiled boiler tubes.

This last statement leads to the main area in which study might produce interesting and original work.

This study has added a flow regime to those already known and established for two-phase flow. This is the two-phase secondary flow slugging which caused substantial vibrations in the test coil. The flow visualisation tests carried out were very crude. No mention of either the vibration caused or the phenomenon itself has been traced in the literature survey. Lacey has discussed annular flow in a coiled tube with liquid entrainment but this flow regime is believed to occur at much higher qualities. It is suggested that the presence of secondary flow might lead to some very interesting results at high mass velocities with many different flow pattern combinations and effects, the knowledge of which will be very useful to design engineers.

Finally it would be of great interest to know more about the effects of vibration on flow in coils and particularly for two-phase flow. If vibration is a characteristic of two-phase flow in coils and the friction factor increases as suggested by Hsien-wen hsu(18) then such knowledge will be of great importance to anyone involved in plant design.

REFERENCES

1) Akagawa K., Sakaguchi T., and Ueda M. (1971) 'Study on a gas-liquid two-phase flow in helically coiled tubes'. Bulletin J.S.M.E. Vol 14 No. 72 pp 564-571.

2) Srinivasan P.S., Nandapurkar S.S., and Holland F.A., (1970) 'Friction factors for coils'. Trans Instn Chem Engr. Vol 48 pp T156-T161.

3) Ramana M.V. and Sadasivudu D., 'Pressure drop in helical coils' (1972) India Jour Tecny Vol 12 Nov 1974 pp 473-474.

4) Mohan Reddy C. J. and Satyanarayan A. 'Two-phase flow in helical coils - flow pattern, pressure drop and hold-up' IE(I) Journal-CH Vol 58, Oct 1977.

5) Boyce B.E., Collier J.G. and Levy J. 'Hold-up and pressure drop measurement in the two-phase flow of air-water mixtures in helical coils' (1969) Concurrent gas liquid flow, Plenum Press.

6) Engineering Sciences Data Unit 'Pressure losses in curved ducts : coils' (1977) Item Number 77029.

7) Rogers G. F. C. and Mayhew Y. R. 'Heat transfer and pressure loss in helically coiled tubes with turbulent flow' (1964) Int. J. Heat Mass Transfer Vol 7 pp 1207-1216 Pergamon Press.

8) Kasturi G. and Stepanek J. B. 'Two-phase flow - I. Pressure drop and void fraction measurements in concurrent gas-liquid flow in a coil' (1972) Chem Eng Sci Vol 27 pp 1871-1880 Pergamon Press.

9) Kasturi G. and Stepanek J. B. 'Two-phase flow - II. Parameters for void fraction and pressure drop correlations' Chem Eng Sci Vol 27 pp 1881-1891 Pergamon Press.

10) Banerjee S., Rhodes E. and Scott D. S. 'Studies on concurrent gas-liquid flow in helically coiled tubes - I' (1969) Cana Jour Chem Eng Vol 47 Oct 1969.

11) Puri A., Srivastava R. P. S., Varma A. P. and Saksena R. K. 'Hydrodynamics fo air-water two-phase flow in helical coils' (1977) Chem and Petro Chem Jour 1977 pp 19-24.

12) Mishra P. and Gupta S.N. 'Momentum transfer in curved pipes I. Newtonian fluids' (1979) Ind Eng Chem Process Des Dev Vol 18 No 1 1979.

13) Tarbell J. M. and Samuels M. R. 'Momentum and heat transfer in helical coils' (1972) Chem Eng Jour Vol 5 (1973) pp 117-227.

14) Keulegal G.H. and Hilding Beji K. 'Pressure losses for fluid flow in curved pipes' (1937) Jour of Res Of the Nat Bur Of Stds Vol 18 Paper RP965.

15) Patankar S. V., Pratap V. S. and Spalding D. B. 'Prediction of turbulent flow in curved pipes' (1975) Jour of Fluid Mech Vol 67 Part 3 pp 583-595.

16) Kozeki M. 'Experimental study on two-phase flow in curved tube' (1970) Mitsui Shipbuilding and Eng Company Ltd, Tokyo, Japan.

17) McConalogue D. J. and Srivastava R. S. 'Motion of a fluid in a curved pipe' (1968) Proc Roy Soc A 307, pp 37-53.

18) Constantine G., Vytoyannis and Hsien-wen Hsu 'Experimental study of effect of vibration on friction factor in flows through curved pipes' (1970) Ind Eng Chem Process Des Dev Vol 9 No 2 pp 186-190.

19) Rangacharyulu K. and Davies G. S. 'Pressure drop and hold-up studies of air-liquid flow in helical coils' (1984) Chem Eng Jour Vol 29 pp 41-46.

20) Lockart R. W. and Martinelli R. C. 'Proposed correlation of data for isothermal two-phase, two component flow in pipes' (1949) Chem Eng Prog Vol 45 No 1 pp 39-48.

21) Martinelli R. C. and Nelson D. B. 'Prediction of pressure drop during forced-circulation boiling of water' (1948) Trans ASME Vol 70 pp 695-702.

22) Dean W. R. 'Note on the motion of fluid in a curved pipe' (1927) Phil Mag (Series 7) Vol 4 pp 208-223.

23) Eustice J. 'Flow of water in curved pipes' (1910) Proc Roy Soc Vol A84 pp 107-118.

24) Wattendorf F. L. 'A study of the effect of curvature on fully developed turbulent flow' (1934) Proc Roy Soc Vol 148A pp 565-598.

25) Lacey P. M. C. 'Two-phase flow in curved ducts' (1970) Ann Mtng DECHEMA.

26) Engineering Sciences Data Unit, 1976, Item No. 76018.

27) Maddock I., Lacey P.M.C. and Patrick M.A. 'The structure of two-phase flow in a curved pipe' (1974) Symp Multi-phase flow systems, Univ Strath Paper J2.

28) Chisholm D. and Sutherland L. A. 'Prediction of pressure gradients in pipeline systems during two-phase flow' (1979) Proc Instn Mech Eng Vol 184 Pt 3C.

29) Thom J. R. C. 'Prediction of pressure drop during forced circulation boiling of water' (1964) Int Jour Heat Mass Transfer Vol 7 pp 709-724.

30) Taylor G. I. 'The criterion for turbulence in curved pipes' (1929) Vol A124 pp 243-249.

31) Dean W. R. 'The streamline motion of fluid in a curved pipe' (1928) Phil Mag S 7 Vol 5 No 30.

32) White C. M. 'Fluid friction and its relation to heat transfer' (1932) Trans Instn Chem Eng Vol 19 pp 66-80.

33) Baroczy C. J. 'A systematic correlation for two-phase pressure drop' (1966) Chem Eng Prog Symp Series Vol 62 No 64 pp 232-249.

34) Chisholm D. 'Two-phase flow in pipelines and heat exchangers' (1983) Pitman Press. In association with the Instn Chem Eng.

35) Chisholm D. and Sutherland L. A. 'Prediction of pressure changes in pipeline systems during two-phase flow' (1969) Inst Chem Eng/Mech Eng Joint Symp, Univ Leeds, Paper 4I.

36) Chisholm D. and Laird A. D. K. 'Two-phase flow in rough tubes' (1958) Trans ASME Vol 80 No 2 pp 276-286.

37) Cichitti A. 'Two-phase cooling experiments - pressure drop, heat transfer and burnout experiments' (1960) Energie Nucleare Vol 7 No 6 pp 407-425.

38) McAdams Wh., Woods W. K. and Heroman L. C. 'Vapourisation inside horizontal tubes II - Benzene oil mixtures' (1942) Trans ASME Vol 64 No 3 pp 193-200.

39) White C. M. Proc. of Royal Society Series 'A' Vol 123 pp 645-663, 1929.

40) James J. E. A. 'Gas Dynamics' (1933) ISBN 0-205-08014-6, Allyn Bacon Inc.

41) Kays W. M. 'Convective heat and mass transfer' (1979) McGraw-Hill Inc.

42) Rogers G. F. C. and Mayhew Y. R. 'Engineering thermodynamics work and heat transfer' (1967) Longman Press.

43) Ito H. 'Frictional factors for turbulent flow in curved pipes' (1959) Jour Bas Eng Vol 81 pp 123-134.

44) Riddel G. R., Eidt C. M. and Jordan H. B. 'Two-phase flow in a coiled tube' (1966) I and EC Process Design & Development.

45) Engineering Sciences Data Unit, 1966, Item No. 66017.

LIST OF TABLES

LIST OF FIGURES

6.10 Double exposure photograph taken with coil at maximum vibration. Note amount of deflection.

6.11 Diagram of possible boiler tube arrangement

6.12 Diagram showing possible boiling nucleation site for inner coil

6.13 Diagram showing liquid film inversion

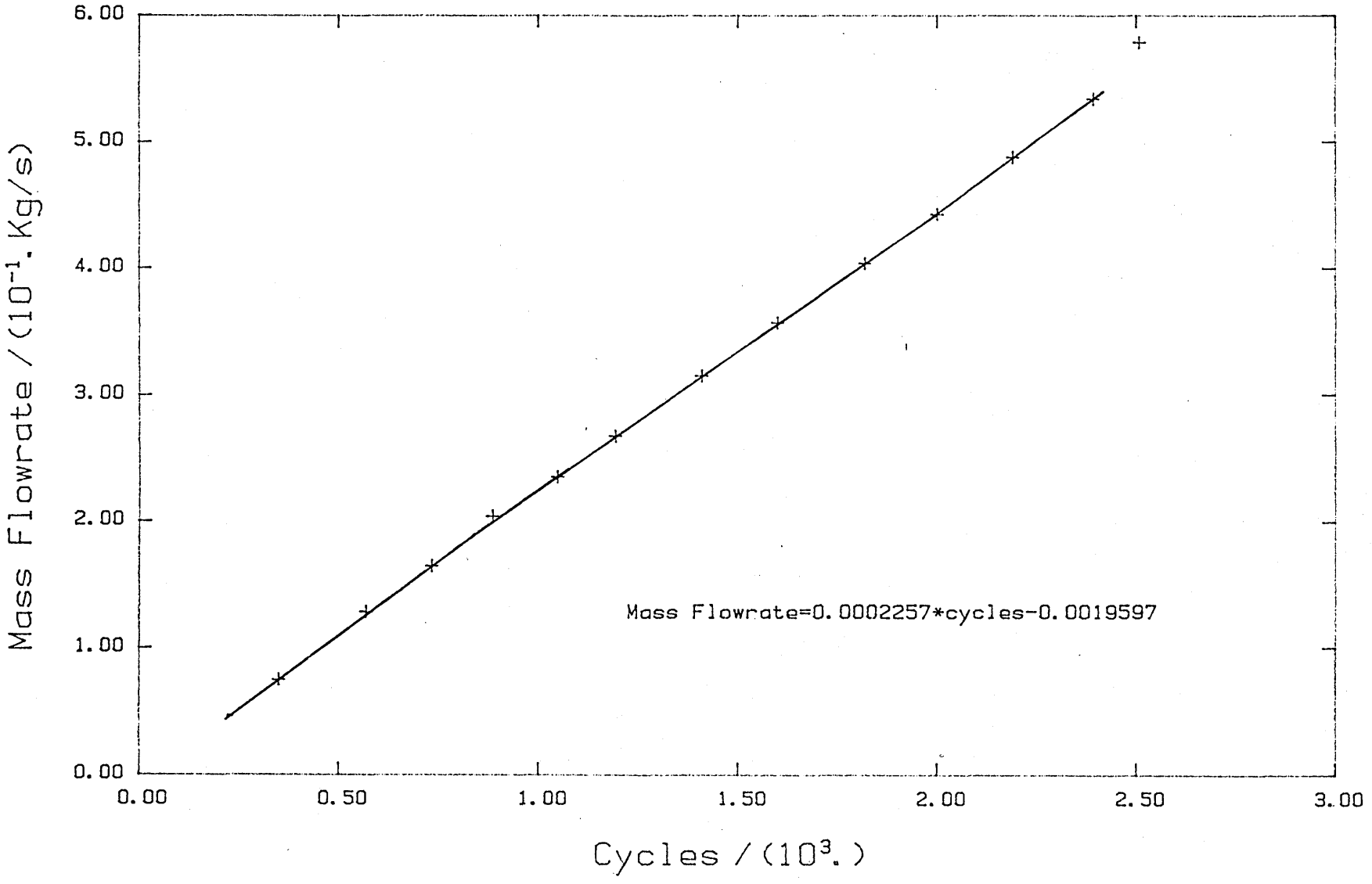

TURBINE METER CALIBRATION GRAPH

APPENDIX 1

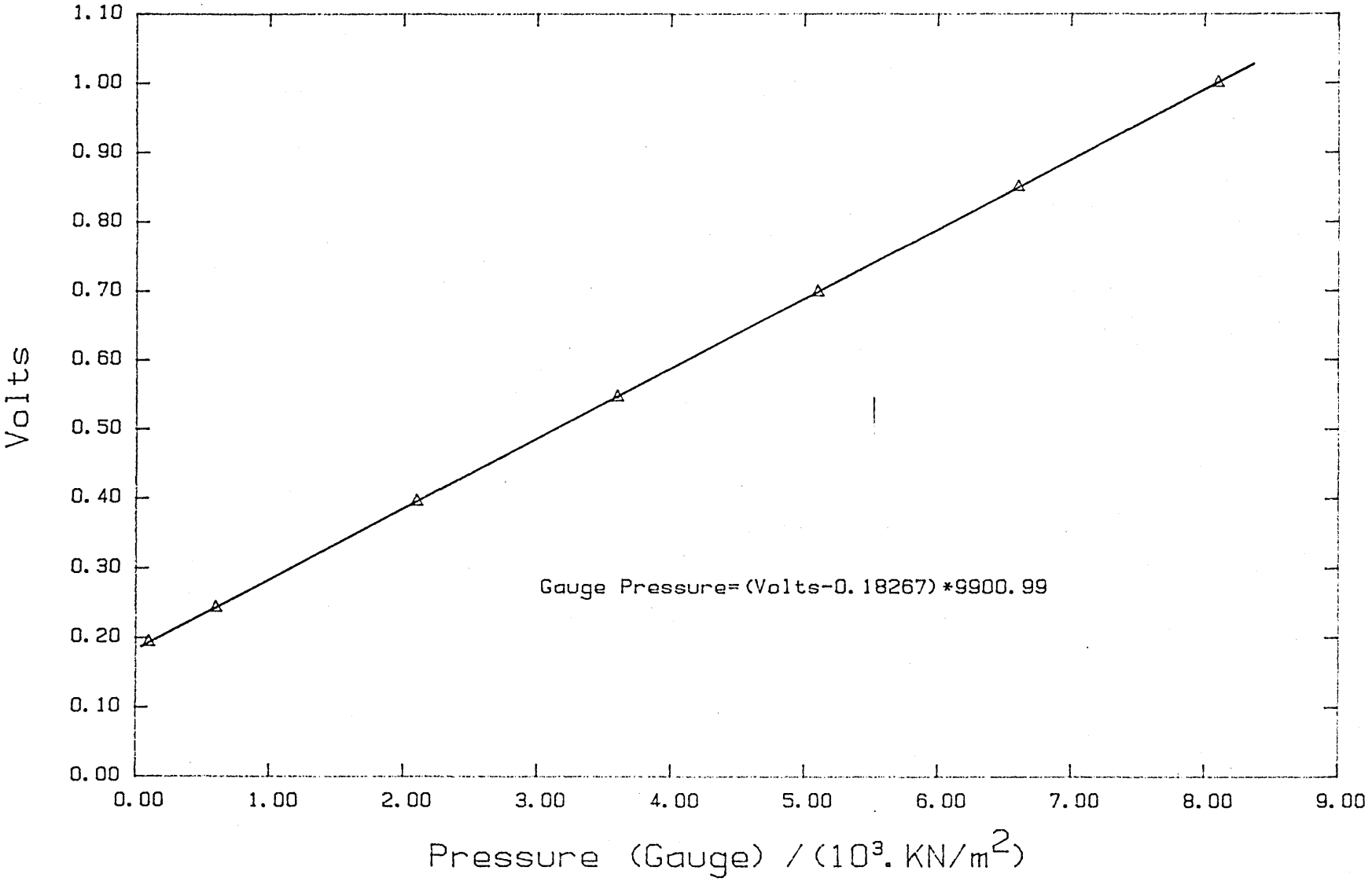

PRESSURE TRANSDUCER CALIBRATION GRAPH

APPENDIX 2

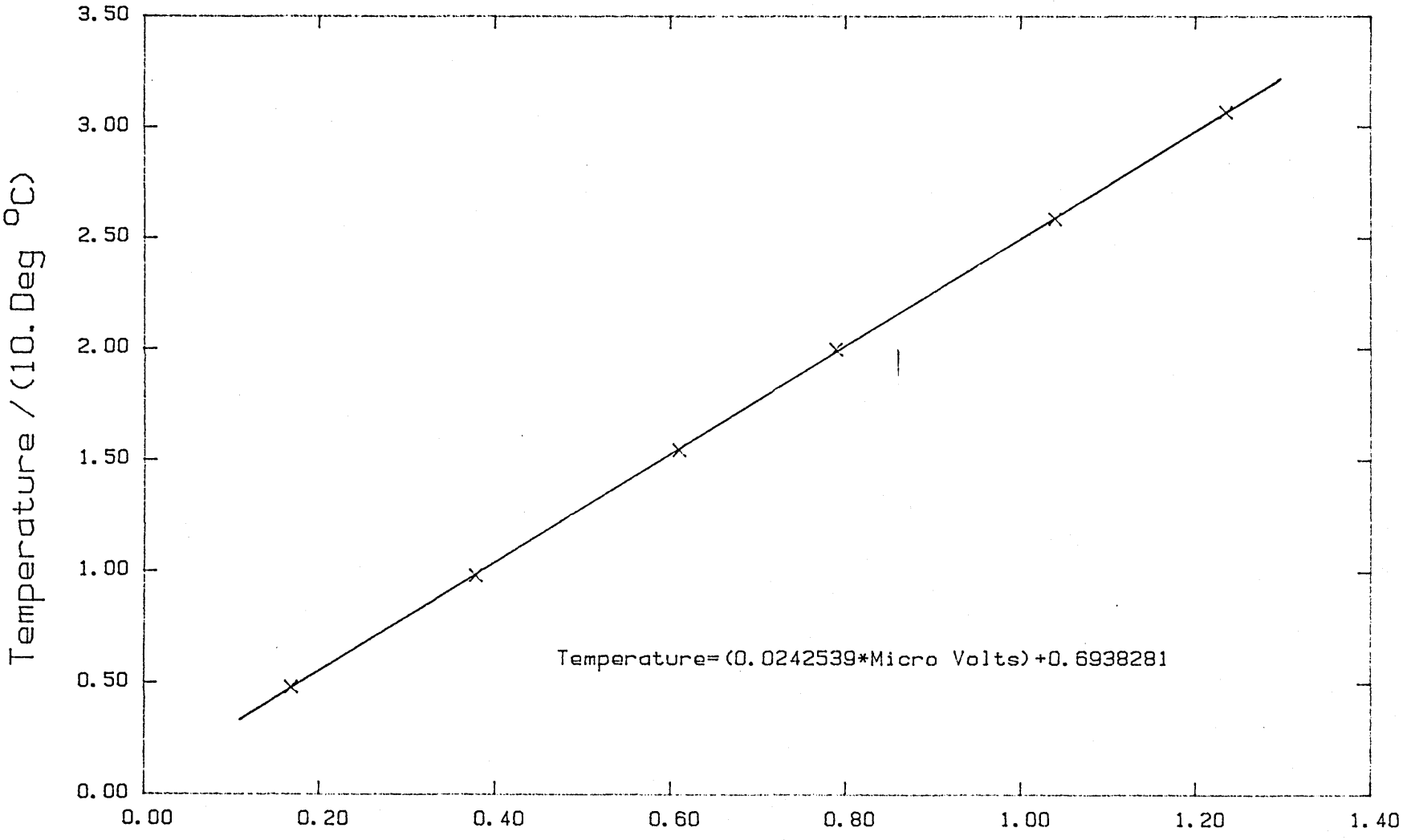

THERMOCOUPLE No1 CALIBRATION GRAPH

APPENDIX 3

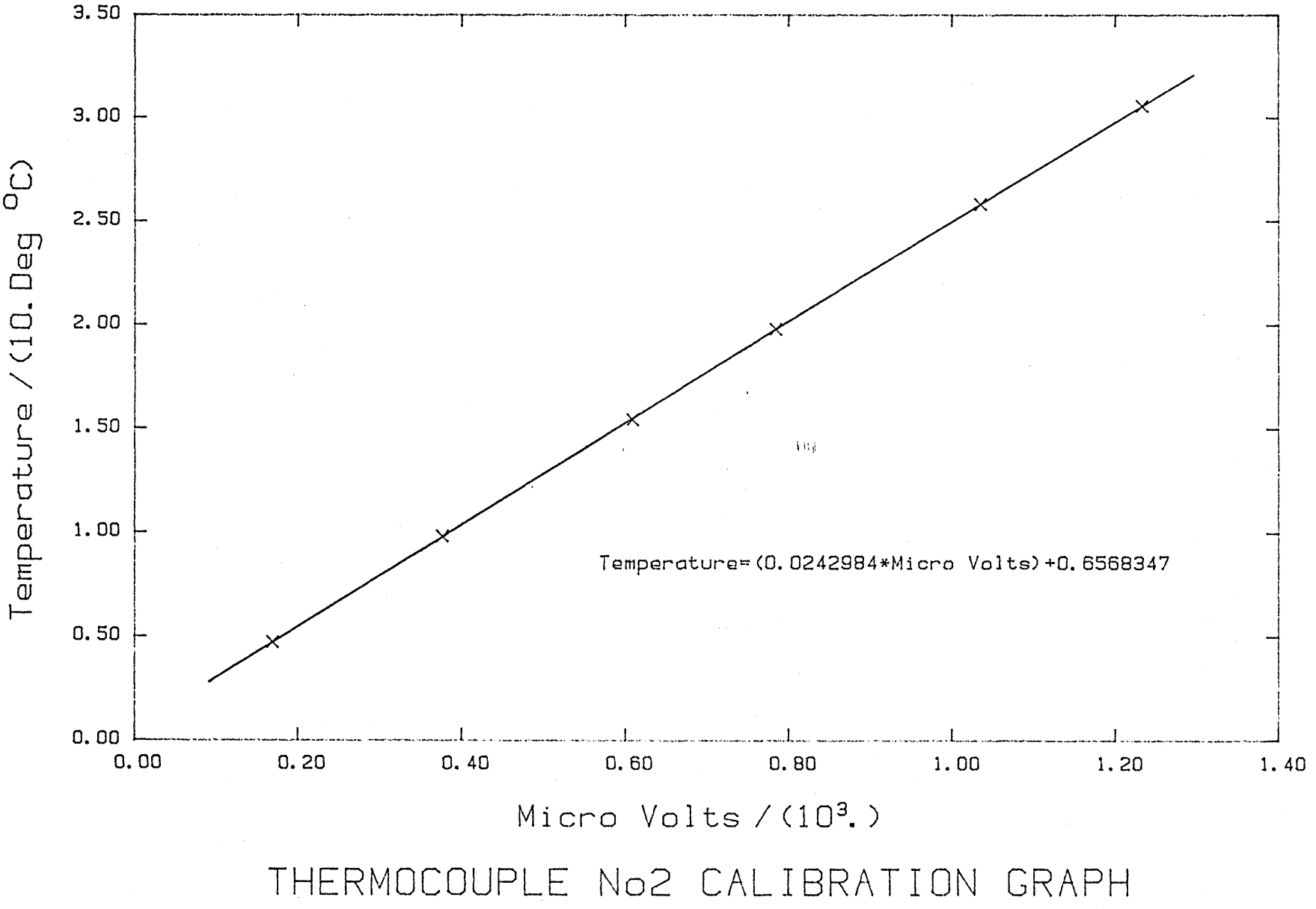

THERMOCOUPLE No2 CALIBRATION GRAPH

APPENDIX 4

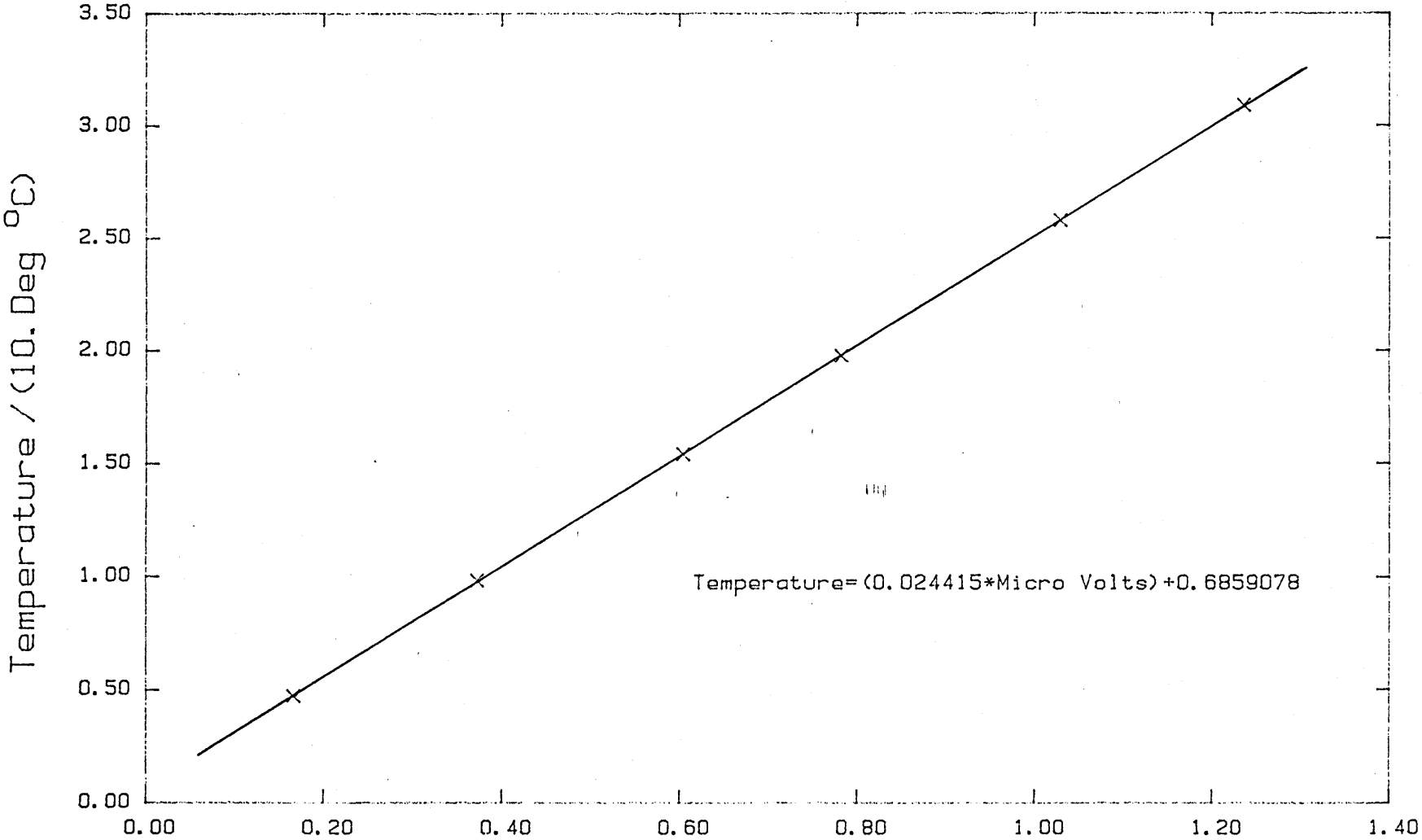

THERMOCOUPLE No3 CALIBRATION GRAPH

APPENDIX 5

Tube Bore = .0124

Mass Flux KG/M2.S	Qual (-)	L-M Param (-)	Mult Ratio C/M	T.P.Mult Meas (-)	T.P.Mult Calc (-)
1152.7	.174	3.275E-01	.924	61.50	56.84
1122.7	.170	3.293E-01	.911	62.70	57.13
1104.0	.153	3.516E-01	.894	60.02	53.68
1086.9	.136	3.793E-01	.922	53.99	49.79
1056.6	.120	4.095E-01	.965	48.00	46.32
1055.0	.100	4.657E-01	1.146	35.25	40.41
1024.4	.083	5.225E-01	1.068	33.74	36.03
985.5	.064	6.281E-01	1.121	26.69	29.92
979.2	.043	8.515E-01	1.016	21.48	21.82
960.6	.023	1.400E+00	.907	14.66	13.30
1968.5	.059	9.130E-01	1.420	11.06	15.71
1933.1	.056	9.350E-01	1.412	11.01	15.54
1924.2	.049	1.005E+00	1.465	9.95	14.57
1911.2	.043	1.093E+00	1.408	9.60	13.53
1910.2	.039	1.168E+00	1.381	9.20	12.70
1894.4	.033	1.310E+00	1.195	9.57	11.44
1855.5	.028	1.440E+00	1.252	8.44	10.56
1882.2	.021	1.763E+00	1.114	7.80	8.69
1865.6	.014	2.454E+00	.952	6.79	6.47
2864.9	.033	1.573E+00	1.412	5.34	7.53
2907.4	.029	1.698E+00	1.352	5.17	6.98
2813.8	.027	1.746E+00	1.513	4.62	7.00
2834.6	.024	1.944E+00	1.225	5.18	6.35
2824.5	.021	2.130E+00	1.211	4.86	5.89
2804.3	.018	2.320E+00	1.406	3.92	5.51
2782.0	.015	2.677E+00	1.069	4.61	4.93
2781.5	.011	3.253E+00	.954	4.42	4.22
2772.7	.008	4.341E+00	.867	3.93	3.40
3721.0	.017	2.828E+00	1.154	3.26	3.76
3723.9	.014	3.199E+00	1.063	3.24	3.44
3701.2	.012	3.425E+00	1.086	3.05	3.31
3749.0	.010	4.015E+00	.850	3.46	2.94
3746.4	.008	4.856E+00	.854	3.05	2.61
3705.7	.002	1.621E+01	.563	2.63	1.48
3709.7	.004	7.937E+00	.923	2.15	1.99
3708.0	.006	5.857E+00	.848	2.76	2.34
3716.1	.008	4.927E+00	.807	3.22	2.59
3710.6	.006	5.757E+00	.783	3.02	2.37
3777.9	.003	9.373E+00	.624	2.91	1.82
4587.2	.008	5.121E+00	.651	3.25	2.12
4599.1	.007	5.620E+00	.637	3.16	2.01
4625.1	.006	6.340E+00	.732	2.58	1.89
4570.5	.006	6.922E+00	.716	2.56	1.83
4576.9	.005	8.012E+00	.608	2.83	1.72
4547.5	.004	9.299E+00	.599	2.72	1.63

TWO-PHASE TEST RESULTS USING 'WHITE'S' EQUATION FOR SINGLE-PHASE FRICTION FACTOR (HTFS CORR)

TABLE 5.1

Tube Bore = .0124

Mass Flux KG/M2.S	Qual (-)	L-M Param (-)	Mult Ratio C/M	T.P.Mult Meas (-)	T.P.Mult Calc (-)
4554.4	.003	1.144E+01	.573	2.63	1.51
4559.4	.002	1.852E+01	.634	2.07	1.31
4566.6	.001	3.350E+01	.742	1.58	1.17
5516.7	.005	8.076E+00	.560	2.60	1.45
5504.3	.005	8.797E+00	.490	2.90	1.42
5537.6	.004	1.036E+01	.526	2.57	1.35
5476.1	.003	1.172E+01	.505	2.62	1.32
5461.0	.002	1.458E+01	.510	2.48	1.26
5468.8	.001	2.098E+01	.573	2.06	1.18
5508.6	.001	3.508E+01	.744	1.49	1.11

TABLE 5,1 (Cont'd)

Mass Flux KG/M2.S	Qual (-)	L-M Param (-)	Mult Ratio C/M	T.P.Mult Meas (-)	T.P.Mult Calc (-)
1152.7	.174	3.208E-01	.873	66.69	58.21
1122.7	.170	3.226E-01	.860	68.01	58.48
1104.0	.153	3.449E-01	.843	65.10	54.86
1086.9	.136	3.726E-01	.867	58.55	50.79
1056.6	.120	4.028E-01	.906	52.07	47.18
1055.0	.100	4.589E-01	1.074	38.23	41.05
1024.4	.083	5.159E-01	.998	36.60	36.53
985.5	.064	6.218E-01	1.044	28.96	30.24
979.2	.043	8.459E-01	.943	23.29	21.97
960.6	.023	1.398E+00	.838	15.90	13.32
1968.5	.059	9.028E-01	1.336	11.90	15.89
1933.1	.056	9.251E-01	1.327	11.84	15.71
1924.2	.049	9.952E-01	1.375	10.70	14.71
1911.2	.043	1.084E+00	1.320	10.33	13.64
1910.2	.039	1.160E+00	1.293	9.89	12.79
1894.4	.033	1.303E+00	1.117	10.29	11.50
1855.5	.028	1.434E+00	1.168	9.08	10.61
1882.2	.021	1.760E+00	1.038	8.39	8.70
1865.6	.014	2.458E+00	.885	7.30	6.46
2864.9	.033	1.562E+00	1.328	5.71	7.58
2907.4	.029	1.688E+00	1.270	5.53	7.02
2813.8	.027	1.736E+00	1.421	4.95	7.03
2834.6	.024	1.936E+00	1.149	5.55	6.37
2824.5	.021	2.124E+00	1.134	5.21	5.90
2804.3	.018	2.316E+00	1.316	4.20	5.52
2782.0	.015	2.677E+00	.998	4.94	4.93
2781.5	.011	3.260E+00	.890	4.73	4.21
2772.7	.008	4.363E+00	.807	4.20	3.39
3721.0	.017	2.825E+00	1.084	3.48	3.77
3723.9	.014	3.200E+00	.997	3.45	3.44
3701.2	.012	3.434E+00	1.019	3.25	3.31
3749.0	.010	4.033E+00	.798	3.68	2.94
3746.4	.008	4.886E+00	.800	3.24	2.60
3705.7	.002	1.646E+01	.526	2.80	1.47
3709.7	.004	8.016E+00	.862	2.29	1.98
3708.0	.006	5.899E+00	.794	2.94	2.33
3716.1	.008	4.953E+00	.755	3.43	2.59
3710.6	.006	5.796E+00	.732	3.22	2.36
3777.9	.003	9.478E+00	.583	3.10	1.81
4587.2	.008	5.151E+00	.613	3.44	2.11
4599.1	.007	5.658E+00	.599	3.35	2.01
4625.1	.006	6.392E+00	.689	2.73	1.88
4570.5	.006	6.985E+00	.673	2.71	1.83
4576.9	.005	8.097E+00	.572	2.99	1.71
4547.5	.004	9.411E+00	.563	2.88	1.62

TWO-PHASE RESULTS USING TEST EQUATION FOR SINGLE-PHASE FRICTION FACTOR (HTFS CORR)

TABLE 5.2

Mass Flux KG/M2.S	Qual (-)	L-M Param (-)	Mult Ratio C/M	T.P.Mult Meas (-)	T.P.Mult Calc (-)
4554.4	.003	1.160E+01	.538	2.79	1.50
4559.4	.002	1.885E+01	.596	2.19	1.31
4566.6	.001	3.423E+01	.698	1.67	1.17
5516.7	.005	8.158E+00	.529	2.74	1.45
5504.3	.005	8.894E+00	.463	3.06	1.42
5537.6	.004	1.049E+01	.497	2.71	1.35
5476.1	.003	1.188E+01	.477	2.76	1.32
5461.0	.002	1.481E+01	.482	2.61	1.26
5468.8	.001	2.137E+01	.542	2.18	1.18
5508.6	.001	3.588E+01	.703	1.57	1.10

TABLE 5,2 (Cont'd)

Tube Bore = .0077

Mass Flux KG/M2.S	Qual (-)	L-M Param (-)	Mult Ratio C/M	T.P.Mult Meas (-)	T.P.Mult Calc (-)
2617.7	.068	7.248E-01	.572	30.46	17.43
2615.6	.061	7.709E-01	.578	28.36	16.40
2584.8	.056	8.151E-01	.508	30.77	15.64
2559.4	.048	8.857E-01	.537	26.95	14.48
2565.6	.043	9.459E-01	.537	25.20	13.54
2567.0	.036	1.072E+00	.549	21.74	11.94
2542.0	.031	1.161E+00	.580	19.10	11.07
2562.0	.022	1.443E+00	.657	13.48	8.86
3510.5	.031	1.271E+00	.387	20.88	8.09
3491.0	.028	1.331E+00	.420	18.54	7.78
3477.1	.025	1.433E+00	.440	16.55	7.28
3452.5	.023	1.536E+00	.433	15.83	6.86
3491.6	.019	1.736E+00	.414	14.61	6.05
3472.0	.016	1.910E+00	.475	11.69	5.55
3446.5	.013	2.211E+00	.481	10.18	4.89
3445.0	.009	2.660E+00	.510	8.14	4.15
3391.5	.006	3.437E+00	.537	6.29	3.38
3404.8	.003	5.415E+00	.799	3.01	2.40
4453.7	.020	2.226E+00	.322	11.97	3.85
4429.8	.018	2.377E+00	.387	9.55	3.69
4442.1	.016	2.505E+00	.333	10.64	3.54
4417.8	.014	2.744E+00	.365	9.14	3.34
4425.1	.012	2.923E+00	.372	8.57	3.18
4415.8	.010	3.273E+00	.366	8.04	2.95
4385.1	.009	3.642E+00	.369	7.47	2.76
4414.1	.007	4.341E+00	.378	6.45	2.44
4373.2	.005	5.223E+00	.466	4.71	2.19
4352.3	.002	8.496E+00	.649	2.62	1.70
5258.9	.013	3.217E+00	.321	7.47	2.40
5256.7	.011	3.439E+00	.327	7.07	2.31
5275.3	.010	3.632E+00	.314	7.11	2.23
5279.3	.009	3.890E+00	.315	6.80	2.14
5277.6	.008	4.240E+00	.324	6.31	2.05
5258.5	.007	4.551E+00	.343	5.78	1.98
5253.3	.006	5.000E+00	.356	5.30	1.89
5265.9	.005	5.723E+00	.354	4.99	1.77
5233.7	.003	7.375E+00	.430	3.70	1.59
5273.5	.002	1.057E+01	.465	2.99	1.39
6184.6	.008	4.605E+00	.288	5.43	1.57
6351.2	.007	5.324E+00	.295	4.84	1.43
6266.3	.006	5.690E+00	.309	4.61	1.43
6289.3	.005	6.284E+00	.336	4.09	1.38
6246.2	.004	6.999E+00	.343	3.93	1.35
6258.9	.003	8.292E+00	.361	3.57	1.29
6413.6	.002	1.048E+01	.426	2.82	1.20

TWO-PHASE TEST RESULTS USING 'WHITE'S' EQUATION FOR SINGLE-PHASE FRICTION FACTOR (HTFS CORR)

TABLE 5.3

Tube Bore = .0077

Mass Flux KG/M2.S	Qual (-)	L-M Param (-)	Mult Ratio C/M	T.P.Mult Meas (-)	T.P.Mult Calc (-)
6257.6	.002	1.305E+01	.464	2.53	1.17

TABLE 5.3 (Cont'd)

Mass Flux KG/M2.S	Qual (-)	L-M Param (-)	Mult Ratio C/M	T.P.Mult Meas (-)	T.P.Mult Calc (-)
2617.7	.068	7.158E-01	.538	32.86	17.66
2615.6	.061	7.620E-01	.543	30.60	16.60
2584.8	.056	8.065E-01	.476	33.20	15.81
2559.4	.048	8.776E-01	.503	29.08	14.62
2565.6	.043	9.381E-01	.502	27.18	13.65
2567.0	.036	1.065E+00	.513	23.45	12.02
2542.0	.031	1.155E+00	.540	20.60	11.13
2562.0	.022	1.439E+00	.610	14.54	8.87
3510.5	.031	1.265E+00	.363	22.38	8.12
3491.0	.028	1.326E+00	.393	19.87	7.81
3477.1	.025	1.429E+00	.411	17.75	7.30
3452.5	.023	1.532E+00	.405	16.98	6.87
3491.6	.019	1.735E+00	.387	15.67	6.06
3472.0	.016	1.912E+00	.443	12.54	5.55
3446.5	.013	2.216E+00	.447	10.92	4.89
3445.0	.009	2.672E+00	.474	8.74	4.14
3391.5	.006	3.463E+00	.498	6.75	3.36
3404.8	.003	5.478E+00	.740	3.23	2.39
4453.7	.020	2.224E+00	.301	12.78	3.85
4429.8	.018	2.377E+00	.362	10.20	3.69
4442.1	.016	2.506E+00	.312	11.36	3.54
4417.8	.014	2.749E+00	.342	9.76	3.33
4425.1	.012	2.931E+00	.347	9.15	3.18
4415.8	.010	3.288E+00	.342	8.59	2.94
4385.1	.009	3.662E+00	.344	7.97	2.75
4414.1	.007	4.374E+00	.353	6.89	2.43
4373.2	.005	5.274E+00	.434	5.03	2.18
4352.3	.002	8.617E+00	.604	2.80	1.69
5258.9	.013	3.226E+00	.301	7.95	2.40
5256.7	.011	3.451E+00	.306	7.53	2.31
5275.3	.010	3.648E+00	.294	7.57	2.22
5279.3	.009	3.910E+00	.295	7.24	2.14
5277.6	.008	4.266E+00	.304	6.72	2.04
5258.5	.007	4.583E+00	.321	6.15	1.97
5253.3	.006	5.042E+00	.333	5.65	1.88
5265.9	.005	5.778E+00	.331	5.31	1.76
5233.7	.003	7.466E+00	.402	3.94	1.58
5273.5	.002	1.074E+01	.435	3.18	1.38
6184.6	.008	4.632E+00	.271	5.77	1.56
6351.2	.007	5.364E+00	.277	5.14	1.42
6266.3	.006	5.736E+00	.290	4.90	1.42
6289.3	.005	6.343E+00	.316	4.35	1.37
6246.2	.004	7.073E+00	.322	4.17	1.34
6258.9	.003	8.395E+00	.339	3.79	1.28
6413.6	.002	1.064E+01	.400	2.99	1.20

TWO-PHASE RESULTS USING TEST EQUATION FOR SINGLE-PHASE FRICTION FACTOR (HTFS CORR)

TABLE 5.4

Mass Flux KG/M2.S	Quality (-)	Flow Param (-)	Mass Ratio C/M	Pressure Meas (-)	Pressure Calc (-)
6257.6	.002	1.327E+01	.436	2.69	1.17

TABLE 5.4 (Cont'd)

Mass Flux KG/M2.S	Qual (-)	L-M Param (-)	Mult Ratio C/M	T.P.Mult Meas (-)	T.P.Mult Calc (-)
1063.1	.124	4.279E-01	1.059	40.95	43.37
1044.4	.110	4.418E-01	1.114	38.25	42.59
1038.9	.098	4.704E-01	1.061	37.71	40.02
1013.7	.088	4.925E-01	1.099	34.99	38.46
1002.8	.077	5.341E-01	1.283	27.59	35.39
999.0	.064	5.925E-01	1.269	24.97	31.69
952.5	.053	6.413E-01	1.283	22.81	29.26
954.3	.039	7.980E-01	1.305	17.74	23.14
962.2	.026	1.020E+00	1.238	14.22	17.60
943.7	.013	1.610E+00	1.068	10.06	10.74
1401.8	.072	6.876E-01	1.035	23.41	24.24
1381.0	.068	7.113E-01	1.064	22.19	23.62
1374.4	.062	7.459E-01	1.102	20.51	22.60
1360.0	.054	8.003E-01	1.049	20.18	21.17
1348.2	.047	8.656E-01	1.078	18.21	19.64
1340.4	.039	9.594E-01	1.159	15.29	17.73
1336.5	.031	1.101E+00	1.074	14.34	15.40
1327.0	.024	1.321E+00	1.153	11.15	12.85
1315.9	.016	1.694E+00	1.137	8.76	9.96
1295.8	.007	5.988E+00	.596	5.64	3.36
1729.9	.049	1.009E+00	.975	15.54	15.15
1711.2	.046	1.046E+00	1.002	14.70	14.73
1719.1	.041	1.107E+00	1.060	13.17	13.96
1719.2	.038	1.160E+00	1.002	13.34	13.37
1698.5	.035	1.206E+00	1.082	11.98	12.97
1691.2	.031	1.304E+00	1.029	11.72	12.06
1695.9	.027	1.406E+00	1.038	10.80	11.21
1692.9	.023	1.553E+00	.972	10.50	10.20
1674.5	.019	1.736E+00	1.109	8.29	9.19
1676.8	.014	2.075E+00	1.076	7.17	7.71
1662.4	.008	3.201E+00	.965	5.39	5.20
2083.3	.034	1.422E+00	.954	10.48	10.00
2058.3	.032	1.474E+00	.899	10.84	9.75
2069.5	.027	1.616E+00	.956	9.38	8.96
2049.8	.025	1.684E+00	.933	9.33	8.70
2062.9	.021	1.857E+00	.984	8.08	7.95
2048.9	.018	2.024E+00	1.021	7.23	7.38
2024.6	.016	2.158E+00	.907	7.72	7.01
2027.6	.013	2.440E+00	.904	6.93	6.27
2032.7	.010	2.803E+00	.986	5.60	5.52
1993.6	.006	4.077E+00	1.000	4.06	4.06
2415.5	.024	1.915E+00	.876	8.05	7.05
2420.8	.023	1.986E+00	.886	7.72	6.84
2405.8	.021	2.078E+00	.897	7.37	6.61
2410.0	.019	2.195E+00	.914	6.90	6.31

LARGE BORE COIL DATA - HTFS CORRELATION

TABLE 5,5

Mass Flux KG/M2.S	Qual (-)	L-M Param (-)	Mult Ratio C/M	T.P.Mult Meas (-)	T.P.Mult Calc (-)
2411.9	.018	2.324E+00	.893	6.74	6.01
2398.8	.016	2.458E+00	.885	6.51	5.76
2391.4	.014	2.667E+00	.946	5.70	5.39
2366.1	.011	2.987E+00	.852	5.78	4.93
2379.9	.009	3.440E+00	.976	4.48	4.37
2356.4	.007	4.145E+00	.896	4.24	3.80
2380.6	.004	1.248E+01	.525	3.61	1.89

TABLE 5.5 (Cont'd)

Mass Flux KG/M2.S	Qual (-)	L-M Param (-)	Mult Ratio C/M	T.P.Mult Meas (-)	T.P.Mult Calc (-)
2507.8	.038	1.244E+00	.898	11.51	10.34
2524.5	.035	1.314E+00	.949	10.32	9.80
2491.1	.032	1.250E+00	.866	12.08	10.46
2494.1	.027	1.537E+00	.941	9.11	8.57
2502.1	.023	1.709E+00	.990	7.86	7.77
2475.7	.018	1.960E+00	1.132	6.10	6.90
2450.7	.014	2.317E+00	1.041	5.72	5.96
2454.2	.009	7.515E+00	.600	4.11	2.46
2447.6	.005	9.129E+00	.898	2.40	2.15
2963.8	.026	1.762E+00	.866	7.76	6.72
2958.9	.023	1.877E+00	.882	7.25	6.40
2979.4	.020	2.040E+00	.856	6.93	5.93
2961.5	.018	2.210E+00	.905	6.16	5.58
2944.0	.015	2.437E+00	.908	5.68	5.16
2959.0	.012	2.836E+00	.948	4.78	4.54
2969.8	.009	3.285E+00	.973	4.12	4.01
2946.2	.006	9.992E+00	.624	3.14	1.96
2919.9	.004	1.152E+01	.843	2.16	1.82
3438.0	.019	2.320E+00	.821	5.80	4.76
3420.9	.017	2.496E+00	.786	5.74	4.52
3422.2	.015	2.703E+00	.850	5.01	4.25
3380.8	.012	3.033E+00	.851	4.62	3.93
3401.4	.010	3.487E+00	.917	3.84	3.52
3404.9	.008	3.901E+00	.989	3.27	3.24
3417.9	.006	1.152E+01	.562	3.09	1.74
3422.2	.005	1.231E+01	.663	2.53	1.68
3388.1	.003	1.376E+01	.642	2.49	1.60
3891.5	.014	3.077E+00	.762	4.51	3.43
3919.4	.013	3.303E+00	.775	4.19	3.25
3918.4	.011	3.560E+00	.797	3.88	3.09
3913.4	.010	3.823E+00	.799	3.70	2.95
3915.5	.008	4.344E+00	.819	3.32	2.72
3883.0	.007	4.697E+00	.835	3.12	2.60
3872.5	.006	1.364E+01	.614	2.51	1.54
3862.2	.004	1.477E+01	.718	2.09	1.50
3862.4	.003	1.614E+01	.697	2.08	1.45
4367.3	.010	4.038E+00	.722	3.56	2.57
4334.5	.009	4.279E+00	.737	3.39	2.50
4389.5	.008	4.832E+00	.766	3.01	2.30
4364.1	.006	5.518E+00	.788	2.73	2.15
4313.1	.005	1.558E+01	.558	2.53	1.41
4362.7	.004	1.736E+01	.612	2.22	1.36
4352.7	.003	1.945E+01	.721	1.83	1.32
4805.5	.008	4.998E+00	.702	2.94	2.06
4772.1	.007	5.403E+00	.714	2.80	2.00

SMALL BORE COIL DATA - HTFS CORRELATION

TABLE 5,6

Mass Flux KG/M2.S	Qual (-)	L-M Param (-)	Mult Ratio C/M	T.P.Mult Meas (-)	T.P.Mult Calc (-)
4787.0	.006	5.913E+00	.697	2.74	1.91
4806.9	.006	6.442E+00	.684	2.67	1.83
4788.6	.005	1.823E+01	.591	2.18	1.29
4821.1	.004	1.983E+01	.636	1.99	1.26
4735.8	.003	2.134E+01	.698	1.79	1.25

TABLE 5.6 (Cont'd)

Mass Flux KG/M2.S	Qual (-)	L-M Param (-)	Adit Ratio C/M	T.T.Adit Meas (-)	Calc (-)
1063.1	.124	4.398E-01	.918	45.81	42.08
1044.4	.110	4.533E-01	.968	42.78	41.41
1038.9	.098	4.820E-01	.924	42.19	38.98
1013.7	.088	5.038E-01	.959	39.13	37.53
1002.8	.077	5.454E-01	1.122	30.85	34.61
999.0	.064	6.036E-01	1.112	27.94	31.08
952.5	.053	6.516E-01	1.129	25.50	28.78
954.3	.039	8.076E-01	1.153	19.83	22.86
962.2	.026	1.027E+00	1.099	15.90	17.48
943.7	.013	1.606E+00	.957	11.25	10.76
1401.8	.072	7.012E-01	.898	26.43	23.75
1381.0	.068	7.248E-01	.925	25.04	23.16
1374.4	.062	7.592E-01	.959	23.14	22.19
1360.0	.054	8.132E-01	.915	22.77	20.83
1348.2	.047	8.781E-01	.942	20.54	19.35
1340.4	.039	9.708E-01	1.015	17.25	17.52
1336.5	.031	1.111E+00	.944	16.18	15.27
1327.0	.024	1.328E+00	1.016	12.58	12.78
1315.9	.016	1.694E+00	1.008	9.88	9.95
1295.8	.007	5.638E+00	.551	6.36	3.51
1729.9	.049	1.024E+00	.846	17.65	14.93
1711.2	.046	1.061E+00	.871	16.69	14.53
1719.1	.041	1.121E+00	.923	14.94	13.79
1719.2	.038	1.173E+00	.873	15.14	13.22
1698.5	.035	1.218E+00	.944	13.60	12.83
1691.2	.031	1.316E+00	.899	13.30	11.95
1695.9	.027	1.416E+00	.908	12.26	11.13
1692.9	.023	1.561E+00	.852	11.92	10.15
1674.5	.019	1.741E+00	.975	9.41	9.17
1676.8	.014	2.073E+00	.950	8.13	7.72
1662.4	.008	3.172E+00	.857	6.12	5.24
2083.3	.034	1.436E+00	.829	11.96	9.91
2058.3	.032	1.487E+00	.781	12.37	9.67
2069.5	.027	1.628E+00	.832	10.71	8.91
2049.8	.025	1.694E+00	.813	10.64	8.65
2062.9	.021	1.864E+00	.859	9.22	7.92
2048.9	.018	2.028E+00	.894	8.25	7.37
2024.6	.016	2.158E+00	.795	8.81	7.00
2027.6	.013	2.435E+00	.794	7.90	6.28
2032.7	.010	2.788E+00	.868	6.39	5.54
1993.6	.006	4.032E+00	.885	4.63	4.10
2415.5	.024	1.925E+00	.761	9.22	7.02
2420.8	.023	1.995E+00	.770	8.84	6.81
2405.8	.021	2.085E+00	.780	8.44	6.59
2410.0	.019	2.200E+00	.796	7.91	6.30

TEST SINGLE-PHASE CORRELATION USED-
HTFS CORRELATION

TABLE 5.7

Mass Flux KG/M2.S	Quality (-)	Lockhart Param (-)	Void Ratio C/M	Void Meas (-)	Void Calc (-)
2411.9	.018	2.326E+00	.778	7.72	6.01
2398.8	.016	2.458E+00	.772	7.45	5.76
2391.4	.014	2.662E+00	.827	6.53	5.40
2366.1	.011	2.975E+00	.746	6.63	4.95
2379.9	.009	3.415E+00	.856	5.13	4.39
2356.4	.007	4.106E+00	.789	4.85	3.83
2380.6	.004	1.167E+01	.474	4.13	1.96

TABLE 5.7 (Cont'd)

Mass Flux KG/M2.S	Qual (-)	L-M Param (-)	Mult Ratio C/M	T.P.Mult Meas (-)	T.P.Mult Calc (-)
2507.8	.038	1.258E+00	.753	13.59	10.23
2524.5	.035	1.328E+00	.796	12.19	9.71
2491.1	.032	1.261E+00	.727	14.26	10.38
2494.1	.027	1.548E+00	.792	10.75	8.52
2502.1	.023	1.717E+00	.835	9.28	7.74
2475.7	.018	1.963E+00	.958	7.20	6.89
2450.7	.014	2.312E+00	.884	6.76	5.97
2454.2	.009	6.917E+00	.534	4.85	2.59
2447.6	.005	8.403E+00	.796	2.83	2.25
2963.8	.026	1.775E+00	.726	9.19	6.68
2958.9	.023	1.886E+00	.741	8.60	6.37
2979.4	.020	2.047E+00	.720	8.22	5.92
2961.5	.018	2.213E+00	.763	7.30	5.57
2944.0	.015	2.436E+00	.766	6.73	5.16
2959.0	.012	2.826E+00	.802	5.67	4.55
2969.8	.009	3.263E+00	.824	4.89	4.03
2946.2	.006	9.175E+00	.549	3.73	2.05
2919.9	.004	1.058E+01	.740	2.56	1.89
3438.0	.019	2.326E+00	.689	6.89	4.75
3420.9	.017	2.499E+00	.661	6.83	4.51
3422.2	.015	2.701E+00	.715	5.95	4.26
3380.8	.012	3.024E+00	.717	5.49	3.94
3401.4	.010	3.467E+00	.774	4.56	3.54
3404.9	.008	3.870E+00	.836	3.89	3.26
3417.9	.006	1.056E+01	.491	3.67	1.80
3422.2	.005	1.128E+01	.578	3.01	1.74
3388.1	.003	1.261E+01	.559	2.97	1.66
3891.5	.014	3.075E+00	.639	5.37	3.43
3919.4	.013	3.297E+00	.651	5.00	3.25
3918.4	.011	3.547E+00	.670	4.62	3.10
3913.4	.010	3.805E+00	.672	4.41	2.96
3915.5	.008	4.312E+00	.690	3.96	2.73
3883.0	.007	4.654E+00	.704	3.72	2.62
3872.5	.006	1.249E+01	.532	2.99	1.59
3862.2	.004	1.353E+01	.621	2.49	1.54
3862.4	.003	1.478E+01	.602	2.48	1.49
4367.3	.010	4.017E+00	.605	4.26	2.58
4334.5	.009	4.253E+00	.618	4.06	2.51
4389.5	.008	4.791E+00	.643	3.60	2.32
4364.1	.006	5.457E+00	.663	3.27	2.17
4313.1	.005	1.425E+01	.479	3.02	1.45
4362.7	.004	1.588E+01	.525	2.65	1.39
4352.7	.003	1.779E+01	.616	2.19	1.35
4805.5	.008	4.958E+00	.588	3.53	2.07
4772.1	.007	5.351E+00	.598	3.36	2.01

TEST SINGLE-PHASE CORRELATION USED - HTFS CORRELATION

TABLE 5.8

Mass Flux KG/M2.S	Qual (-)	L-M Param (-)	Mult Ratio C/M	T.P.Mult Meas (-)	T.P.Mult Calc (-)
4787.0	.006	5.847E+00	.585	3.29	1.92
4806.9	.006	6.360E+00	.574	3.21	1.84
4788.6	.005	1.664E+01	.503	2.62	1.32
4821.1	.004	1.811E+01	.541	2.38	1.29
4735.8	.003	1.949E+01	.594	2.15	1.28

TABLE 5.8 (Cont'd)

Mass Flux KG/M2.S	Qual (-)	L-M Param (-)	Mult Ratio C/M	T.P.Mult Meas (-)	T.P.Mult Calc (-)
1152.7	.174	3.275E-01	.924	61.50	56.84
1122.7	.170	3.293E-01	.911	62.70	57.13
1104.0	.153	3.516E-01	.894	60.02	53.68
1086.9	.136	3.793E-01	.922	53.99	49.79
1056.6	.120	4.095E-01	.965	48.00	46.32
1055.0	.100	4.657E-01	1.146	35.25	40.41
1024.4	.083	5.225E-01	1.068	33.74	36.03
985.5	.064	6.281E-01	1.121	26.69	29.92
979.2	.043	8.515E-01	1.016	21.48	21.82
960.6	.023	1.400E+00	.907	14.66	13.30
1968.5	.059	9.130E-01	1.420	11.06	15.71
1933.1	.056	9.350E-01	1.412	11.01	15.54
1924.2	.049	1.005E+00	1.465	9.95	14.57
1911.2	.043	1.093E+00	1.408	9.60	13.53
1910.2	.039	1.168E+00	1.381	9.20	12.70
1894.4	.033	1.310E+00	1.195	9.57	11.44
1855.5	.028	1.440E+00	1.252	8.44	10.56
1882.2	.021	1.763E+00	1.114	7.80	8.69
1865.6	.014	2.454E+00	.952	6.79	6.47
2864.9	.033	1.573E+00	1.412	5.34	7.53
2907.4	.029	1.698E+00	1.352	5.17	6.98
2813.8	.027	1.746E+00	1.513	4.62	7.00
2834.6	.024	1.944E+00	1.225	5.18	6.35
2824.5	.021	2.130E+00	1.211	4.86	5.89
2804.3	.018	2.320E+00	1.406	3.92	5.51
2782.0	.015	2.677E+00	1.069	4.61	4.93
2781.5	.011	3.253E+00	.954	4.42	4.22
2772.7	.008	4.341E+00	.867	3.93	3.40
3721.0	.017	2.828E+00	1.154	3.26	3.76
3723.9	.014	3.199E+00	1.063	3.24	3.44
3701.2	.012	3.425E+00	1.086	3.05	3.31
3749.0	.010	4.015E+00	.850	3.46	2.94
3746.4	.008	4.856E+00	.854	3.05	2.61
3705.7	.002	1.621E+01	.563	2.63	1.48
3709.7	.004	7.937E+00	.923	2.15	1.99
3708.0	.006	5.857E+00	.848	2.76	2.34
3716.1	.008	4.927E+00	.807	3.22	2.59
3710.6	.006	5.757E+00	.783	3.02	2.37
3777.9	.003	9.373E+00	1.035	2.91	3.01
4587.2	.008	5.121E+00	1.157	3.25	3.76
4599.1	.007	5.620E+00	1.133	3.16	3.58
4625.1	.006	6.340E+00	1.305	2.58	3.37
4570.5	.006	6.922E+00	1.270	2.56	3.26
4576.9	.005	8.012E+00	1.080	2.83	3.05
4547.5	.004	9.299E+00	1.062	2.72	2.88

LARGE BORE STRAIGHT TUBE DATA - TEST CORRELATION ON HTFS CORRELATION

TABLE 5.9

Mass Flux KG/M2.S	Void (-)	Param (-)	Ratio C/M	Meas (-)	Calc (-)
4554.4	.003	1.144E+01	1.016	2.63	2.67
4559.4	.002	1.852E+01	1.125	2.07	2.33
4566.6	.001	3.350E+01	1.316	1.58	2.08
5516.7	.005	8.076E+00	1.065	2.60	2.76
5504.3	.005	8.797E+00	.930	2.90	2.70
5537.6	.004	1.036E+01	1.001	2.57	2.57
5476.1	.003	1.172E+01	.958	2.62	2.51
5461.0	.002	1.458E+01	.966	2.48	2.39
5468.8	.001	2.098E+01	1.086	2.06	2.24

TABLE 5.9 (Cont'd)

Tube Bore = .0077

Mass Flux KG/M2.S	Qual (-)	L-M Param (-)	Mult Ratio C/M	T.P.Mult Meas (-)	T.P.Mult Calc (-)
2617.7	.068	7.248E-01	1.007	30.46	30.68
2615.6	.061	7.709E-01	1.018	28.36	28.86
2584.8	.056	8.151E-01	.890	30.77	27.39
2559.4	.048	8.857E-01	.938	26.95	25.28
2565.6	.043	9.459E-01	.939	25.20	23.66
2567.0	.036	1.072E+00	.960	21.74	20.87
2542.0	.031	1.161E+00	1.010	19.10	19.28
2562.0	.022	1.443E+00	1.147	13.48	15.47
3510.5	.031	1.271E+00	.759	20.88	15.85
3491.0	.028	1.331E+00	.820	18.54	15.21
3477.1	.025	1.433E+00	.858	16.55	14.20
3452.5	.023	1.536E+00	.843	15.83	13.35
3491.6	.019	1.736E+00	.810	14.61	11.83
3472.0	.016	1.910E+00	.927	11.69	10.84
3446.5	.013	2.211E+00	.935	10.18	9.52
3445.0	.009	2.660E+00	.992	8.14	8.08
3391.5	.006	3.437E+00	1.039	6.29	6.54
3404.8	.003	5.415E+00	1.548	3.01	4.66
4453.7	.020	2.226E+00	.689	11.97	8.25
4429.8	.018	2.377E+00	.827	9.55	7.90
4442.1	.016	2.505E+00	.713	10.64	7.59
4417.8	.014	2.744E+00	.780	9.14	7.13
4425.1	.012	2.923E+00	.795	8.57	6.81
4415.8	.010	3.273E+00	.782	8.04	6.29
4385.1	.009	3.642E+00	.786	7.47	5.87
4414.1	.007	4.341E+00	.808	6.45	5.21
4373.2	.005	5.223E+00	.992	4.71	4.67
4352.3	.002	8.496E+00	1.378	2.62	3.62
5258.9	.013	3.217E+00	.734	7.47	5.49
5256.7	.011	3.439E+00	.747	7.07	5.28
5275.3	.010	3.632E+00	.718	7.11	5.10
5279.3	.009	3.890E+00	.722	6.80	4.91
5277.6	.008	4.240E+00	.742	6.31	4.69
5258.5	.007	4.551E+00	.784	5.78	4.53
5253.3	.006	5.000E+00	.815	5.30	4.32
5265.9	.005	5.723E+00	.810	4.99	4.04
5233.7	.003	7.375E+00	.981	3.70	3.63
5273.5	.002	1.057E+01	1.065	2.99	3.18
6184.6	.008	4.605E+00	.703	5.43	3.81
6351.2	.007	5.324E+00	.725	4.84	3.51
6266.3	.006	5.690E+00	.757	4.61	3.49
6289.3	.005	6.284E+00	.825	4.09	3.38
6246.2	.004	6.999E+00	.839	3.93	3.30
6258.9	.003	8.292E+00	.884	3.57	3.15
6413.6	.002	1.048E+01	1.053	2.82	2.97

SMALL BORE STRAIGHT TUBE DATA - TEST CORRELATION ON HTFS CORRELATION

TABLE 5.10

Tube Bore = .0124 Coil Mean Diameter =.2739

Mass Flux KG/M2.S	Qual (-)	L-M Param (-)	Mult Ratio C/M	T.P.Mult Meas (-)	T.P.Mult Calc (-)
1063.1	.124	4.398E-01	.918	45.81	42.08
1044.4	.110	4.533E-01	.968	42.78	41.41
1038.9	.098	4.820E-01	.924	42.19	38.98
1013.7	.088	5.038E-01	.959	39.13	37.53
1002.8	.077	5.454E-01	1.122	30.85	34.61
999.0	.064	6.036E-01	1.112	27.94	31.08
952.5	.053	6.516E-01	1.129	25.50	28.78
954.3	.039	8.076E-01	1.153	19.83	22.86
962.2	.026	1.027E+00	1.099	15.90	17.48
943.7	.013	1.606E+00	.957	11.25	10.76
1401.8	.072	7.012E-01	.898	26.43	23.75
1381.0	.068	7.248E-01	.925	25.04	23.16
1374.4	.062	7.592E-01	.959	23.14	22.19
1360.0	.054	8.132E-01	.915	22.77	20.83
1348.2	.047	8.781E-01	.942	20.54	19.35
1340.4	.039	9.708E-01	1.015	17.25	17.52
1336.5	.031	1.111E+00	.944	16.18	15.27
1327.0	.024	1.328E+00	1.016	12.58	12.78
1315.9	.016	1.694E+00	1.008	9.88	9.95
1295.8	.007	5.638E+00	.551	6.36	3.51
1729.9	.049	1.024E+00	.846	17.65	14.93
1711.2	.046	1.061E+00	.871	16.69	14.53
1719.1	.041	1.121E+00	.923	14.94	13.79
1719.2	.038	1.173E+00	.873	15.14	13.22
1698.5	.035	1.218E+00	.944	13.60	12.83
1691.2	.031	1.316E+00	.899	13.30	11.95
1695.9	.027	1.416E+00	.908	12.26	11.13
1692.9	.023	1.561E+00	.852	11.92	10.15
1674.5	.019	1.741E+00	.975	9.41	9.17
1676.8	.014	2.073E+00	.950	8.13	7.72
1662.4	.008	3.172E+00	.857	6.12	5.24
2083.3	.034	1.436E+00	.923	11.96	11.04
2058.3	.032	1.487E+00	.867	12.37	10.73
2069.5	.027	1.628E+00	.925	10.71	9.90
2049.8	.025	1.694E+00	.901	10.64	9.59
2062.9	.021	1.864E+00	.954	9.22	8.79
2048.9	.018	2.028E+00	.990	8.25	8.17
2024.6	.016	2.158E+00	.878	8.81	7.73
2027.6	.013	2.435E+00	.877	7.90	6.93
2032.7	.010	2.788E+00	.959	6.39	6.13
1993.6	.006	4.032E+00	.885	4.63	4.10
2415.5	.024	1.925E+00	.888	9.22	8.19
2420.8	.023	1.995E+00	.900	8.84	7.96
2405.8	.021	2.085E+00	.910	8.44	7.68
2410.0	.019	2.200E+00	.930	7.91	7.35

LARGE BORE COILED TUBE DATA - TEST CORRELATION ON HTFS CORRELATION

TABLE 5.11

Tube Bore = .0124 Coil Mean Diameter =.2739

Mass Flux KG/M2.S	Qual (-)	L-M Param (-)	Mult Ratio C/M	T.P.Mult Meas (-)	T.P.Mult Calc (-)
2411.9	.018	2.328E+00	.909	7.72	7.01
2398.8	.016	2.458E+00	.900	7.45	6.71
2391.4	.014	2.662E+00	.963	6.53	6.28
2366.1	.011	2.975E+00	.866	6.63	5.74
2379.9	.009	3.415E+00	.996	5.13	5.11
2356.4	.007	4.105E+00	.914	4.85	4.43

TABLE 5,11 (Cont'd)

Tube Bore = .0077 Coil Mean Diameter =.0745

Mass Flux KG/M2.S	Qual (-)	L-M Param (-)	Mult Ratio C/M	T.P.Mult Meas (-)	T.P.Mult Calc (-)
2507.8	.038	1.258E+00	1.050	13.59	14.27
2524.5	.035	1.328E+00	1.113	12.19	13.56
2491.1	.032	1.261E+00	1.012	14.26	14.44
2494.1	.027	1.548E+00	1.103	10.75	11.86
2502.1	.023	1.717E+00	1.163	9.28	10.79
2475.7	.018	1.963E+00	1.330	7.20	9.57
2450.7	.014	2.312E+00	1.223	6.76	8.26
2454.2	.009	6.917E+00	.740	4.85	3.59
2447.6	.005	8.403E+00	1.102	2.83	3.12
2963.8	.026	1.775E+00	1.069	9.19	9.83
2956.9	.023	1.886E+00	1.090	8.60	9.37
2979.4	.020	2.047E+00	1.062	8.22	8.73
2961.5	.018	2.213E+00	1.123	7.30	8.20
2944.0	.015	2.436E+00	1.126	6.73	7.58
2959.0	.012	2.825E+00	1.180	5.67	6.69
2969.8	.009	3.263E+00	1.215	4.89	5.94
2946.2	.006	9.175E+00	.807	3.73	3.01
2919.9	.004	1.058E+01	1.084	2.56	2.77
3438.0	.019	2.326E+00	1.065	6.89	7.34
3420.9	.017	2.499E+00	1.019	6.83	6.96
3422.2	.015	2.701E+00	1.103	5.95	6.57
3380.8	.012	3.024E+00	1.102	5.49	6.05
3401.4	.010	3.467E+00	1.193	4.56	5.45
3404.9	.008	3.870E+00	1.288	3.89	5.02
3417.5	.006	1.056E+01	.758	3.57	2.78
3422.2	.005	1.120E+01	.892	3.01	2.69
3388.1	.003	1.261E+01	.859	2.97	2.55
3891.5	.014	3.075E+00	1.029	5.37	5.53
3919.4	.013	3.297E+00	1.050	5.00	5.25
3918.4	.011	3.547E+00	1.081	4.62	5.00
3913.4	.010	3.805E+00	1.084	4.41	4.78
3915.5	.008	4.312E+00	1.113	3.96	4.40
3883.0	.007	4.654E+00	1.133	3.72	4.21
3872.5	.006	1.249E+01	.855	2.99	2.56
3862.2	.004	1.353E+01	.997	2.49	2.48
3862.4	.003	1.478E+01	.966	2.48	2.39
4367.3	.010	4.017E+00	1.012	4.26	4.31
4334.5	.009	4.253E+00	1.031	4.06	4.19
4389.5	.008	4.791E+00	1.077	3.60	3.88
4364.1	.006	5.457E+00	1.108	3.27	3.62
4313.1	.005	1.425E+01	.798	3.02	2.41
4362.7	.004	1.588E+01	.877	2.65	2.33
4352.7	.003	1.779E+01	1.029	2.19	2.25
4805.5	.008	4.958E+00	1.014	3.53	3.58
4772.1	.007	5.351E+00	1.030	3.36	3.46

SMALL BORE COILED TUBE DATA - TEST CORRELATION ON HTFS CORRELATION

TABLE 5.12

Mass Flux KG/M2.S	Dual (-)	L-M Param (-)	Mult Ratio C/M	T.P. Mult Meas (-)	T.P. Mult Calc (-)
4787.0	.006	5.847E+00	1.007	3.29	3.31
4806.9	.006	5.360E+00	.990	3.21	3.18
4788.6	.005	1.664E+01	.867	2.62	2.27
4821.1	.004	1.811E+01	.934	2.38	2.23

TABLE 5.12 (Cont'd)

1 Mean meter.	kg/m^2.s	Two-phase Multiplier	Two-phase Multiplier (HTFS)	Calculated Ratio	Mean)^2	Count
0.0124	1063.1	45.81	42.06	1.089	0.004	1
	1044.4	42.75	41.41	1.032	0.015	1
	1038.9	42.19	38.98	1.082	0.005	1
	1013.7	39.13	37.53	1.043	0.013	1
	1002.8	30.85	34.61	0.891	0.069	0
	999.0	27.94	31.08	0.899	0.065	0
	952.5	25.51	28.78	0.886	0.072	0
	954.3	19.83	22.86	0.867	0.082	0
	952.2	15.90	17.48	0.910	0.060	1
	943.7	11.25	10.76	1.046	0.012	1
	1401.8	26.43	23.75	1.113	0.002	0
	1381.0	25.04	23.16	1.081	0.005	1
	1374.4	23.14	22.19	1.043	0.012	1
	1360.0	22.77	20.83	1.093	0.004	1
	1348.2	20.54	19.35	1.061	0.009	1
	1340.4	17.26	17.52	0.985	0.029	1
	1336.5	16.18	15.27	1.060	0.009	1
	1327.0	12.58	12.78	0.984	0.029	1
	1315.9	9.88	9.95	0.993	0.026	1
	1295.8	6.36	3.51	1.812	0.432	0
	1729.9	17.65	14.93	1.182	0.001	0
	1711.2	16.69	14.53	1.149	0.000	0
	1719.1	14.94	13.79	1.083	0.005	1
	1719.2	15.14	13.22	1.145	0.000	0
	1698.5	13.60	12.83	1.060	0.009	1
	1691.2	13.30	11.95	1.113	0.002	0
	1695.9	12.26	11.13	1.102	0.003	0
	1692.9	11.82	10.15	1.174	0.000	0
	1674.5	9.41	9.17	1.026	0.018	1
	1676.8	8.13	7.72	1.053	0.010	1
	1562.4	6.13	5.24	1.168	0.000	0
	2083.3	11.96	9.91	1.207	0.003	0
	2058.3	12.37	9.67	1.279	0.016	0
	2069.5	10.71	8.91	1.202	0.002	0
	2049.8	10.64	8.65	1.230	0.006	0
	2052.9	9.22	7.92	1.164	0.000	0
	2048.9	8.25	7.37	1.119	0.001	0
	2024.6	8.81	7.00	1.259	0.011	0
	2027.6	7.90	6.28	1.258	0.011	0
	2032.7	6.39	5.54	1.153	0.000	0
	1993.6	4.63	4.10	1.129	0.001	0
	2415.5	9.22	7.02	1.313	0.025	0
	2420.8	8.84	6.81	1.298	0.021	0
	2405.8	8.45	6.59	1.282	0.016	0
	2410.0	7.91	6.30	1.256	0.010	0
	2411.9	7.72	6.01	1.285	0.017	0
	2398.8	7.38	5.76	1.281	0.016	0
	2391.4	6.53	5.40	1.209	0.003	0
	2366.1	6.63	4.95	1.339	0.034	0
	2379.9	5.13	4.39	1.169	0.000	0
	2356.4	4.85	3.83	1.266	0.013	0
	2380.6	4.13	1.96	2.107	0.908	0
				Mean	Std Dev	10% Limit
				1.154	0.204	35%

Table 5.13

2524.5	12.19	9.71	1.255	0.073	0
2491.1	14.26	10.38	1.374	0.023	0
2494.1	10.75	8.52	1.262	0.070	0
2502.1	9.28	7.74	1.199	0.107	0
2475.7	7.20	6.89	1.045	0.231	1
2450.7	6.76	5.97	1.132	0.155	0
2454.2	4.85	2.59	1.873	0.120	0
2447.6	2.83	2.25	1.258	0.072	0
2963.8	9.19	6.68	1.376	0.022	0
2958.9	8.60	6.37	1.350	0.031	0
2979.4	8.22	5.92	1.389	0.019	0
2961.5	7.30	5.57	1.311	0.046	0
2944.0	6.73	5.16	1.304	0.049	0
2959.0	5.67	4.55	1.246	0.078	0
2969.8	4.89	4.03	1.213	0.098	0
2946.2	3.73	2.05	1.820	0.086	0
2919.9	2.56	1.89	1.354	0.029	0
3438.0	6.89	4.75	1.451	0.006	0
3420.9	6.83	4.51	1.514	0.000	0
3422.2	5.95	4.26	1.397	0.017	0
3380.3	5.49	3.94	1.393	0.017	0
3401.4	4.56	3.54	1.288	0.056	0
3404.9	3.89	3.26	1.193	0.110	0
3417.9	3.67	1.80	2.039	0.263	0
3422.2	3.01	1.74	1.730	0.042	0
3388.1	2.97	1.66	1.789	0.069	0
3891.5	5.37	3.43	1.566	0.002	0
3919.4	5.00	3.25	1.538	0.000	0
3918.4	4.62	3.10	1.490	0.001	0
3913.4	4.41	2.96	1.490	0.001	0
3915.5	3.96	2.73	1.451	0.006	0
3883.0	3.72	2.62	1.420	0.011	0
3872.5	2.99	1.59	1.881	0.126	0
3862.2	2.49	1.54	1.617	0.008	0
3862.4	2.48	1.49	1.664	0.019	0
4367.3	4.26	2.58	1.651	0.016	0
4334.5	4.06	2.51	1.618	0.008	0
4389.5	3.60	2.32	1.552	0.001	0
4364.1	3.27	2.17	1.507	0.000	0
4313.1	3.02	1.45	2.083	0.310	0
4362.7	2.65	1.39	1.906	0.145	0
4352.7	2.19	1.35	1.622	0.009	0
4805.5	3.53	2.07	1.705	0.032	0
4772.1	3.36	2.01	1.672	0.021	0
4787.0	3.29	1.92	1.714	0.035	0
4806.9	3.21	1.84	1.745	0.048	0
4788.6	2.62	1.32	1.985	0.211	0
4821.1	2.38	1.29	1.845	0.102	0
4735.8	2.15	1.28	1.680	0.024	0
			Mean	Std Dev	10% Limit
			1.526	0.250	2%
			Total Mean	Group Std Dev	
			1.340	0.227	

Table 5.13 contd

Two-phase Multiplier (tm=B/d^n)	Calculated Ratio	Mean)^2	Count
22.37	2.048	0.372	0
21.63	1.977	0.290	0
20.25	2.083	0.417	0
19.02	2.057	0.383	0
17.36	1.778	0.115	0
15.53	1.800	0.131	0
13.71	1.861	0.179	0
10.91	1.818	0.144	0
8.41	1.891	0.205	0
5.08	2.216	0.605	0
16.65	1.588	0.022	0
15.99	1.566	0.016	0
15.25	1.517	0.006	0
14.17	1.607	0.029	0
13.05	1.575	0.019	0
11.74	1.469	0.001	0
10.21	1.585	0.022	0
8.48	1.483	0.002	0
6.55	1.509	0.005	0
2.27	2.796	1.846	0
12.91	1.367	0.005	0
12.43	1.342	0.009	0
11.85	1.260	0.032	0
11.36	1.332	0.011	0
10.90	1.248	0.036	0
10.11	1.316	0.015	0
9.44	1.299	0.019	0
8.59	1.387	0.003	0
7.66	1.225	0.045	0
6.47	1.256	0.033	0
4.36	1.405	0.001	0
10.32	1.158	0.078	0
9.95	1.243	0.038	0
9.22	1.162	0.076	0
8.87	1.200	0.057	0
8.17	1.129	0.096	0
7.55	1.093	0.119	1
7.09	1.243	0.038	0
6.37	1.241	0.039	0
5.63	1.135	0.092	0
4.09	1.133	0.093	0
8.48	1.087	0.123	1
8.24	1.072	0.134	1
7.93	1.066	0.138	1
7.59	1.042	0.157	1
7.25	1.065	0.139	1
6.91	1.068	0.137	1
6.46	1.011	0.182	1
5.86	1.132	0.094	0
5.22	0.982	0.208	1
4.51	1.075	0.132	1
2.33	1.770	0.110	0
	Mean	Std Dev	10% Limit
	1.438	0.378	19%

Table 5.14

20.38	0.598	0.005	0
21.50	0.663	0.019	0
17.67	0.608	0.007	0
16.10	0.576	0.002	0
14.18	0.508	0.000	0
12.16	0.556	0.001	0
5.28	0.918	0.153	1
4.58	0.618	0.008	0
16.46	0.558	0.001	0
15.67	0.549	0.000	0
14.66	0.561	0.001	0
13.71	0.532	0.000	0
12.63	0.533	0.000	0
11.19	0.507	0.000	0
9.95	0.491	0.001	0
5.02	0.743	0.047	0
4.59	0.558	0.001	0
13.58	0.507	0.000	0
12.83	0.532	0.000	0
12.12	0.491	0.001	0
11.07	0.496	0.001	0
10.01	0.455	0.005	0
9.23	0.422	0.011	0
5.12	0.717	0.036	0
4.95	0.608	0.007	0
4.68	0.635	0.012	0
11.10	0.484	0.002	0
10.59	0.472	0.003	0
10.10	0.457	0.005	0
9.63	0.458	0.005	0
8.89	0.446	0.007	0
8.46	0.440	0.008	0
5.12	0.584	0.003	0
4.95	0.504	0.001	0
4.78	0.518	0.000	0
9.37	0.455	0.005	0
9.05	0.449	0.006	0
8.47	0.425	0.010	0
7.87	0.415	0.012	0
5.20	0.581	0.003	0
5.04	0.526	0.000	0
4.89	0.448	0.006	0
8.27	0.427	0.010	0
7.98	0.421	0.011	0
7.64	0.431	0.009	0
7.35	0.437	0.008	0
5.26	0.499	0.001	0
5.17	0.460	0.004	0
5.04	0.427	0.010	0

Mean	Std Dev	10% Limit
0.527	0.097	2%

Total Mean	Group Std Dev
0.991	0.238

Table 5.14 contd

Two-phase Multiplier (ct=0.1)	Calculated Ratio	Mean)^2	Count
26.58	1.724	0.210	0
25.77	1.659	0.155	0
24.15	1.747	0.232	0
22.78	1.718	0.204	0
20.82	1.482	0.047	0
18.63	1.499	0.055	0
16.59	1.538	0.074	0
13.19	1.503	0.056	0
10.16	1.565	0.090	0
6.15	1.828	0.316	0
19.02	1.389	0.015	0
18.31	1.368	0.010	0
17.47	1.325	0.003	0
16.25	1.401	0.018	0
14.98	1.371	0.011	0
13.49	1.278	0.000	0
11.73	1.379	0.013	0
9.76	1.289	0.001	0
7.54	1.310	0.002	0
2.63	2.423	1.338	0
14.41	1.225	0.002	0
13.89	1.202	0.004	0
13.23	1.129	0.019	0
12.69	1.193	0.005	0
12.18	1.117	0.022	0
11.30	1.177	0.008	0
10.55	1.162	0.011	0
9.61	1.241	0.001	0
8.60	1.095	0.029	1
7.25	1.122	0.021	0
4.88	1.254	0.000	0
11.31	1.057	0.044	1
10.92	1.133	0.018	0
10.11	1.059	0.043	1
9.73	1.093	0.030	1
8.96	1.029	0.056	1
8.29	0.995	0.073	1
7.79	1.131	0.018	0
7.00	1.129	0.019	0
6.19	1.033	0.054	1
4.50	1.030	0.056	1
9.18	1.004	0.068	1
8.92	0.991	0.076	1
8.59	0.984	0.079	1
8.22	0.962	0.092	1
7.85	0.984	0.080	1
7.49	0.986	0.078	1
7.00	0.933	0.111	1
6.35	1.044	0.049	1
5.66	0.906	0.130	1
4.90	0.991	0.076	1
2.53	1.633	0.135	0
	Mean	Std Dev	10% Limit
	1.266	0.292	35%

Table 5.15

21.35	0.571	0.004	0
22.54	0.633	0.013	0
18.52	0.580	0.005	0
16.88	0.550	0.002	0
14.87	0.484	0.001	0
12.76	0.530	0.000	0
5.54	0.875	0.134	0
4.80	0.589	0.007	0
17.13	0.537	0.001	0
16.31	0.527	0.000	0
15.26	0.539	0.001	0
14.27	0.511	0.000	0
13.15	0.512	0.000	0
11.65	0.487	0.000	0
10.35	0.472	0.001	0
5.23	0.714	0.042	0
4.78	0.536	0.001	0
14.05	0.490	0.000	0
13.28	0.514	0.000	0
12.55	0.474	0.001	0
11.47	0.479	0.001	0
10.37	0.440	0.005	0
9.55	0.407	0.010	0
5.30	0.693	0.034	0
5.12	0.587	0.006	0
4.84	0.613	0.011	0
11.44	0.469	0.002	0
10.92	0.458	0.003	0
10.41	0.444	0.004	0
9.93	0.444	0.004	0
9.16	0.432	0.006	0
8.72	0.427	0.007	0
5.28	0.566	0.003	0
5.10	0.488	0.000	0
4.93	0.503	0.000	0
9.63	0.443	0.004	0
9.30	0.437	0.005	0
8.70	0.414	0.009	0
8.09	0.404	0.011	0
5.34	0.565	0.003	0
5.18	0.511	0.000	0
5.02	0.438	0.005	0
8.48	0.416	0.008	0
8.18	0.411	0.009	0
7.83	0.420	0.008	0
7.54	0.426	0.007	0
5.39	0.486	0.000	0
5.30	0.449	0.004	0
5.17	0.416	0.009	0
	Mean	Std Dev	10% Limit
	0.508	0.091	0%
	Total Mean	Group Std Dev	
	0.895	0.192	

Table 5.15 contd

Two-phase Multiplier (ct=0.11)	Calculated Ratio	Mean)^2	Count
27.00	1.697	0.199	0
26.18	1.633	0.146	0
24.54	1.719	0.219	0
23.15	1.690	0.193	0
21.16	1.458	0.043	0
18.94	1.475	0.050	0
16.87	1.512	0.068	0
13.42	1.477	0.051	0
10.33	1.539	0.083	0
6.26	1.797	0.298	0
19.26	1.372	0.015	0
18.54	1.351	0.010	0
17.69	1.308	0.003	0
16.46	1.384	0.018	0
15.17	1.354	0.011	0
13.67	1.262	0.000	0
11.88	1.361	0.012	0
9.89	1.272	0.000	0
7.64	1.293	0.002	0
2.66	2.391	1.299	0
14.56	1.212	0.001	0
14.03	1.189	0.004	0
13.37	1.117	0.018	0
12.82	1.181	0.005	0
12.31	1.105	0.021	0
11.42	1.165	0.007	0
10.66	1.150	0.010	0
9.71	1.228	0.001	0
8.69	1.083	0.028	1
7.32	1.110	0.020	0
4.93	1.241	0.000	0
11.41	1.048	0.041	1
11.02	1.123	0.016	0
10.20	1.050	0.040	1
9.82	1.084	0.029	1
9.04	1.020	0.053	1
8.36	0.987	0.070	1
7.86	1.121	0.017	0
7.06	1.119	0.017	0
6.24	1.024	0.052	1
4.54	1.020	0.053	1
9.25	0.997	0.065	1
8.99	0.983	0.072	1
8.65	0.977	0.075	1
8.29	0.955	0.088	1
7.91	0.976	0.076	1
7.54	0.978	0.074	1
7.05	0.926	0.106	1
6.40	1.036	0.046	1
5.71	0.899	0.124	0
4.93	0.983	0.072	1
2.55	1.620	0.136	0
	Mean	Std Dev	10% Limit
	1.251	0.285	33%

Table 5.16

21.45	0.568	0.004	0
22.64	0.630	0.015	0
18.60	0.578	0.005	0
16.95	0.547	0.002	0
14.94	0.482	0.001	0
12.82	0.527	0.000	0
5.57	0.871	0.133	0
4.83	0.586	0.006	0
17.20	0.534	0.001	0
16.37	0.525	0.000	0
15.32	0.537	0.001	0
14.33	0.510	0.000	0
13.20	0.510	0.000	0
11.69	0.485	0.000	0
10.39	0.470	0.001	0
5.25	0.711	0.042	0
4.80	0.534	0.001	0
14.10	0.489	0.000	0
13.32	0.513	0.000	0
12.59	0.473	0.001	0
11.51	0.477	0.001	0
10.40	0.438	0.005	0
9.59	0.406	0.010	0
5.31	0.691	0.034	0
5.14	0.585	0.006	0
4.86	0.611	0.011	0
11.48	0.468	0.001	0
10.95	0.457	0.002	0
10.44	0.443	0.004	0
9.95	0.443	0.004	0
9.19	0.431	0.006	0
8.75	0.425	0.007	0
5.29	0.565	0.003	0
5.11	0.487	0.000	0
4.95	0.501	0.000	0
9.65	0.441	0.004	0
9.32	0.436	0.005	0
8.72	0.413	0.009	0
8.11	0.403	0.011	0
5.36	0.564	0.003	0
5.19	0.510	0.000	0
5.03	0.435	0.005	0
8.50	0.415	0.008	0
8.20	0.410	0.009	0
7.85	0.419	0.008	0
7.56	0.425	0.007	0
5.40	0.485	0.000	0
5.31	0.448	0.003	0
5.18	0.415	0.008	0

Mean	Std Dev	10% Limit
0.507	0.090	0%

Total Mean	Group Std Dev
0.886	0.188

Table 5.16 contd

Two-phase Multiplier (ct=0.09)	Calculated Ratio	(Mean)^2	Count
26.16	1.751	0.221	0
25.35	1.686	0.164	0
23.76	1.776	0.245	0
22.40	1.747	0.217	0
20.47	1.507	0.051	0
18.32	1.525	0.059	0
16.30	1.565	0.081	0
12.97	1.529	0.062	0
9.98	1.593	0.097	0
6.05	1.861	0.336	0
18.79	1.407	0.016	0
18.08	1.385	0.011	0
17.25	1.342	0.004	0
16.04	1.420	0.019	0
14.79	1.389	0.012	0
13.32	1.295	0.000	0
11.58	1.397	0.014	0
9.63	1.306	0.001	0
7.44	1.327	0.002	0
2.59	2.455	1.379	0
14.26	1.238	0.002	0
13.74	1.215	0.004	0
13.10	1.141	0.020	0
12.55	1.206	0.006	0
12.09	1.128	0.023	0
11.18	1.189	0.008	0
10.44	1.174	0.011	0
9.51	1.254	0.001	0
8.50	1.107	0.030	0
7.17	1.134	0.022	0
4.83	1.268	0.000	0
11.22	1.066	0.046	1
10.82	1.143	0.019	0
10.02	1.069	0.045	1
9.64	1.103	0.032	0
8.88	1.038	0.059	1
8.21	1.004	0.077	1
7.72	1.142	0.019	0
6.93	1.140	0.020	0
6.13	1.042	0.057	1
4.46	1.039	0.059	1
9.11	1.012	0.072	1
8.86	0.998	0.080	1
8.52	0.992	0.084	1
8.16	0.969	0.097	1
7.79	0.991	0.084	1
7.43	0.994	0.083	1
6.94	0.940	0.116	1
6.30	1.052	0.052	1
5.62	0.913	0.135	1
4.86	0.998	0.080	1
2.51	1.646	0.133	0
	Mean	Std Dev	10% Limit
	1.281	0.299	31%

Table 5.17

21.25	0.574	0.004	0
22.43	0.636	0.016	0
18.43	0.583	0.005	0
16.80	0.552	0.002	0
14.80	0.486	0.001	0
12.70	0.532	0.000	0
5.52	0.879	0.136	0
4.78	0.592	0.007	0
17.06	0.539	0.001	0
16.24	0.529	0.000	0
15.20	0.541	0.001	0
14.22	0.513	0.000	0
13.09	0.514	0.000	0
11.60	0.489	0.000	0
10.31	0.474	0.001	0
5.21	0.716	0.043	0
4.76	0.538	0.001	0
14.01	0.492	0.000	0
13.23	0.516	0.000	0
12.50	0.476	0.001	0
11.43	0.480	0.001	0
10.33	0.441	0.005	0
9.52	0.409	0.010	0
5.28	0.695	0.034	0
5.11	0.589	0.006	0
4.83	0.615	0.011	0
11.41	0.471	0.002	0
10.88	0.459	0.003	0
10.30	0.445	0.004	0
9.90	0.446	0.004	0
9.13	0.434	0.006	0
8.69	0.428	0.007	0
5.26	0.568	0.003	0
5.08	0.490	0.000	0
4.92	0.504	0.000	0
9.60	0.444	0.004	0
9.27	0.438	0.005	0
8.68	0.415	0.009	0
8.07	0.405	0.011	0
5.33	0.567	0.003	0
5.17	0.513	0.000	0
5.01	0.437	0.005	0
8.46	0.417	0.009	0
8.16	0.412	0.010	0
7.81	0.421	0.008	0
7.52	0.427	0.007	0
5.37	0.488	0.001	0
5.29	0.450	0.004	0
5.16	0.417	0.009	0
	Mean	Std Dev	10% Limit
	0.510	0.091	0%
	Total Mean	Group Std Dev	
	0.903	0.195	

Tablee 5.17 contd

Two-phase Multiplier (ind=0.5)	Calculated Ratio	Mean)^2	Count
34.89	1.313	0.029	0
34.07	1.255	0.012	0
31.99	1.319	0.031	0
30.47	1.284	0.020	0
27.97	1.103	0.002	0
25.07	1.114	0.001	0
22.74	1.122	0.000	0
18.08	1.097	0.002	1
13.87	1.146	0.000	0
8.47	1.329	0.034	0
22.26	1.187	0.002	0
21.56	1.161	0.000	0
20.61	1.122	0.000	0
19.26	1.182	0.001	0
17.82	1.152	0.000	0
16.10	1.072	0.005	1
14.01	1.155	0.000	0
11.69	1.076	0.005	1
9.07	1.090	0.003	1
3.18	2.002	0.737	0
15.38	1.148	0.000	0
14.89	1.121	0.001	0
14.16	1.055	0.008	1
13.58	1.115	0.001	0
13.11	1.038	0.011	1
12.18	1.092	0.003	1
11.36	1.079	0.004	1
10.35	1.151	0.000	0
9.31	1.011	0.018	1
7.84	1.037	0.011	1
5.30	1.154	0.000	0
11.11	1.077	0.004	1
10.78	1.148	0.000	0
9.95	1.076	0.005	1
9.62	1.106	0.001	0
8.84	1.043	0.010	1
8.20	1.006	0.019	1
7.74	1.138	0.000	0
6.95	1.136	0.000	0
6.14	1.041	0.011	1
4.50	1.028	0.013	1
8.42	1.095	0.002	1
8.17	1.082	0.004	1
7.89	1.071	0.005	1
7.55	1.048	0.009	1
7.20	1.072	0.005	1
6.88	1.072	0.005	1
6.45	1.013	0.017	1
5.88	1.128	0.000	0
5.23	0.981	0.026	1
4.54	1.068	0.006	1
2.33	1.769	0.391	0
	Mean	Std Dev	10% Limit
	1.144	0.170	48%

Table 5.18

15.04	0.811	0.001	0
15.98	0.893	0.003	0
13.12	0.819	0.000	0
11.94	0.777	0.004	0
10.57	0.681	0.026	0
9.12	0.741	0.010	0
3.96	1.225	0.147	0
3.43	0.824	0.000	0
11.15	0.824	0.000	0
10.63	0.809	0.001	0
9.91	0.830	0.000	0
9.30	0.785	0.003	0
8.59	0.784	0.003	0
7.59	0.747	0.009	0
6.74	0.726	0.013	0
3.41	1.093	0.063	1
3.13	0.817	0.001	0
8.51	0.810	0.001	0
8.06	0.848	0.000	0
7.61	0.762	0.004	0
7.00	0.784	0.003	0
6.31	0.723	0.014	0
5.81	0.669	0.030	0
3.21	1.142	0.050	0
3.11	0.968	0.016	1
2.95	1.006	0.027	1
6.51	0.825	0.000	0
6.19	0.808	0.001	0
5.91	0.782	0.003	0
5.64	0.783	0.003	0
5.20	0.752	0.006	0
4.97	0.749	0.009	0
3.01	0.993	0.023	1
2.91	0.835	0.000	0
2.82	0.880	0.001	0
5.17	0.823	0.000	0
5.02	0.809	0.001	0
4.66	0.772	0.003	0
4.35	0.752	0.008	0
2.89	1.043	0.041	1
2.79	0.951	0.012	1
2.70	0.810	0.001	0
4.34	0.812	0.001	0
4.20	0.799	0.002	0
4.02	0.818	0.001	0
3.86	0.831	0.000	0
2.77	0.947	0.011	1
2.71	0.878	0.001	0
2.67	0.806	0.001	0
	Mean	Std Dev	10% Limit
	0.841	0.111	14%
	Total Mean	Group Std Dev	
	0.996	0.141	

Table 5.18 contd

Two-phase Multiplier (inc=0.2)	Calculated Ratio	(Mean)^2	Count
41.29	1.109	0.001	0
40.51	1.055	0.001	1
38.09	1.108	0.001	0
36.51	1.072	0.000	1
33.61	0.918	0.028	1
30.16	0.926	0.025	1
27.69	0.921	0.027	1
22.00	0.901	0.033	1
16.85	0.944	0.020	1
10.34	1.088	0.000	1
24.50	1.079	0.000	1
23.82	1.051	0.001	1
22.81	1.015	0.005	1
21.37	1.066	0.000	1
19.82	1.036	0.002	1
17.92	0.962	0.015	1
15.61	1.036	0.002	1
13.05	0.964	0.014	1
10.15	0.974	0.012	1
3.57	1.782	0.487	0
16.00	1.103	0.000	0
15.54	1.074	0.000	1
14.76	1.012	0.005	1
14.15	1.070	0.000	1
13.70	0.993	0.008	1
12.75	1.043	0.002	1
11.82	1.032	0.003	1
10.83	1.100	0.000	0
9.77	0.963	0.015	1
8.22	0.988	0.009	1
5.57	1.098	0.000	1
10.98	1.089	0.000	1
10.69	1.157	0.005	0
9.86	1.086	0.000	1
9.56	1.113	0.001	0
8.76	1.052	0.001	1
8.14	1.013	0.005	1
7.72	1.142	0.003	0
6.93	1.141	0.003	0
6.11	1.045	0.001	1
4.51	1.027	0.003	1
7.99	1.154	0.005	0
7.76	1.140	0.003	0
7.50	1.127	0.002	0
7.17	1.103	0.000	0
6.84	1.129	0.002	0
6.55	1.127	0.002	0
6.14	1.064	0.000	1
5.61	1.181	0.009	0
4.98	1.029	0.003	1
4.34	1.117	0.001	0
2.23	1.856	0.595	0
	Mean	Std Dev	10% Limit
	1.084	0.163	65%

Table 5.19

12.23	0.996	0.020	1
13.05	1.093	0.002	1
10.71	1.004	0.018	1
9.74	0.953	0.034	1
8.65	0.832	0.093	0
7.48	0.904	0.054	1
3.25	1.494	0.128	0
2.82	1.004	0.018	1
8.67	1.060	0.006	1
8.26	1.041	0.009	1
7.69	1.069	0.005	1
7.23	1.010	0.016	1
6.69	1.006	0.017	1
5.90	0.961	0.031	1
5.23	0.935	0.041	1
2.66	1.404	0.071	0
2.45	1.047	0.008	1
6.34	1.088	0.002	1
6.01	1.137	0.000	0
5.68	1.048	0.008	1
5.24	1.048	0.008	1
4.71	0.968	0.029	1
4.34	0.896	0.058	0
2.40	1.530	0.155	0
2.32	1.298	0.026	0
2.21	1.345	0.043	0
4.68	1.147	0.000	0
4.44	1.126	0.000	0
4.24	1.091	0.002	1
4.04	1.091	0.002	1
3.73	1.062	0.006	1
3.57	1.041	0.009	1
2.17	1.379	0.059	0
2.10	1.186	0.002	0
2.03	1.221	0.007	0
3.60	1.184	0.002	0
3.49	1.162	0.001	0
3.24	1.112	0.001	0
3.03	1.081	0.003	1
2.02	1.497	0.130	0
1.94	1.368	0.053	0
1.88	1.164	0.001	0
2.94	1.202	0.004	0
2.85	1.179	0.002	0
2.72	1.208	0.005	0
2.61	1.229	0.009	0
1.87	1.399	0.069	0
1.83	1.299	0.026	0
1.81	1.187	0.002	0
	Mean	Std Dev	10% Limit
	1.137	0.163	48%
	Total Mean	Group Std Dev	
	1.110	0.163	

Table 5.19 contd

Two-phase Multiplier (ind=0.35)	Calculated Ratio	Mean)^2	Count
37.94	1.207	0.009	0
37.13	1.151	0.001	0
34.89	1.209	0.009	0
33.34	1.174	0.004	0
30.64	1.007	0.011	1
27.49	1.017	0.009	1
25.08	1.017	0.009	1
19.93	0.995	0.014	1
15.28	1.041	0.005	1
9.35	1.203	0.008	0
23.35	1.132	0.000	0
22.66	1.105	0.000	0
21.68	1.067	0.002	1
20.28	1.123	0.000	0
18.79	1.093	0.000	1
16.98	1.016	0.009	1
14.79	1.094	0.000	1
12.35	1.019	0.009	1
9.59	1.030	0.007	1
3.37	1.889	0.603	0
15.68	1.125	0.000	0
15.21	1.097	0.000	1
14.46	1.033	0.006	1
13.86	1.092	0.000	1
13.40	1.015	0.010	1
12.46	1.067	0.002	1
11.62	1.055	0.003	1
10.59	1.126	0.000	0
9.53	0.987	0.016	1
8.03	1.012	0.010	1
5.44	1.126	0.000	0
11.04	1.083	0.001	1
10.74	1.152	0.002	0
9.91	1.081	0.001	1
9.59	1.109	0.000	0
8.80	1.048	0.004	1
8.17	1.010	0.011	1
7.73	1.140	0.001	0
6.94	1.139	0.001	0
6.13	1.043	0.005	1
4.51	1.028	0.007	1
8.20	1.124	0.000	0
7.96	1.110	0.000	0
7.69	1.099	0.000	1
7.36	1.075	0.001	1
7.02	1.100	0.000	1
6.71	1.099	0.000	1
6.29	1.038	0.006	1
5.75	1.154	0.002	0
5.10	1.005	0.012	1
4.44	1.092	0.000	1
2.28	1.812	0.489	0
	Mean	Std Dev	10% Limit
	1.113	0.160	62%

Table 5.20

13.56	0.899	0.006	0
14.43	0.988	0.000	1
11.85	0.907	0.005	1
10.78	0.861	0.014	0
9.56	0.753	0.051	0
8.26	0.819	0.025	0
3.58	1.353	0.141	0
3.11	0.910	0.005	1
9.83	0.935	0.002	1
9.37	0.918	0.004	1
8.72	0.942	0.001	1
8.19	0.891	0.008	0
7.57	0.888	0.008	0
6.69	0.848	0.017	0
5.93	0.824	0.024	0
3.01	1.239	0.068	0
2.77	0.925	0.003	1
7.34	0.939	0.002	1
6.95	0.982	0.000	1
6.57	0.906	0.005	1
6.05	0.907	0.005	1
5.45	0.837	0.020	0
5.02	0.775	0.041	0
2.77	1.323	0.119	0
2.68	1.122	0.021	0
2.55	1.164	0.035	0
5.52	0.973	0.000	1
5.24	0.954	0.001	1
5.00	0.925	0.003	1
4.77	0.925	0.003	1
4.40	0.900	0.006	1
4.21	0.883	0.009	0
2.55	1.171	0.037	0
2.47	1.008	0.001	1
2.39	1.037	0.004	1
4.31	0.988	0.000	1
4.18	0.971	0.000	1
3.68	0.937	0.003	1
3.62	0.902	0.006	1
2.41	1.252	0.075	0
2.32	1.142	0.027	0
2.25	0.972	0.000	1
3.57	0.989	0.000	1
3.46	0.972	0.000	1
3.31	0.995	0.000	1
3.17	1.012	0.001	1
2.27	1.153	0.030	0
2.23	1.069	0.008	1
2.20	0.979	0.000	1
	Mean	Std Dev	10% Limit
	0.978	0.131	60%
	Total Mean	Group Std Dev	
	1.047	0.145	

Table 5.20 contd

Two-phase Multiplier (ime=0.34)	Calculated Ratio	(mean)^2	Count
38.15	1.201	0.008	0
37.34	1.145	0.001	0
35.10	1.202	0.008	0
33.54	1.167	0.003	0
30.83	1.001	0.012	1
27.65	1.010	0.010	1
25.24	1.011	0.010	1
20.06	0.988	0.015	1
15.38	1.034	0.006	1
9.41	1.195	0.007	0
23.42	1.128	0.000	0
22.74	1.101	0.000	0
21.75	1.064	0.002	1
20.35	1.119	0.000	0
18.86	1.089	0.000	1
17.04	1.012	0.010	1
14.84	1.090	0.000	1
12.39	1.015	0.009	1
9.62	1.026	0.007	1
3.38	1.682	0.555	0
15.70	1.124	0.000	0
15.33	1.096	0.000	1
14.48	1.032	0.006	1
13.84	1.091	0.000	1
13.42	1.013	0.003	1
12.49	-1.065	0.002	1
11.64	1.054	0.003	1
10.61	1.124	0.000	0
9.55	0.985	0.016	1
8.04	1.011	0.010	1
5.44	1.124	0.000	0
11.04	1.083	0.001	1
10.73	1.153	0.002	0
9.91	1.081	0.001	1
9.59	1.110	0.000	0
8.80	1.048	0.004	1
8.17	1.010	0.010	1
7.73	1.140	0.001	0
6.94	1.139	0.001	0
6.12	1.043	0.005	1
4.51	1.028	0.007	1
8.19	1.126	0.000	0
7.95	1.112	0.000	0
7.68	1.101	0.000	0
7.34	1.077	0.001	1
7.01	1.102	0.000	0
6.70	1.101	0.000	0
6.28	1.040	0.005	1
5.74	1.156	0.002	0
5.10	1.007	0.011	1
4.43	1.094	0.000	1
2.28	1.815	0.496	0
	Mean	Std Dev	10% Limit
	1.111	0.160	56%

Table 5.21

13.46	0.905	0.007	1
14.33	0.995	0.000	1
11.77	0.913	0.006	1
10.70	0.867	0.015	0
9.50	0.758	0.053	0
8.20	0.824	0.027	0
3.56	1.362	0.140	0
3.09	0.916	0.005	1
9.75	0.943	0.002	1
9.29	0.926	0.004	1
8.65	0.950	0.001	1
8.12	0.899	0.008	0
7.51	0.896	0.008	0
6.63	0.855	0.018	0
5.88	0.831	0.025	0
2.98	1.250	0.068	0
2.74	0.933	0.003	1
7.26	0.949	0.002	1
6.89	0.992	0.000	1
6.50	0.915	0.005	1
5.99	0.916	0.005	1
5.39	0.845	0.020	0
4.97	0.783	0.042	0
2.75	1.336	0.121	0
2.66	1.133	0.021	0
2.53	1.175	0.035	0
5.46	0.984	0.000	1
5.18	0.965	0.001	1
4.94	0.933	0.003	1
4.72	0.935	0.003	1
4.35	0.910	0.006	1
4.16	0.893	0.009	0
2.53	1.184	0.038	0
2.44	1.019	0.001	1
2.36	1.049	0.004	1
4.26	1.001	0.000	1
4.13	0.983	0.000	1
3.83	0.939	0.002	1
3.58	0.913	0.006	1
2.38	1.267	0.078	0
2.29	1.156	0.028	0
2.23	0.984	0.000	1
3.52	1.002	0.000	1
3.41	0.985	0.000	1
3.26	1.008	0.000	1
3.13	1.025	0.001	1
2.24	1.168	0.032	0
2.20	1.083	0.009	1
2.17	0.992	0.000	1
	Mean	Std Dev	10% Limit
	0.988	0.133	62%
	Total Mean	Group Std Dev	
	1.051	0.146	

Table 5.21 contd.

Two-phase Multiplier (ind=0.36)	Calculated Ratio	Mean)^2	Count
37.73	1.214	0.010	0
36.92	1.158	0.002	0
34.69	1.216	0.010	0
33.14	1.181	0.004	0
30.46	1.013	0.010	1
27.32	1.023	0.008	1
24.91	1.024	0.008	1
19.80	1.001	0.013	1
15.18	1.047	0.005	1
9.29	1.211	0.009	0
23.27	1.136	0.000	0
22.59	1.109	0.000	0
21.61	1.071	0.002	1
20.21	1.126	0.000	0
18.72	1.097	0.000	1
16.92	1.019	0.009	1
14.73	1.098	0.000	1
12.30	1.022	0.009	1
9.55	1.034	0.007	1
3.35	1.897	0.611	0
15.66	1.127	0.000	0
15.19	1.099	0.000	1
14.44	1.033	0.006	1
13.84	1.094	0.000	1
13.38	1.016	0.010	1
12.45	1.069	0.002	1
11.60	1.057	0.003	1
10.57	1.127	0.000	0
9.52	0.989	0.016	1
8.02	1.014	0.010	1
5.43	1.128	0.000	0
11.05	1.083	0.001	1
10.74	1.152	0.001	0
9.91	1.081	0.001	1
9.59	1.109	0.000	0
8.80	1.048	0.005	1
8.17	1.010	0.011	1
7.73	1.140	0.001	0
6.94	1.138	0.001	0
6.13	1.043	0.005	1
4.51	1.028	0.008	1
8.22	1.122	0.000	0
7.98	1.108	0.000	0
7.70	1.097	0.000	1
7.37	1.074	0.002	1
7.03	1.098	0.000	1
6.73	1.097	0.000	1
6.30	1.037	0.006	1
5.75	1.152	0.001	0
5.11	1.003	0.012	1
4.45	1.091	0.001	1
2.28	1.809	0.482	0
	Mean	Std Dev	10% Limit
	1.115	0.160	62%

Table 5.22

13.65	0.893	0.006	0
14.53	0.902	0.000	1
11.93	0.901	0.005	1
10.85	0.855	0.013	0
9.62	0.748	0.049	0
8.31	0.813	0.024	0
3.61	1.345	0.141	0
3.13	0.904	0.004	1
9.91	0.927	0.002	1
9.45	0.911	0.003	1
8.80	0.934	0.001	1
8.26	0.884	0.007	0
7.64	0.881	0.008	0
6.75	0.840	0.016	0
5.98	0.817	0.023	0
3.04	1.229	0.068	0
2.79	0.918	0.003	1
7.41	0.930	0.001	1
7.02	0.973	0.000	1
6.63	0.897	0.005	0
6.11	0.899	0.005	0
5.50	0.829	0.019	0
5.07	0.768	0.040	0
2.80	1.310 -	0.117	0
2.71	1.111	0.020	0
2.58	1.153	0.034	0
5.58	0.963	0.000	1
5.30	0.944	0.001	1
5.03	0.914	0.003	1
4.82	0.914	0.003	1
4.45	0.890	0.006	0
4.26	0.874	0.009	0
2.58	1.158	0.036	0
2.50	0.997	0.001	1
2.42	1.026	0.003	1
4.36	0.977	0.000	1
4.23	0.959	0.000	1
3.93	0.916	0.003	1
3.67	0.891	0.006	0
2.44	1.237	0.072	0
2.35	1.128	0.025	0
2.28	0.961	0.000	1
3.62	0.976	0.000	1
3.50	0.959	0.000	1
3.35	0.982	0.000	1
3.21	0.999	0.001	1
2.30	1.138	0.029	0
2.26	1.055	0.008	1
2.22	0.967	0.000	1
	Mean	Std Dev	10% Limit
	0.968	0.129	52%
	Total Mean	Group Std Dev	
	1.043	0.145	

Table 5.22 contd

$a.dp$ = area x shear

= $\pi . d . dz . \tau$

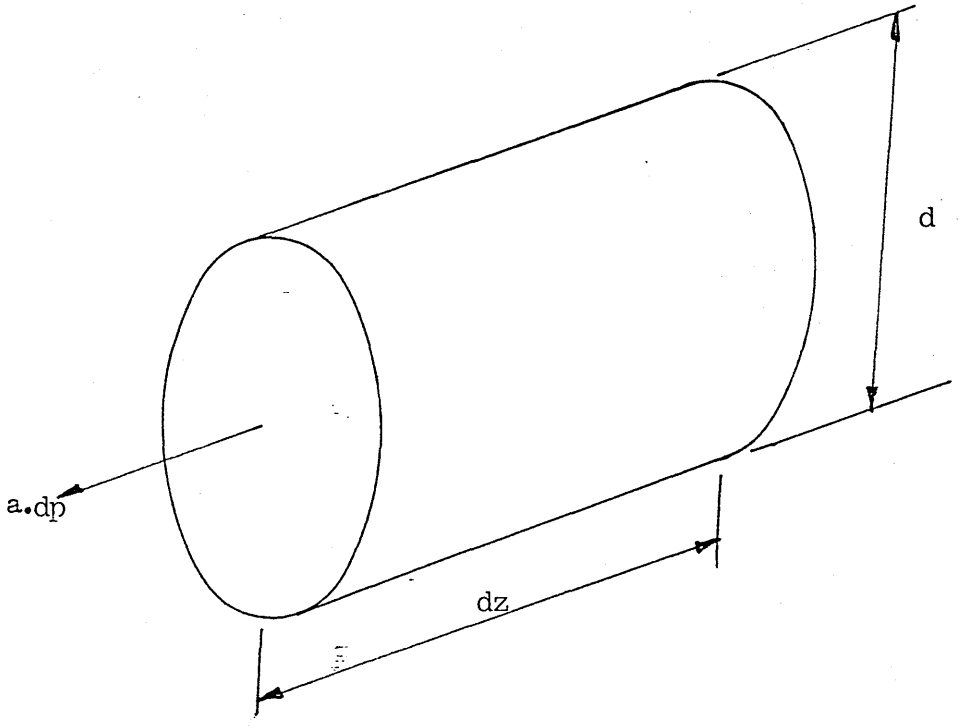

FORCE ON AN ELEMENT OF FLUID IN A PIPE WITH RESPECT TO SHEAR AT THE WALL

FIG. 2.1 SIMPLE SHEAR/FRICTION FACTOR MODEL

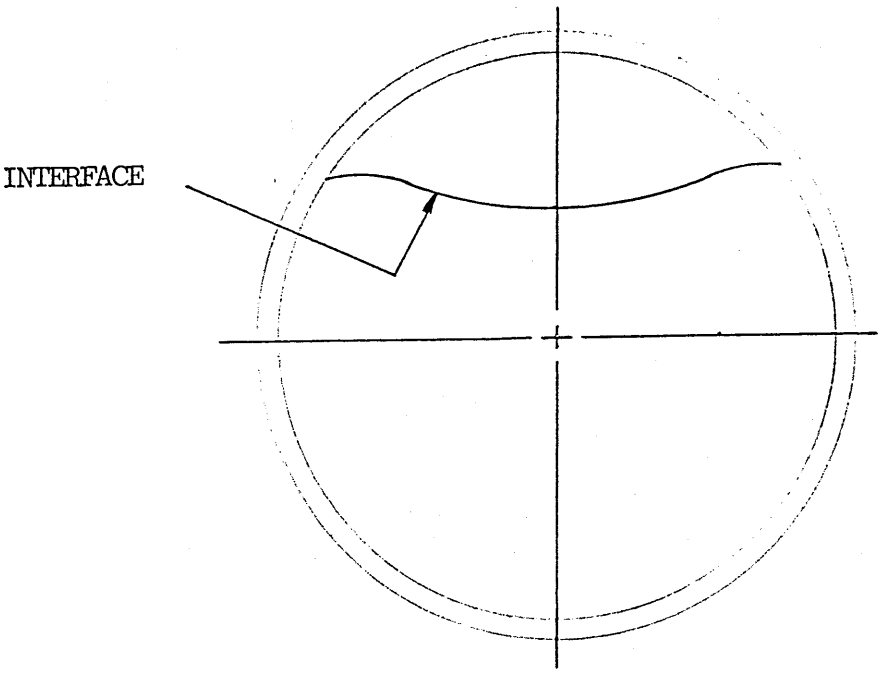

A REPRESENTATIVE PHASE DISTRIBUTION

FIG. 2.2

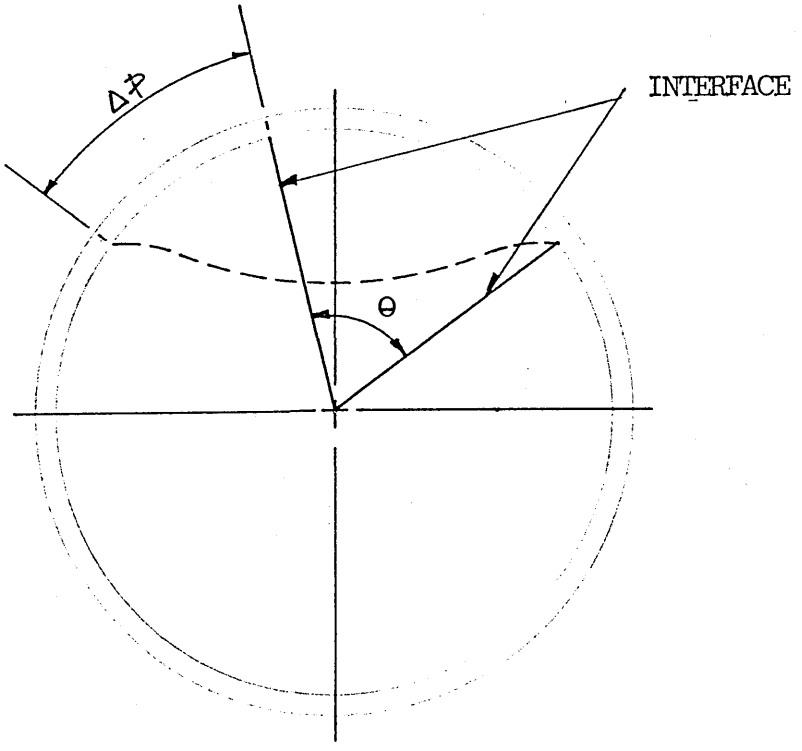

EQUIVALENT CROSS SECTION AS USED IN MODEL

FIG. 2.3

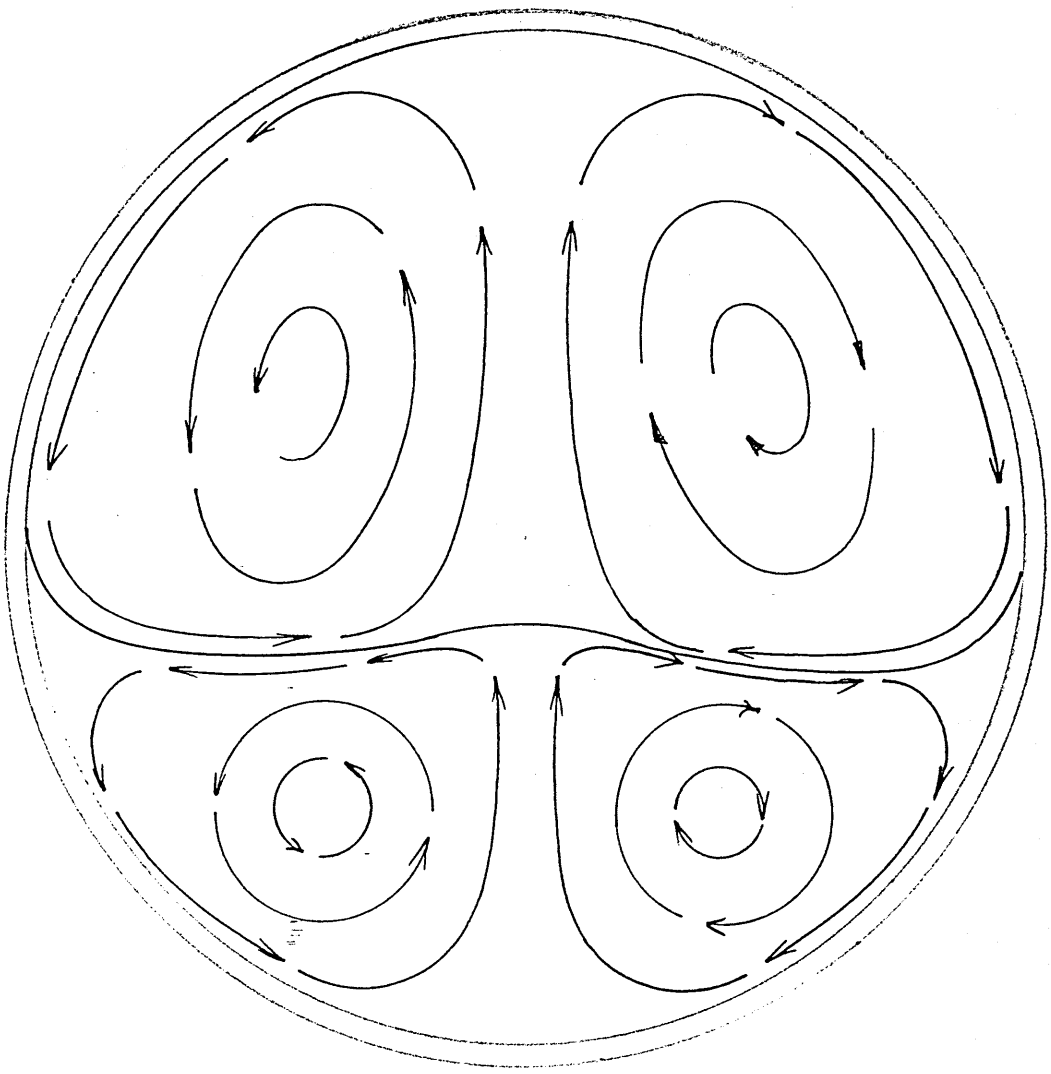

FIG. 2.4 SECONDARY FLOW IN EACH PHASE OF A TWO PHASE FLOW

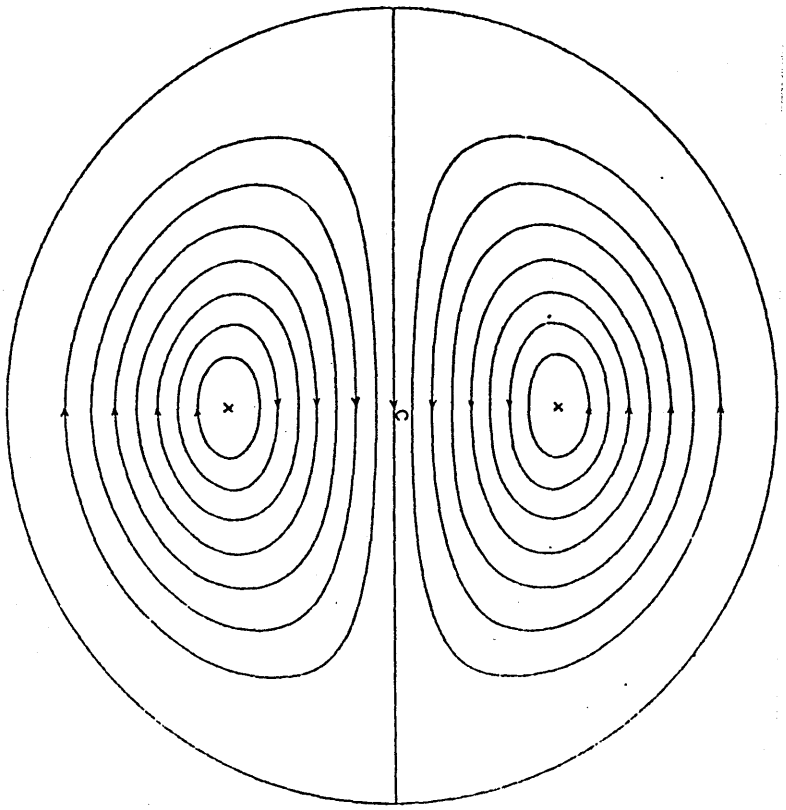

FIG. 3.1 SECONDARY FLOW AS PREDICTED BY DEAN(22)

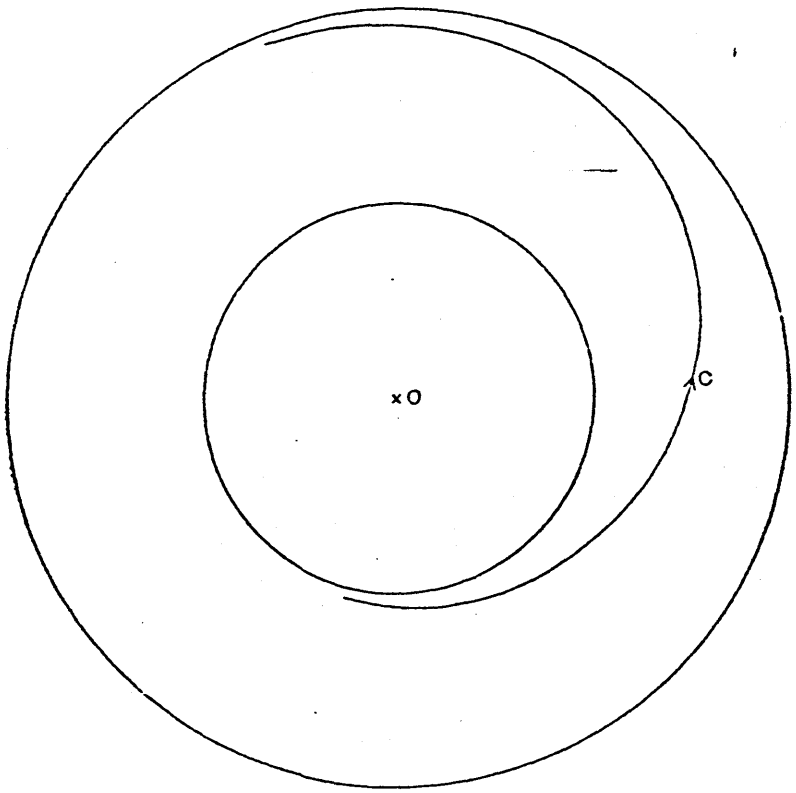

FIG. 3.2 THE STREAMLINE ON THE CENTRAL PLANE (DEAN(22))

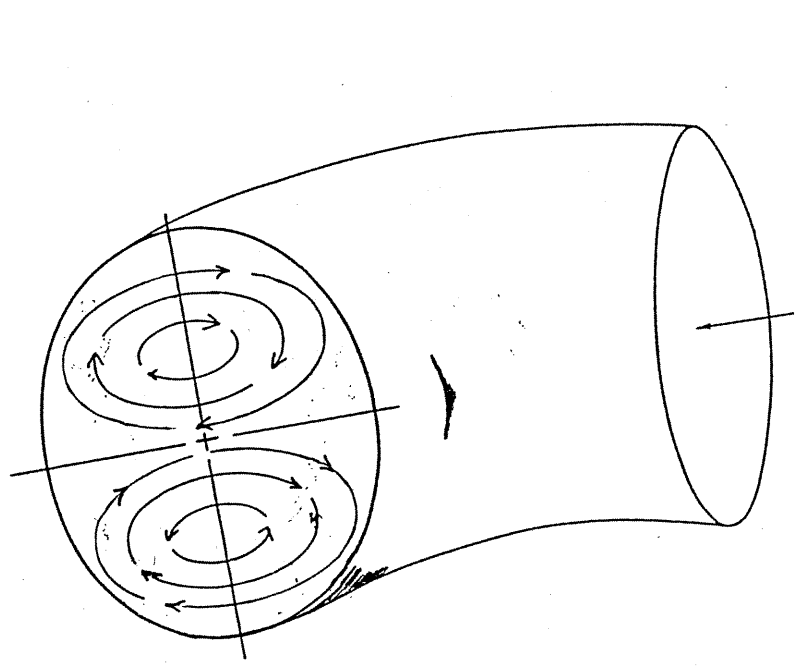

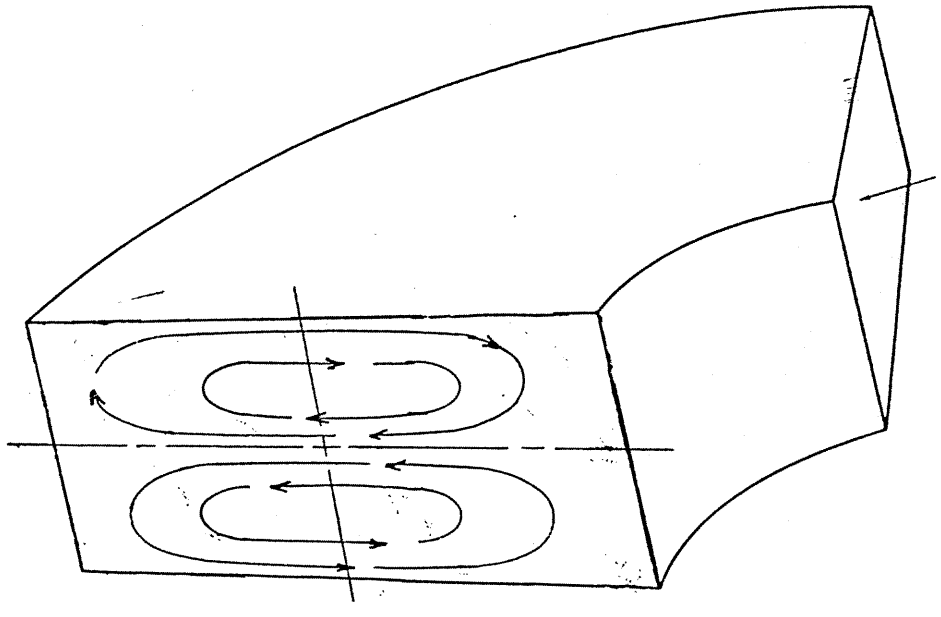

FIG. 3.3 SECONDARY FLOW PATTERN AS DEVELOPED IN RECTANGULAR AND CIRCULAR CROSS SECTIONS

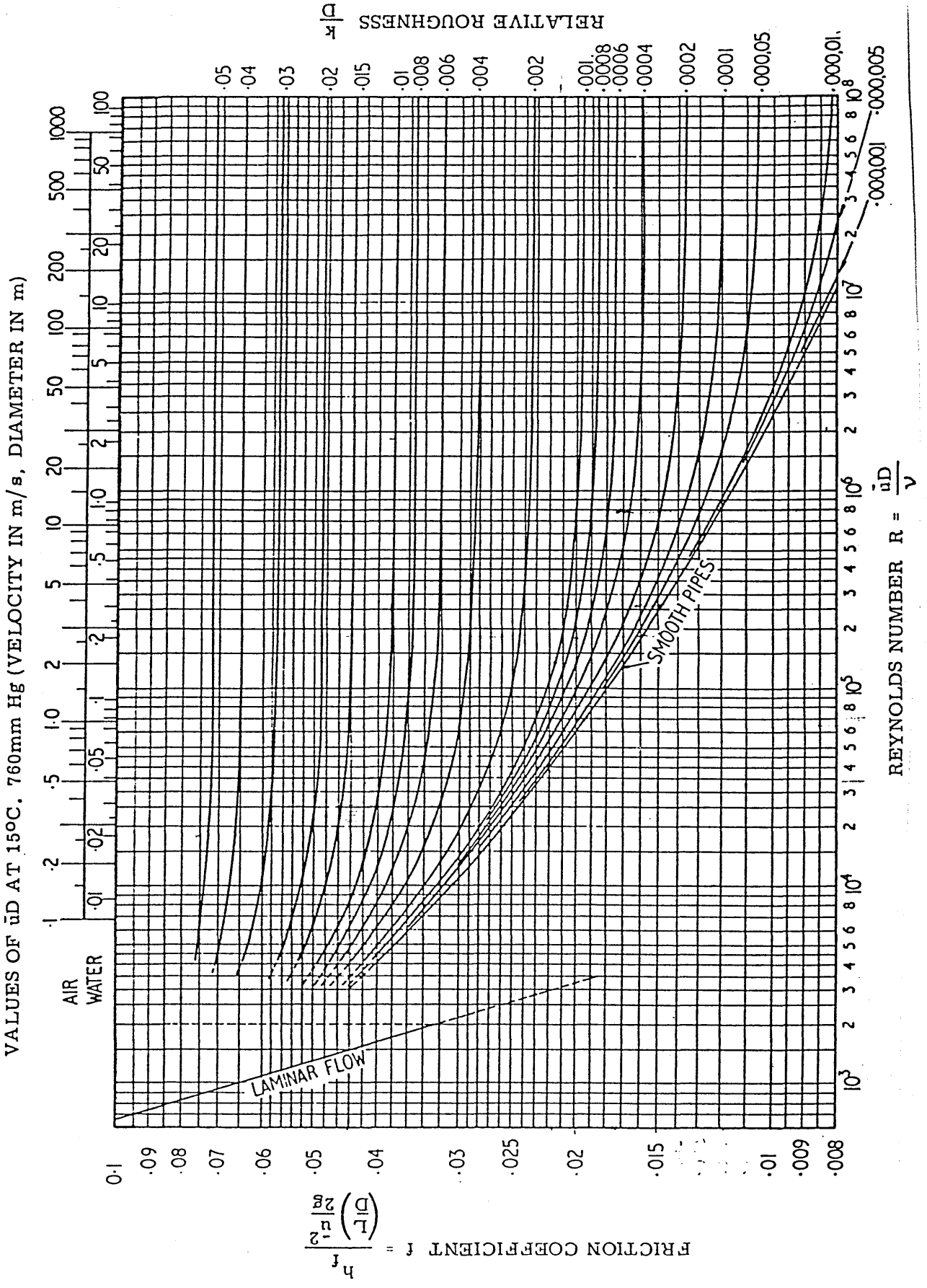

FIG 3.4 THE FRICTION FACTOR/REYNOLDS NUMBER CHART FOR STRAIGHT TUBES (MOODY FRICTION FACTOR)

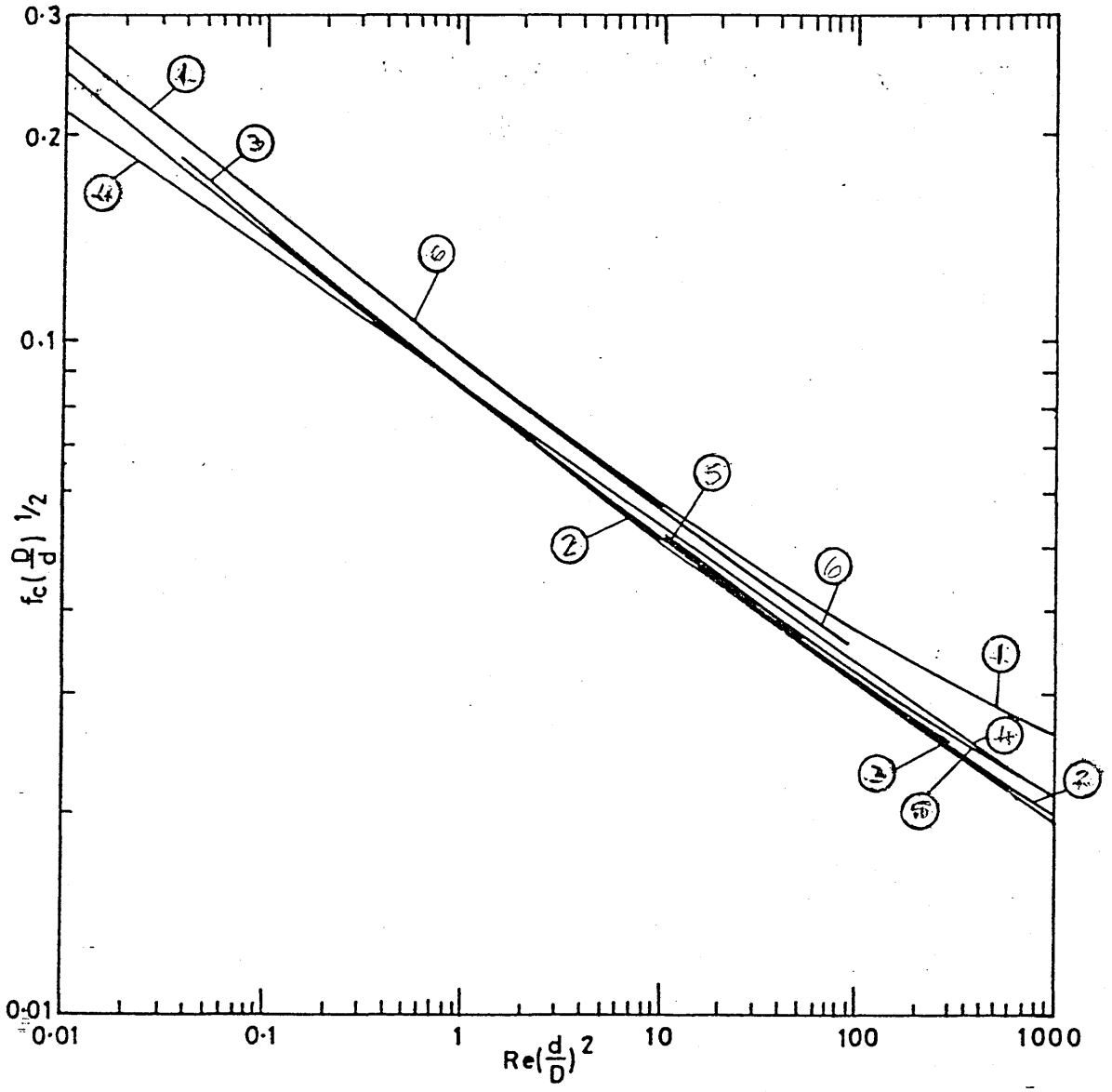

EQUATION	REFERENCE
1	WHITE
2	ITO
3	ITO
4	SRINIVASAN ET AL
5	REJMON
6	ANGLESEA

FIG. 3.5 EQUATIONS FOR TURBULENT FRICTION FACTORS IN COILS

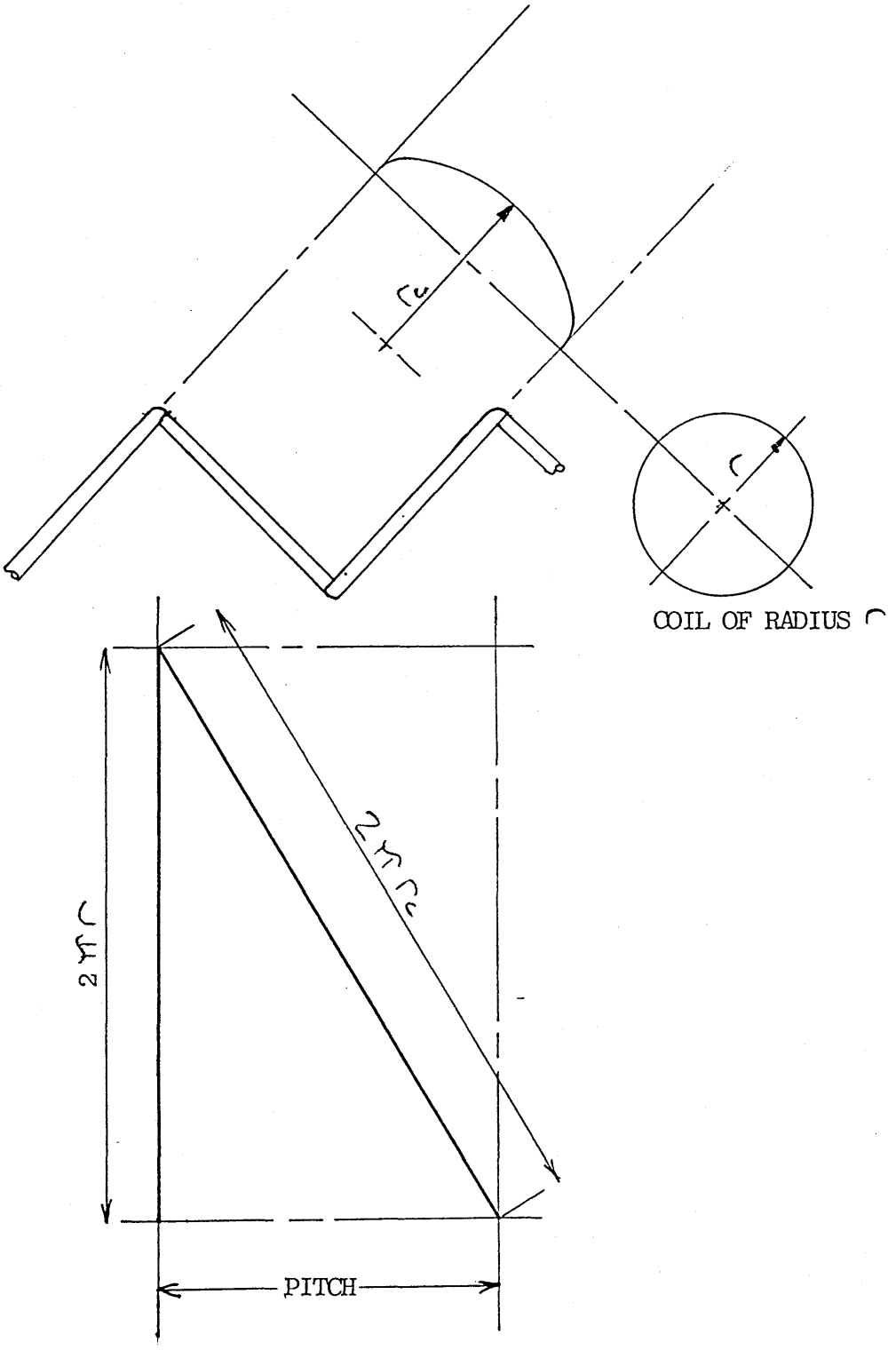

FIG. 3.6 (FROM DEVELOPMENT SHOWN)
THE TRUE RADIUS OF CURVATURE

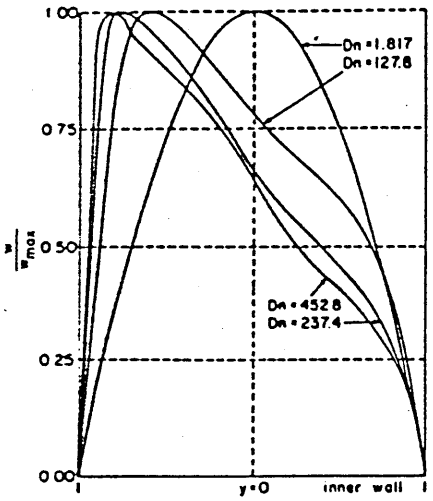

Axial velocities as a function of radius for various Dean numbers (horizontal profiles).

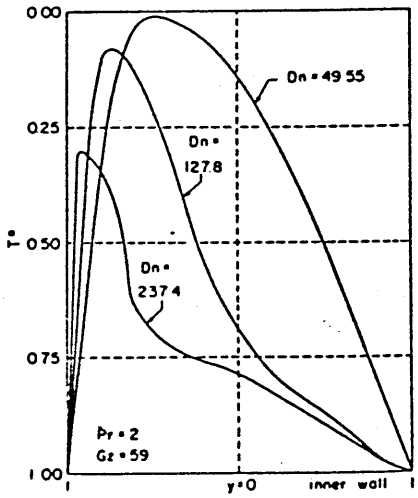

Temperature as a function of radius for various Dean numbers (horizontal profiles).

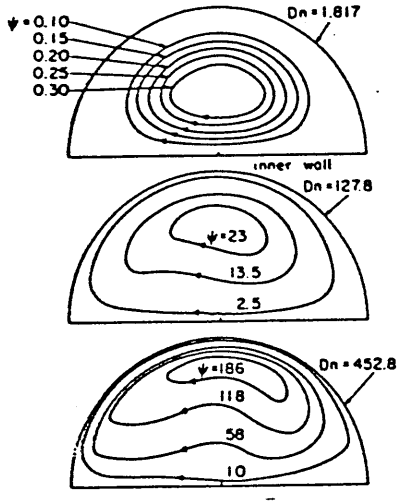

Stream function profiles for various Dean numbers.

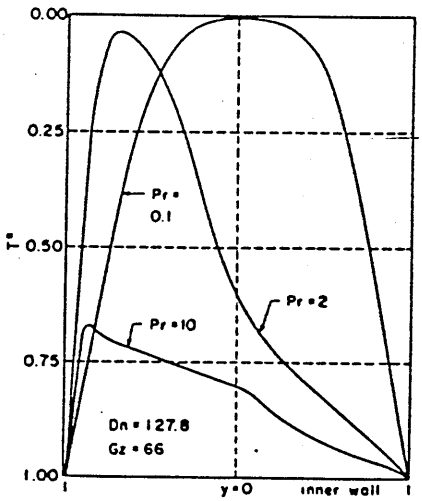

Temperature as a function of radius for various Prandtl numbers (horizontal profiles).

FIG. 3.7 TARBULL AND SAMUELS VELOCITY AND TEMPERATURE PROFILES

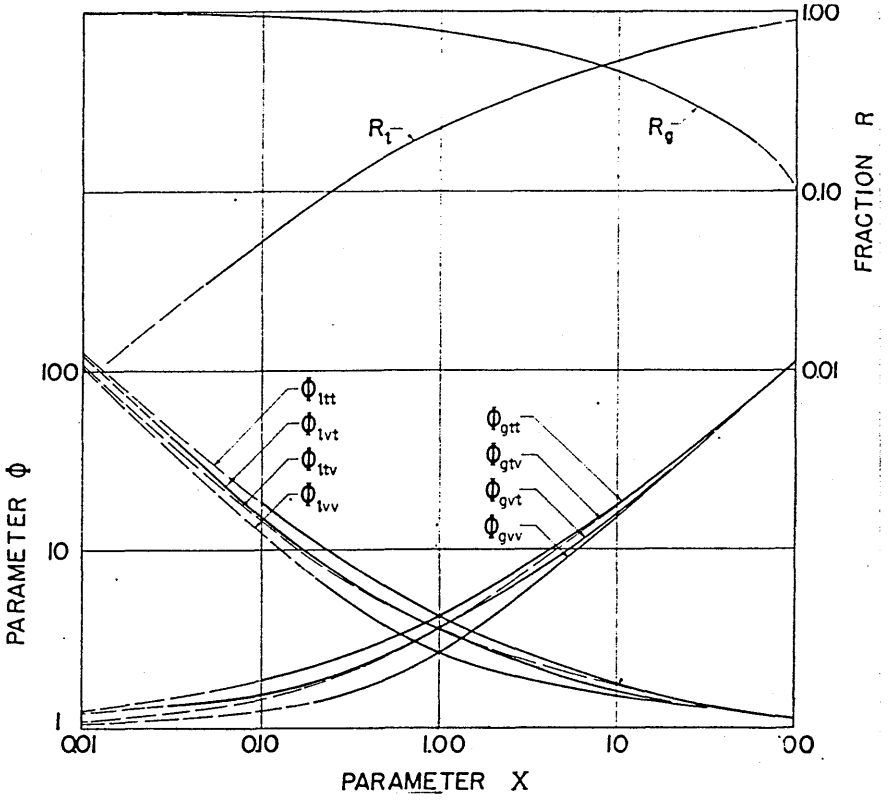

FIG. 3.8 FAIRED CURVES SHOWING THE RELATIONSHIP BETWEEN ϕ_l ϕ_g R_l AND R_g PROPOSED BY LOCKART & MARTINELLI FOR ALL FLOW MECHANISMS

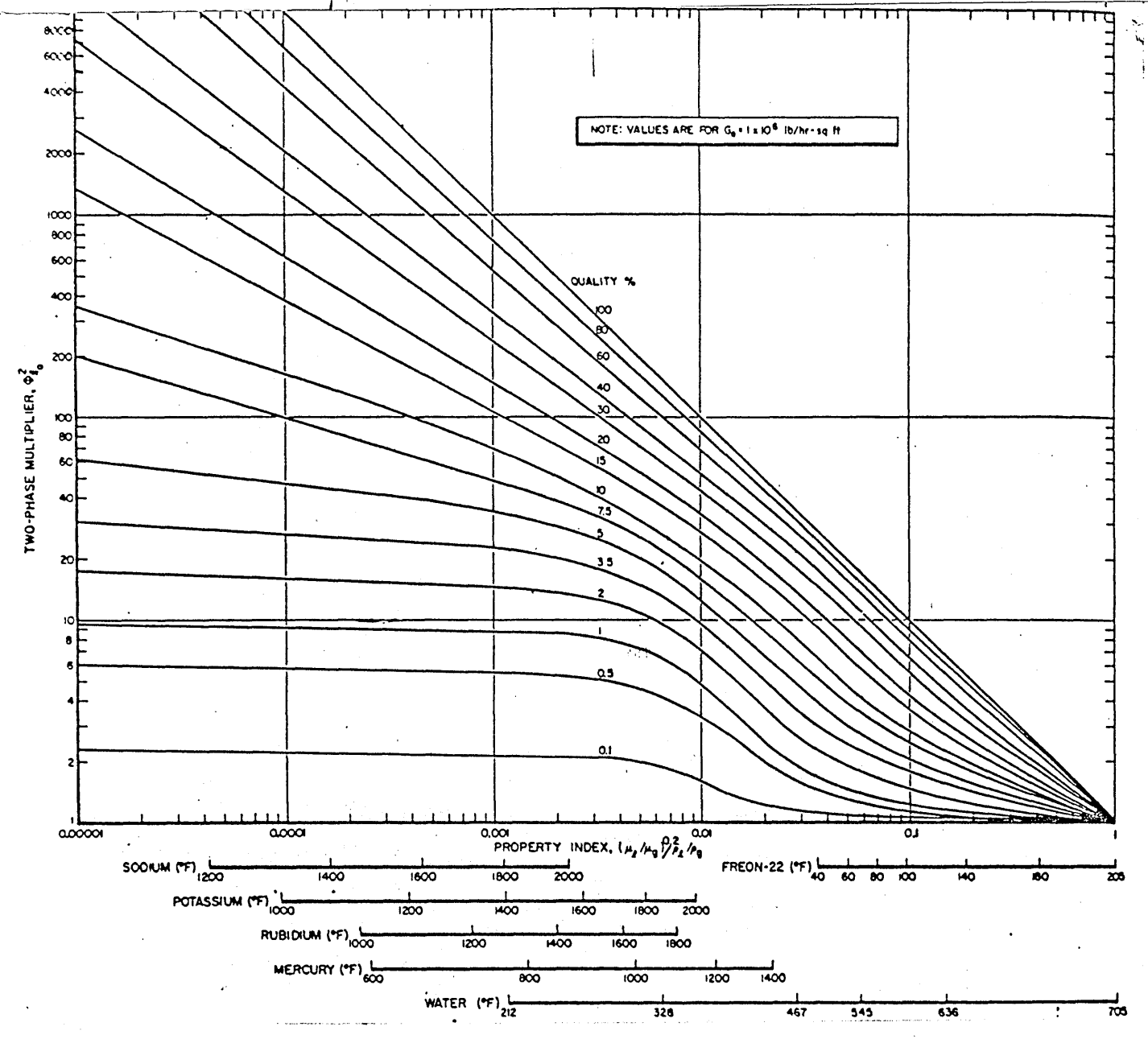

FIG, 3,9 TWO-PHASE FRICTION PRESSURE DROP CORRELATION PROPOS BY BAROCZY(37)

NOTE:- THIS IS FOR FIXED MASS FLUX VAL

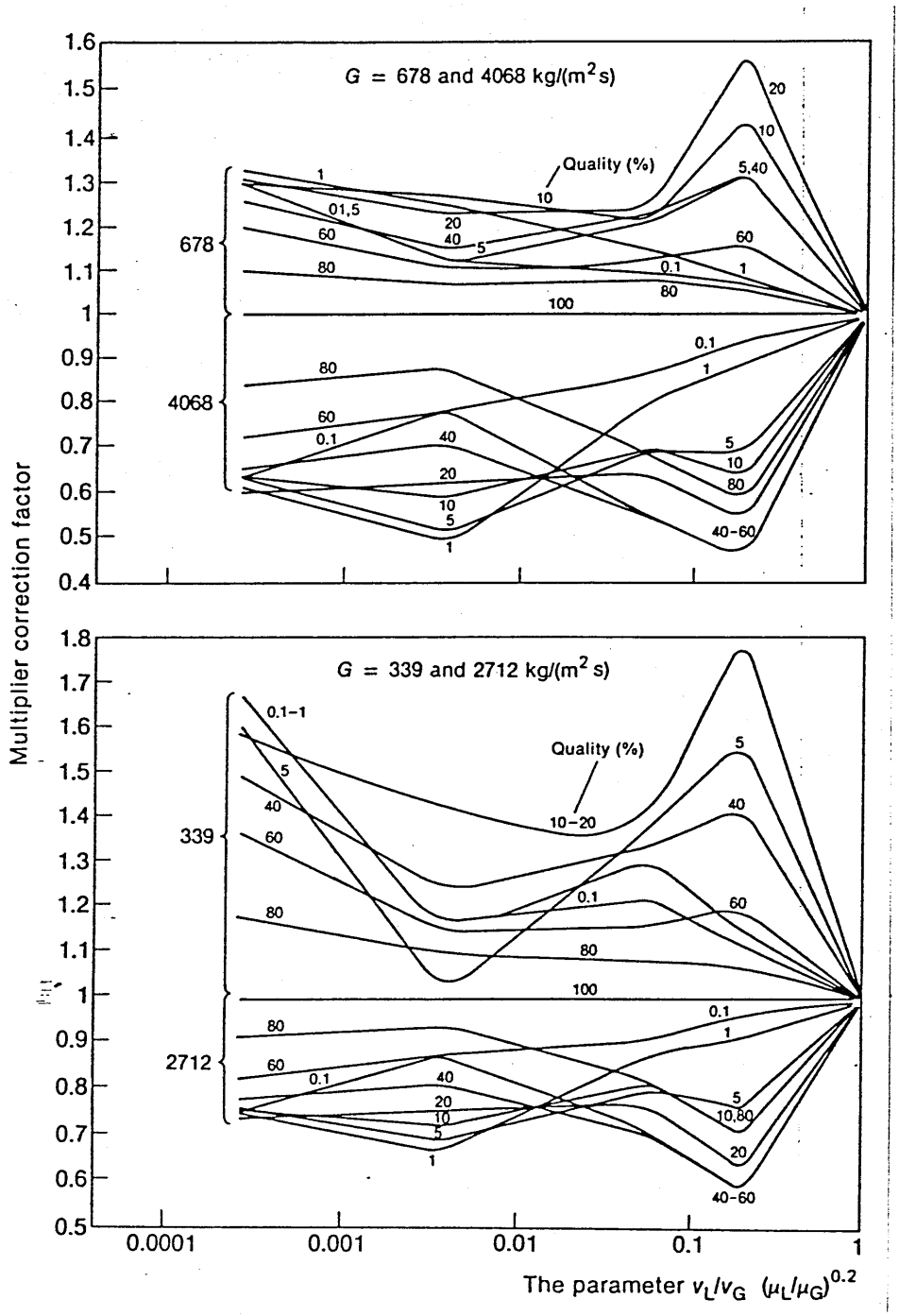

FIG. 3.10 MASS FLUX CORRECTION CURVES FROM BAROCZY(33), FOR VARIOUS FIXED MASS FLUX VALUES

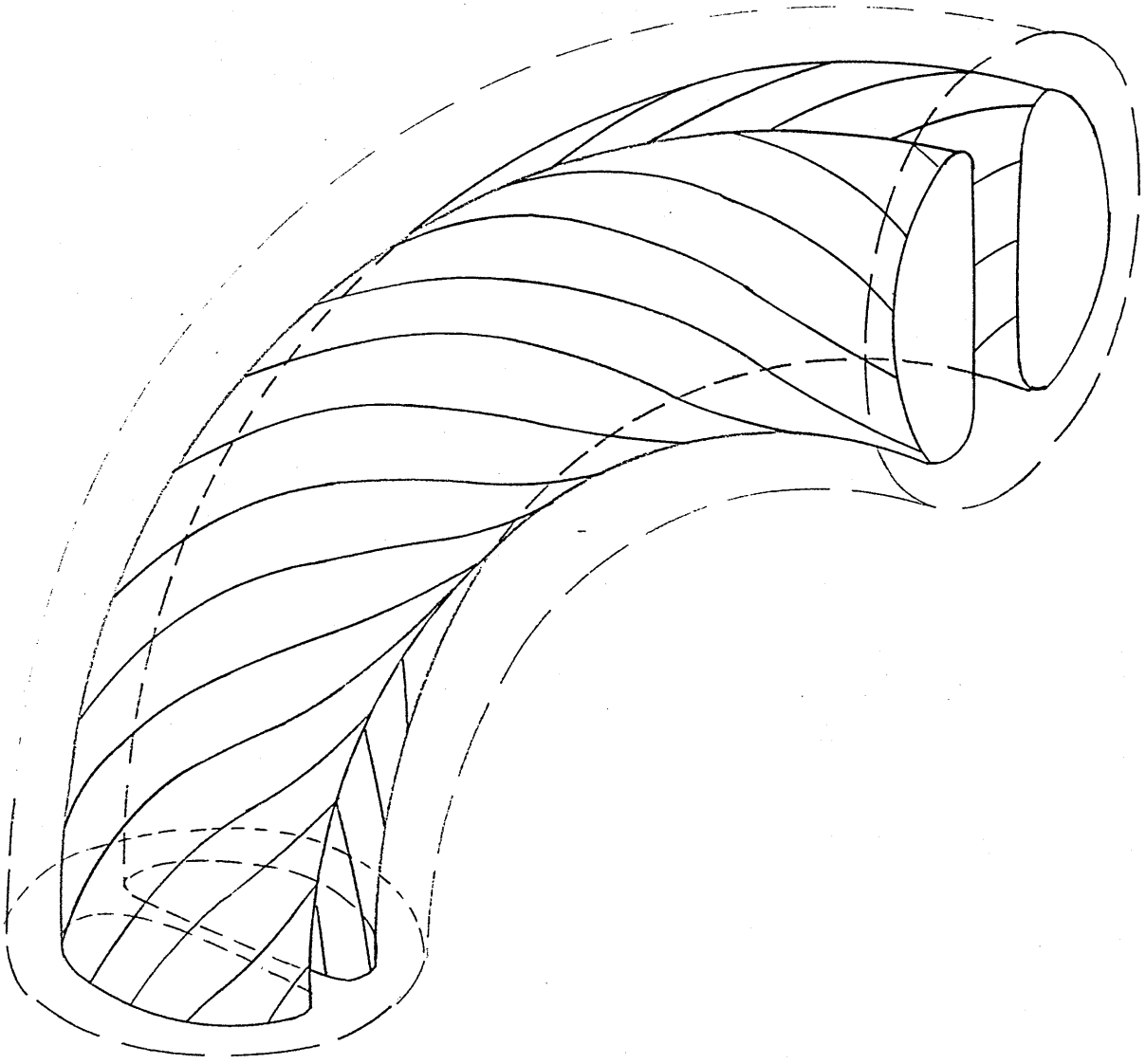

FIG. 3.11 SECONDARY FLOW IN A BEND FROM LACEY(25)

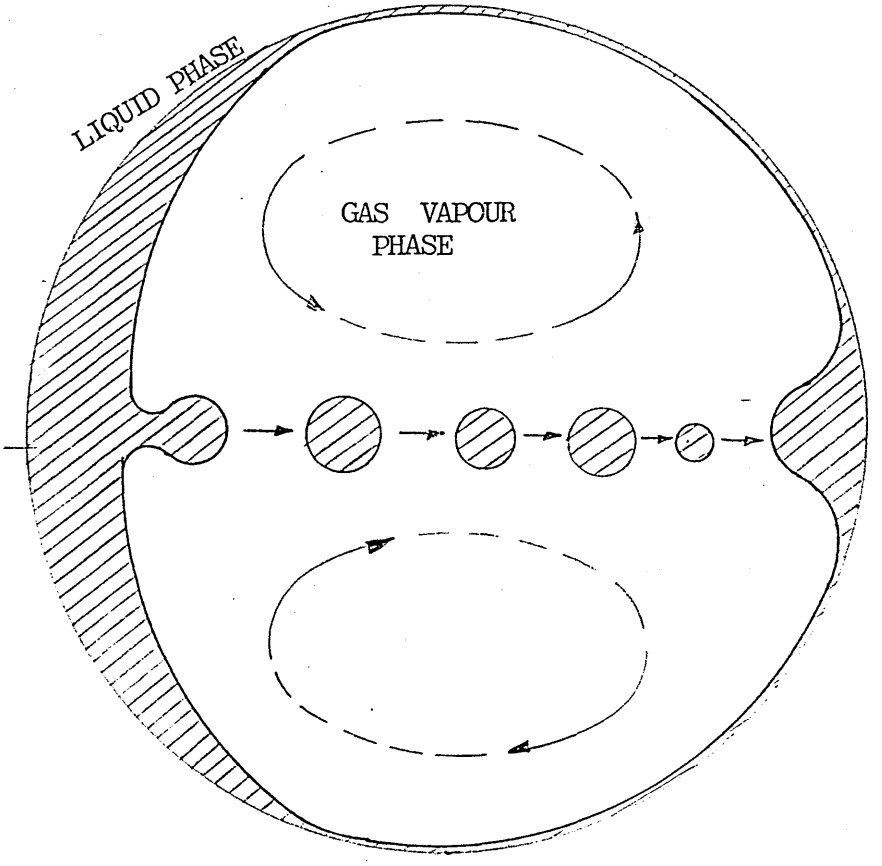

FIG. 3.12 HIGH QUALITY FLOW LIQUID ENTRAINMENT FROM LACEY(25)

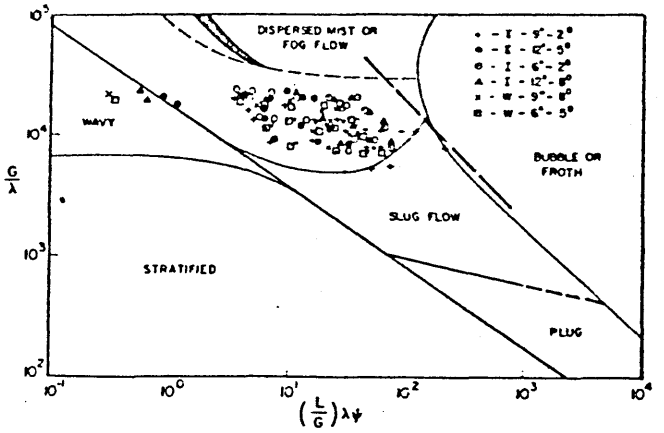

comparison of the data for annular and slug-annular flow with the predictions by Baker.

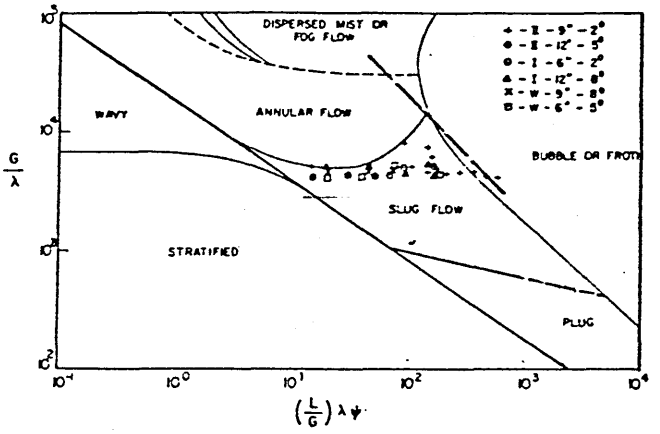

comparison of the data for slug flow with the predictions by Baker.

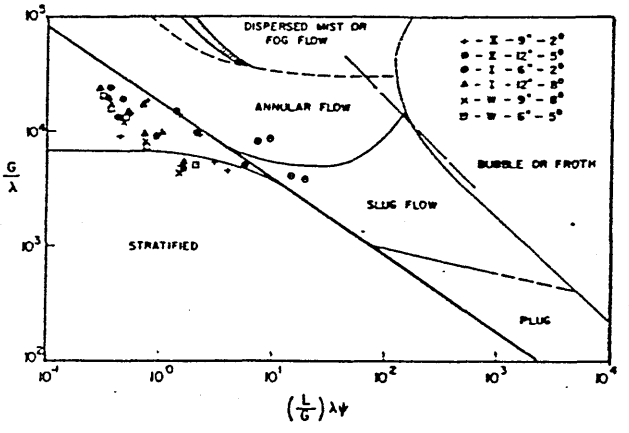

comparison of the data for wavy-stratified flow with the predictions by Baker.

FIG. 3.13 BAKER PLOT (BANNERJEE, RHODES AND SCOTT)

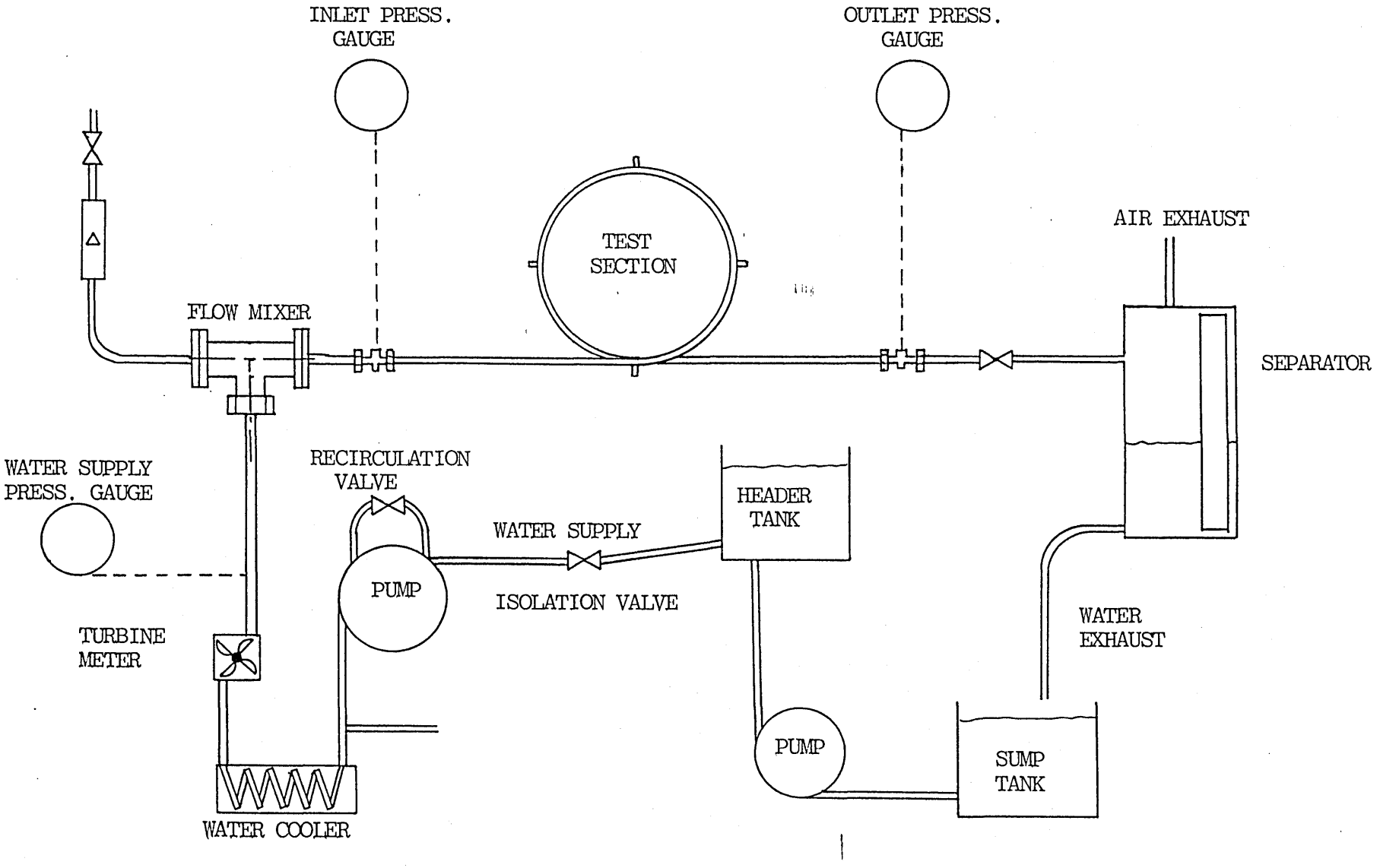

FIG. 4.1 TEST LOOP DIAGRAM

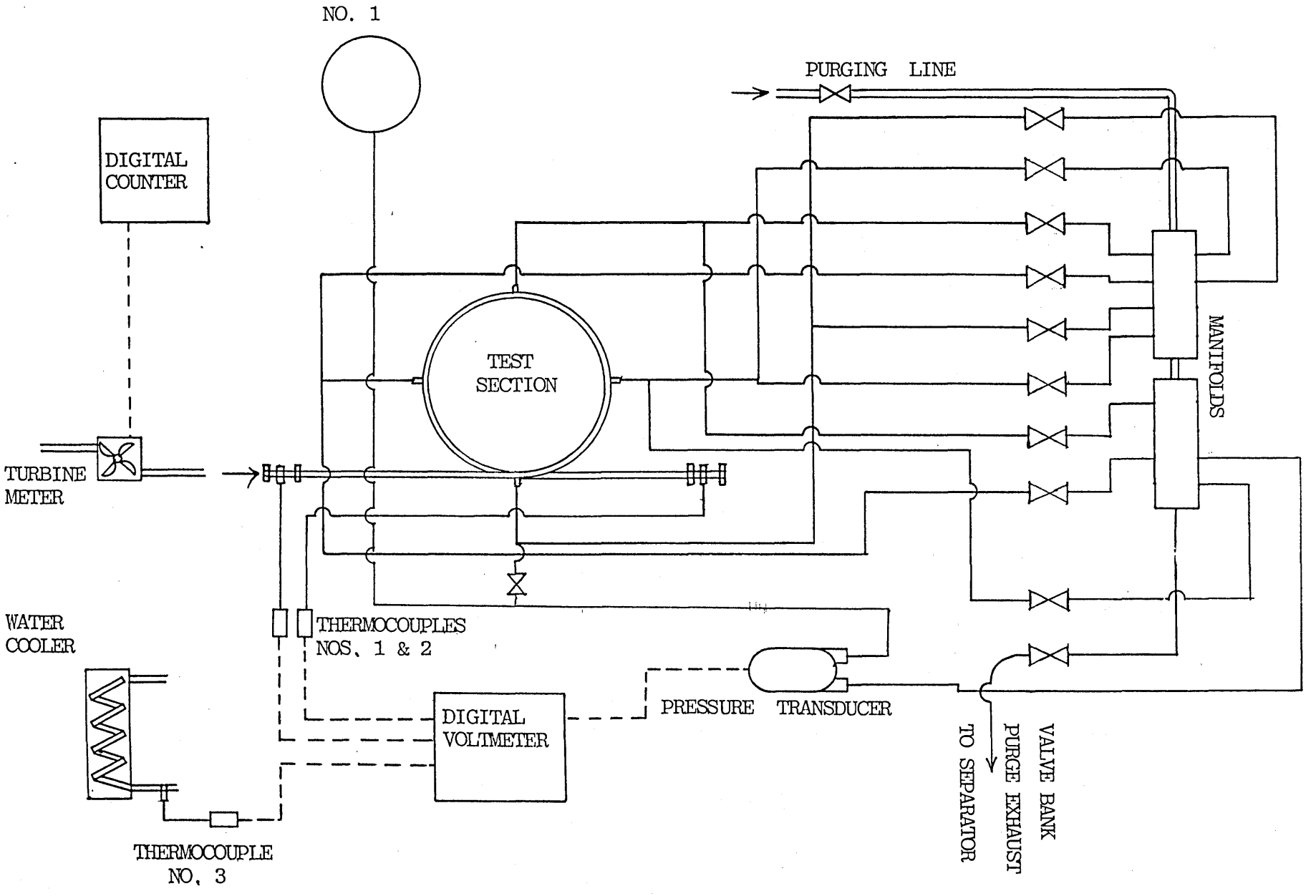

FIG. 4.2 PRESSURE TAPPING CIRCUIT

Tube Bore = .0077

Flux KG/M^2.S	Rey No	Frict Fac
16533.	93756.	.00431
15242.	87791.	.00440
13700.	83159.	.00458
12499.	76570.	.00458
10947.	67409.	.00467
9566.	59406.	.00481
8110.	50923.	.00492
6785.	43081.	.00491
5319.	34304.	.00527
3901.	25671.	.00590
2463.	16656.	.00610

STRAIGHT TUBE SINGLE-PHASE WATER DATA

FIG. 5.1

Tube Bore = .0124

Flux KG/M^2.S	Rey No	Frict Fac
7236.	65834.	.00491
6565.	59812.	.00510
5878.	53720.	.00515
5128.	47055.	.00509
4406.	42140.	.00514
3681.	35739.	.00570
2989.	29538.	.00581
2229.	22517.	.00644
1503.	15531.	.00697

FIG. 5.2

Tube Bore = .0077

Flux KG/M^2.S	Rey No	Frict Fac
353.64	151943.	.00275
315.40	135268.	.00304
275.30	117761.	.00336
228.30	97538.	.00396
185.77	79259.	.00461
153.02	65209.	.00486
120.97	51516.	.00568
89.52	38097.	.00658
58.02	24666.	.00722
464.83	199994.	.00247

STRAIGHT TUBE SINGLE-PHASE AIR DATA

FIG, 5.3

—

Tube Bore = .0134

Flux KG/M^2.S	Rey No	Frict Fac
264.44	186933.	.00398
251.94	178048.	.00423
234.83	165814.	.00405
214.62	151446.	.00411
198.54	140034.	.00430
172.57	121578.	.00431
145.11	101754.	.00486
123.34	86180.	.00554
96.49	67138.	.00565
61.25	42433.	.00563

FIG. 5.4

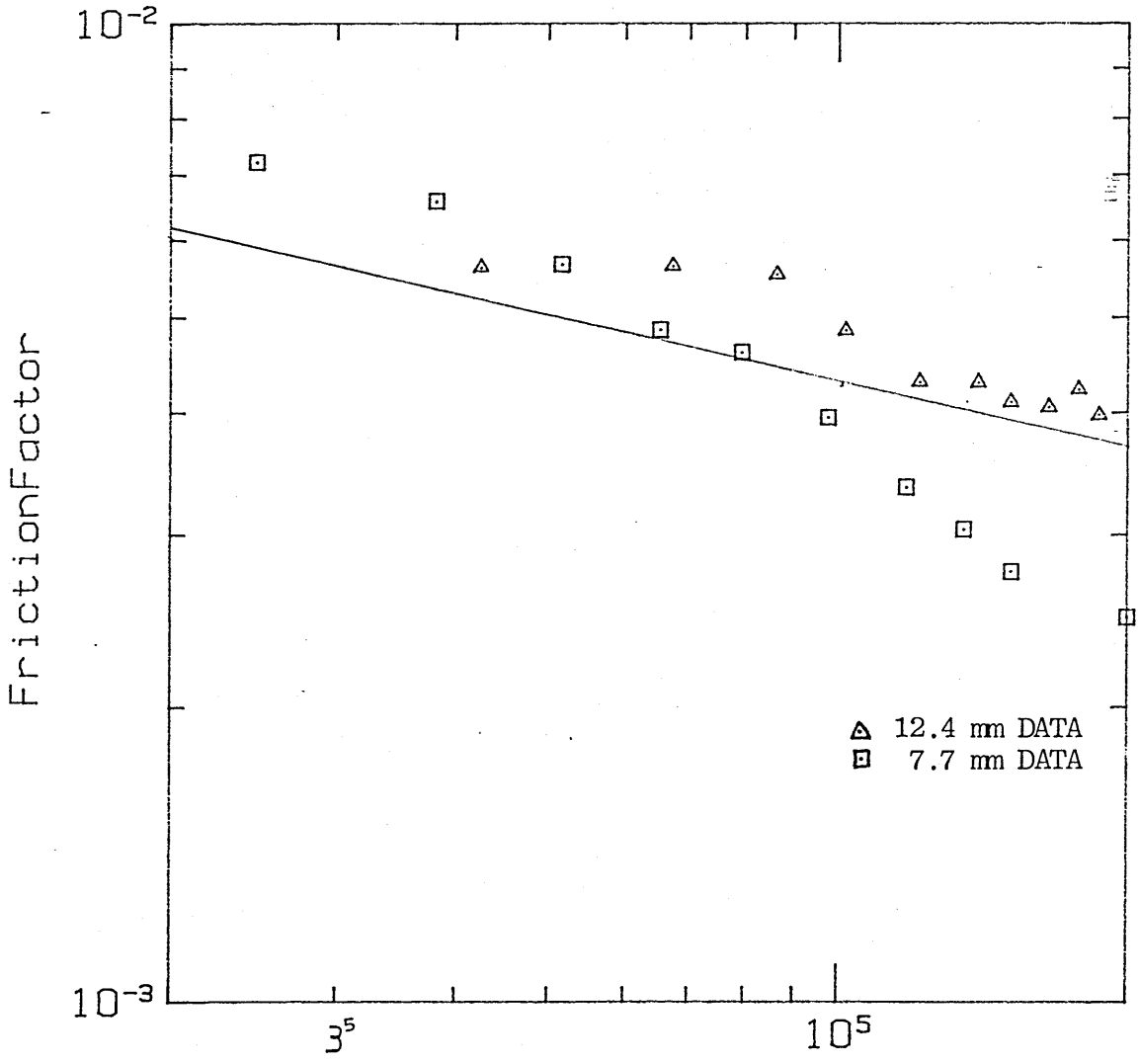

FrictionFactor / Reynolds Number
Single Phase Air, Straight Tube

FIG. 5.5

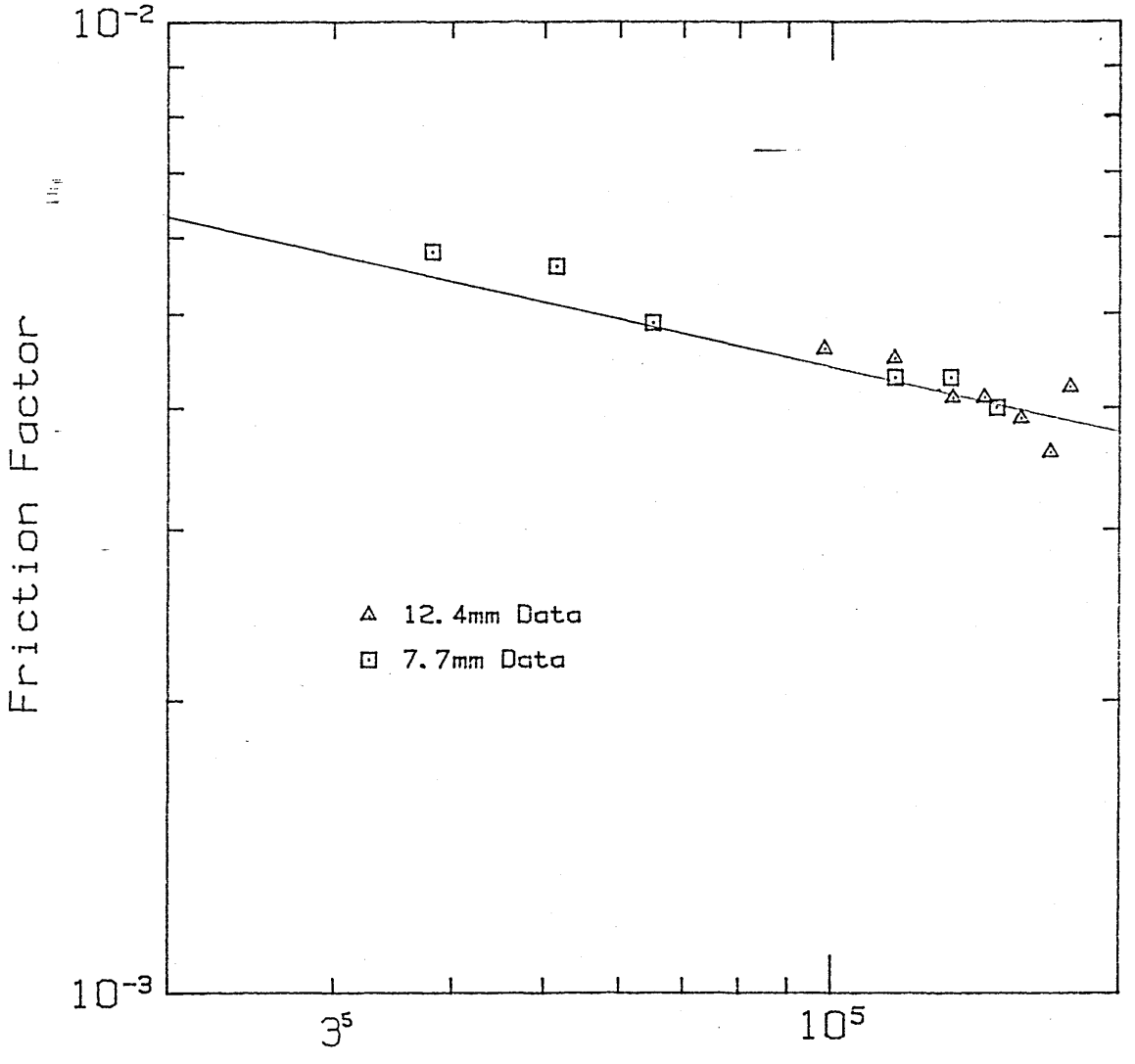

Friction Factor / Reynolds Number
Air , Straight Tube , Fanno Method

FIG. 5.6

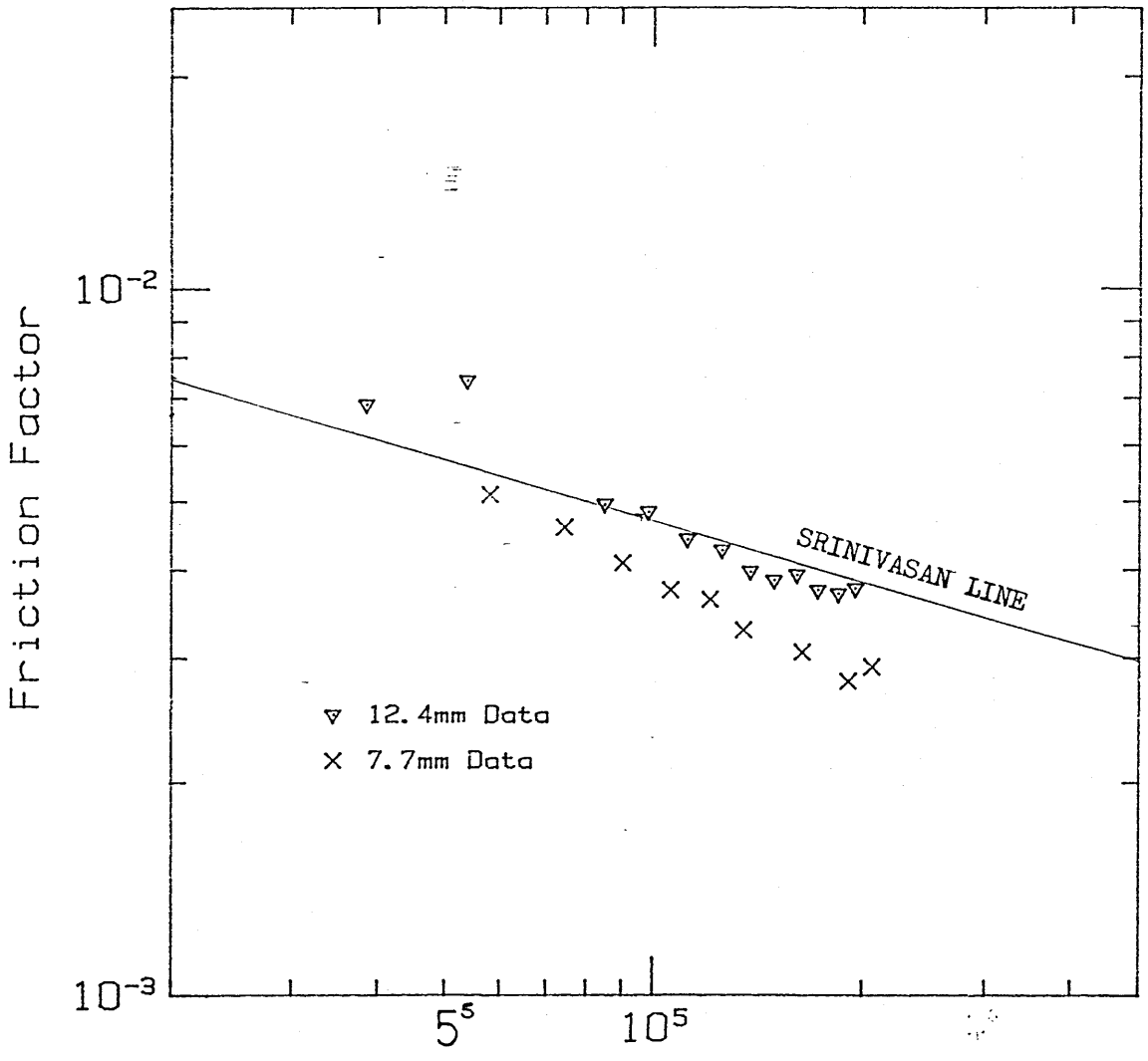

Friction Factor / Reynolds Number
Single Phase Air , Coiled Tube

FIG. 5.7

Tube Bore = .0124 Coil Mean Diameter = .2739

Flux KG/M^2.S	Re(d/D)^2	Rey No	Fric Fac	Fc(D/d)^0.5
275.47	400.13	195226.	.00377	.01770
260.15	378.03	184447.	.00371	.01742
243.15	353.29	172373.	.00375	.01761
226.54	329.22	160630.	.00394	.01853
210.23	305.52	149068.	.00387	.01817
194.26	282.33	137752.	.00398	.01871
176.98	257.03	125408.	.00427	.02006
158.22	229.33	111892.	.00442	.02078
139.32	201.26	98199.	.00484	.02272
120.84	174.14	84966.	.00496	.02330
76.77	110.23	53780.	.00742	.03487
55.15	78.90	38495.	.00686	.03223

Tube Bore = .0077 Coil Mean Diameter = .0745

Flux KG/M^2.S	Re(d/D)^2	Rey No	Fric Fac	Fc(D/d)^0.5
474.76	2190.94	206168.	.00292	.00909
440.27	2025.23	190574.	.00279	.00867
379.75	1739.18	163657.	.00306	.00954
313.45	1431.92	134744.	.00329	.01024
281.32	1283.01	120732.	.00363	.01131
246.90	1124.71	105836.	.00375	.01167
210.73	959.12	90253.	.00409	.01275
173.76	790.22	74360.	.00460	.01432
135.16	616.86	58046.	.00512	.01594

COILED TUBE SINGLE-PHASE AIR DATA

FIG. 5.8

Tube Bore = .0124 Coil Mean Diameter = .2739

Flux KG/M2.s	Re(d/D)^2	Rev No	Frict Fac	Fc(D/d)^0.5
6981.	123.55	60279.	.00603	.02836
6034.	106.24	51834.	.00615	.02890
5477.	95.97	46824.	.00633	.02975
4967.	85.81	42355.	.00634	.02980
4384.	76.72	37431.	.00661	.03109
3851.	67.33	32853.	.00677	.03181
3301.	58.36	28477.	.00685	.03222
2697.	48.02	23429.	.00710	.03336
2187.	39.26	19154.	.00689	.03241
1696.	30.93	15093.	.00715	.03360

Tube Bore = .0077 Coil Mean Diameter = .0745

Flux KG/M2.s	Re(d/D)^2	Rev No	Frict Fac	Fc(D/d)^0.5
10214.	621.48	58481.	.00613	.01908
9500.	579.87	54566.	.00653	.02034
8630.	524.15	49323.	.00658	.02050
7675.	463.66	43630.	.00696	.02168
6715.	406.23	38226.	.00691	.02152
5750.	348.72	32815.	.00709	.02208
4846.	295.50	27807.	.00711	.02214
3877.	237.56	22354.	.00710	.02212
2978.	184.56	17367.	.00761	.02371
1999.	125.28	11789.	.00853	.02656

COILED TUBE SINGLE-PHASE WATER DATA

FIG, 5,9

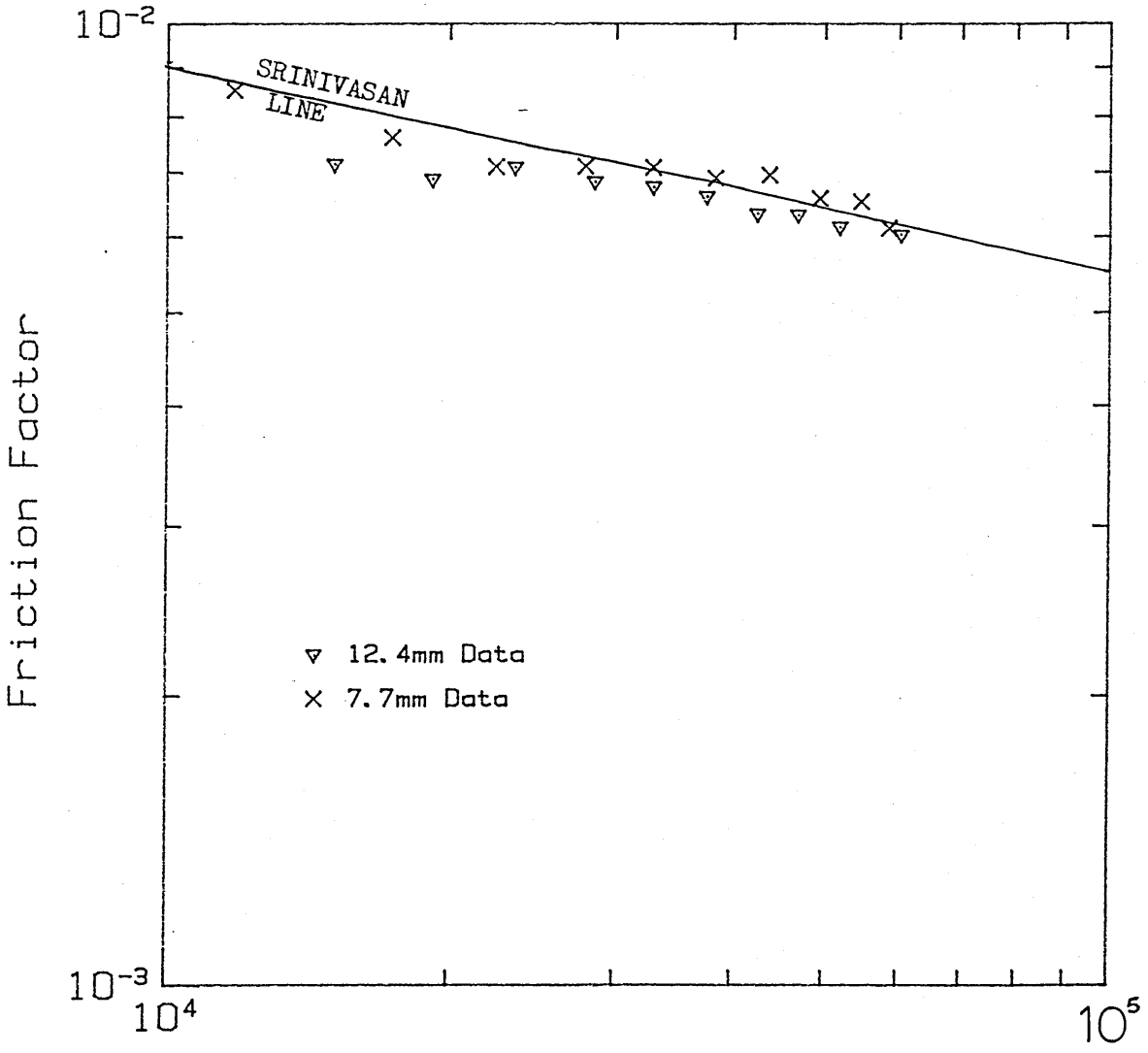

Friction Factor / Reynolds Number
Single Phase Water In Coiled Tubes

FIG. 5.10

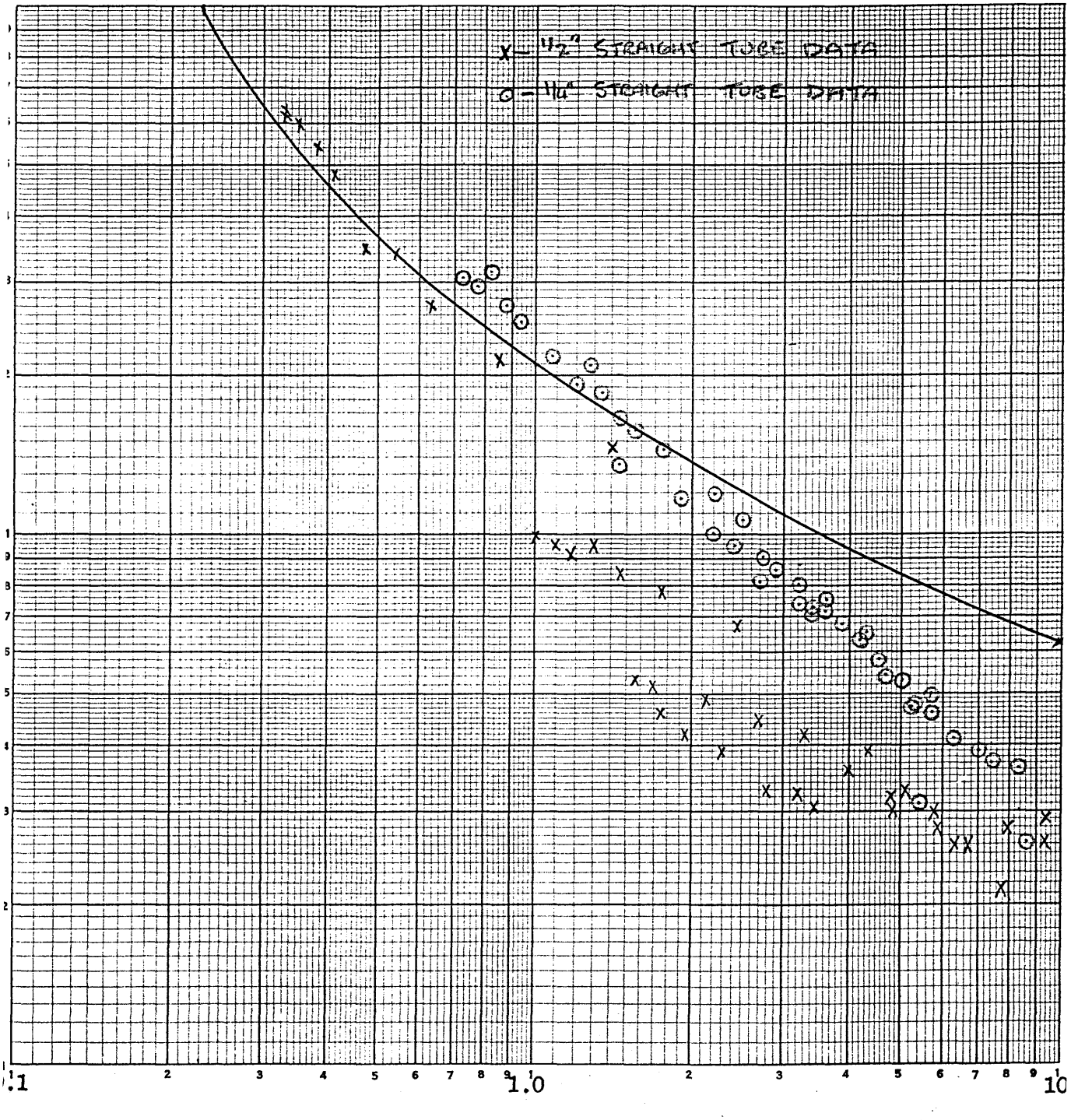

STRAIGHT TUBE TEST DATA AGAINST LOCKART-MARTINELLI LINE

FIG. 5.11

SRINIVASAN'S SINGLE-PHASE EQUATION
USED IN TWO-PHASE MULTIPLIERS

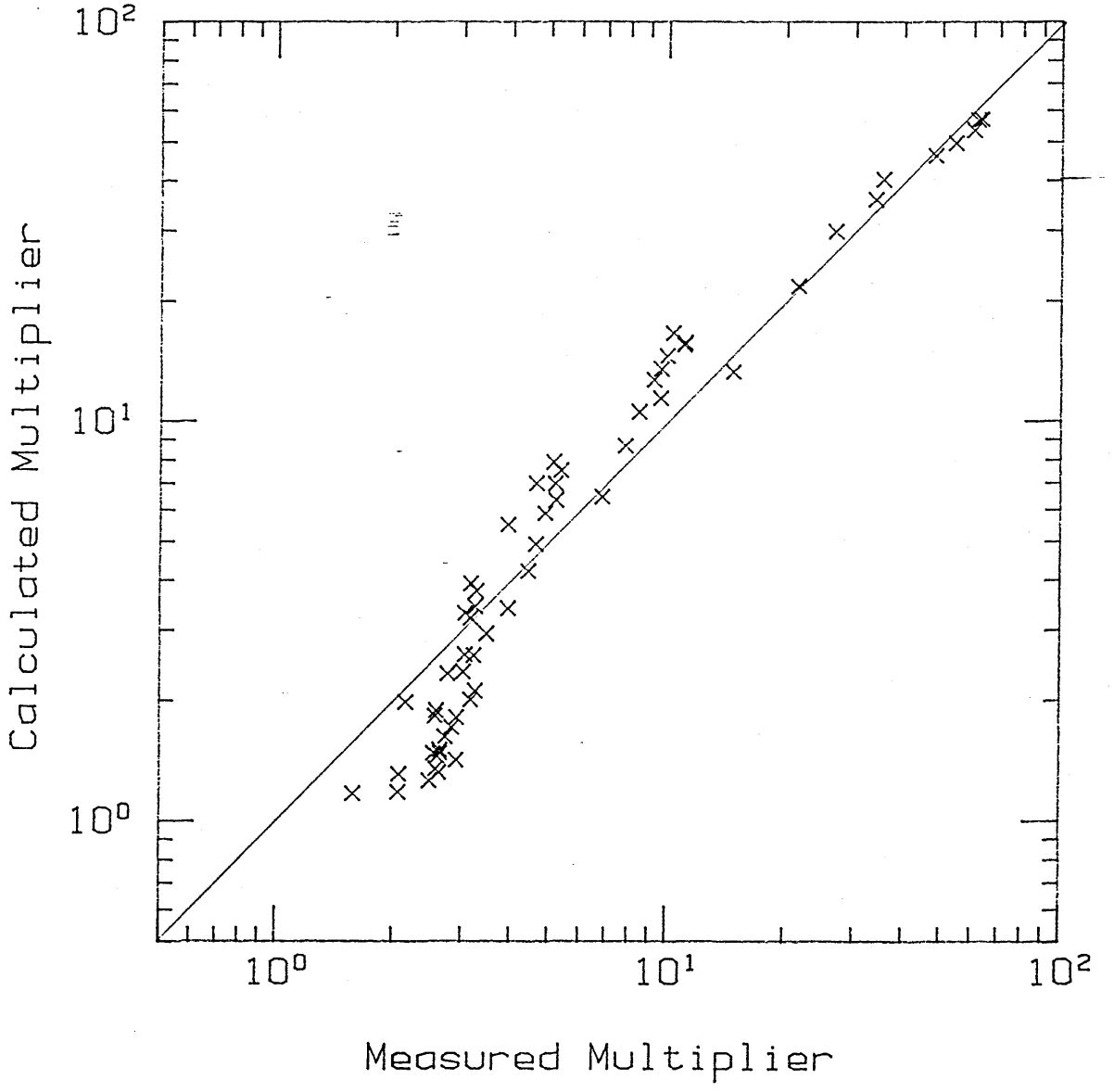

TWO-PHASE MULTIPLIER COMPARISON
FOR 1/2" STRAIGHT TUBE

FIG. 5.12

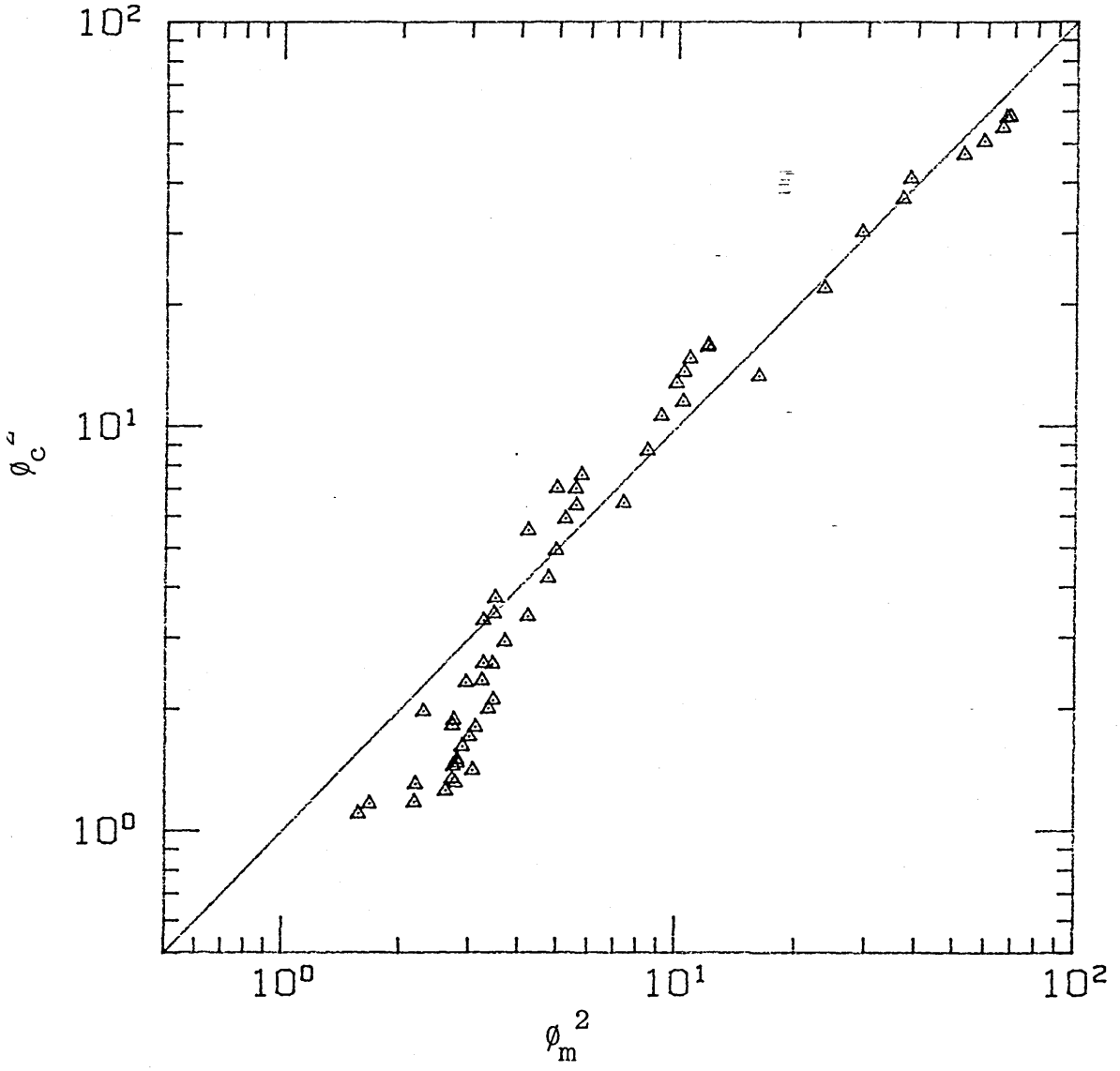

SINGLE-PHASE EQUATION FROM TEST USED
TWO-PHASE MULTIPLIER COMPARISON FOR ½" STRAIGHT TUBE

FIG. 5.13

SRINIVASAN'S SINGLE-PHASE EQUATION
USED IN TWO-PHASE MULTIPLIERS

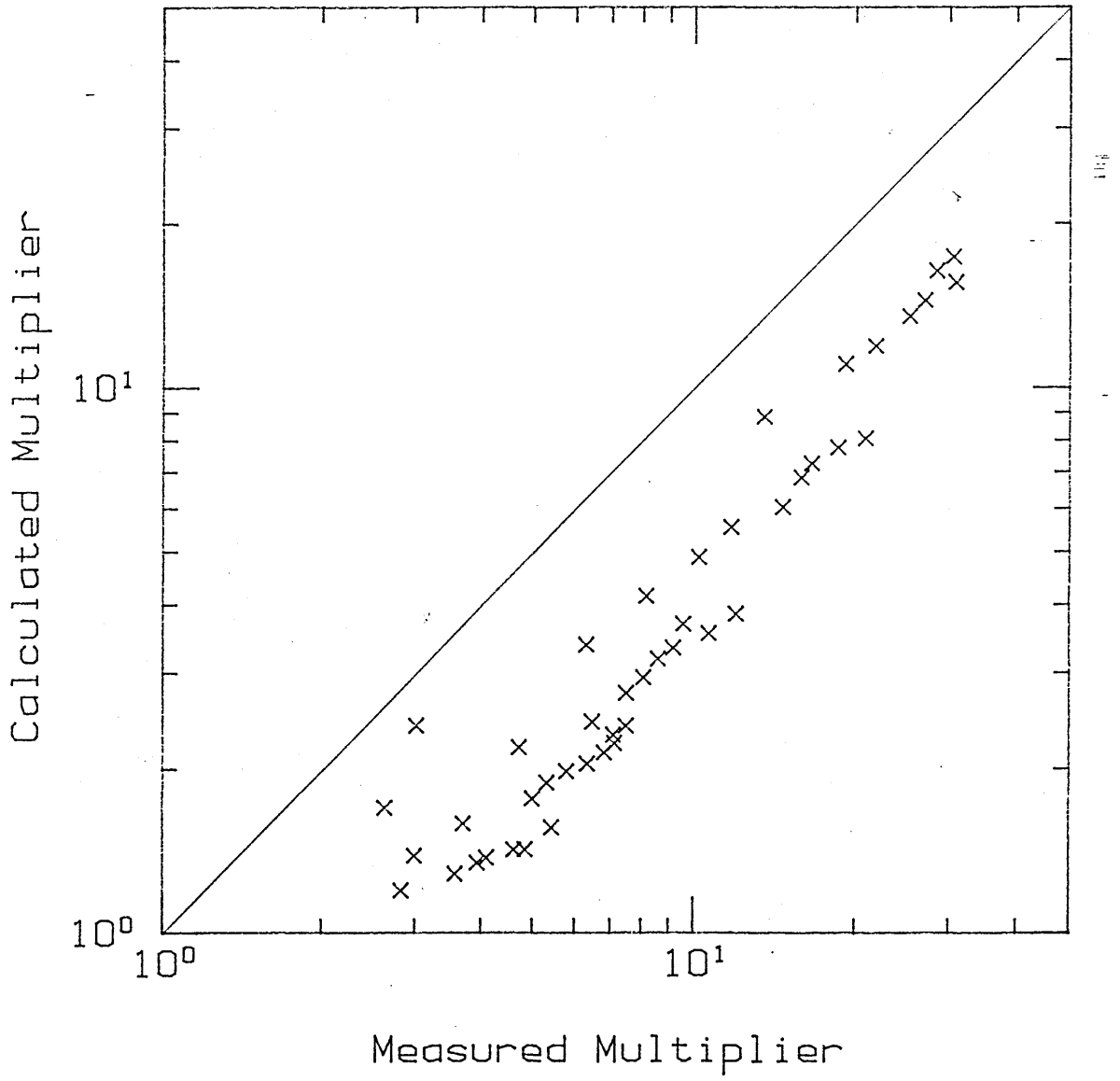

TWO-PHASE MULTIPLIER COMPARISON
FOR 1/4" STRAIGHT TUBE

FIG. 5.14

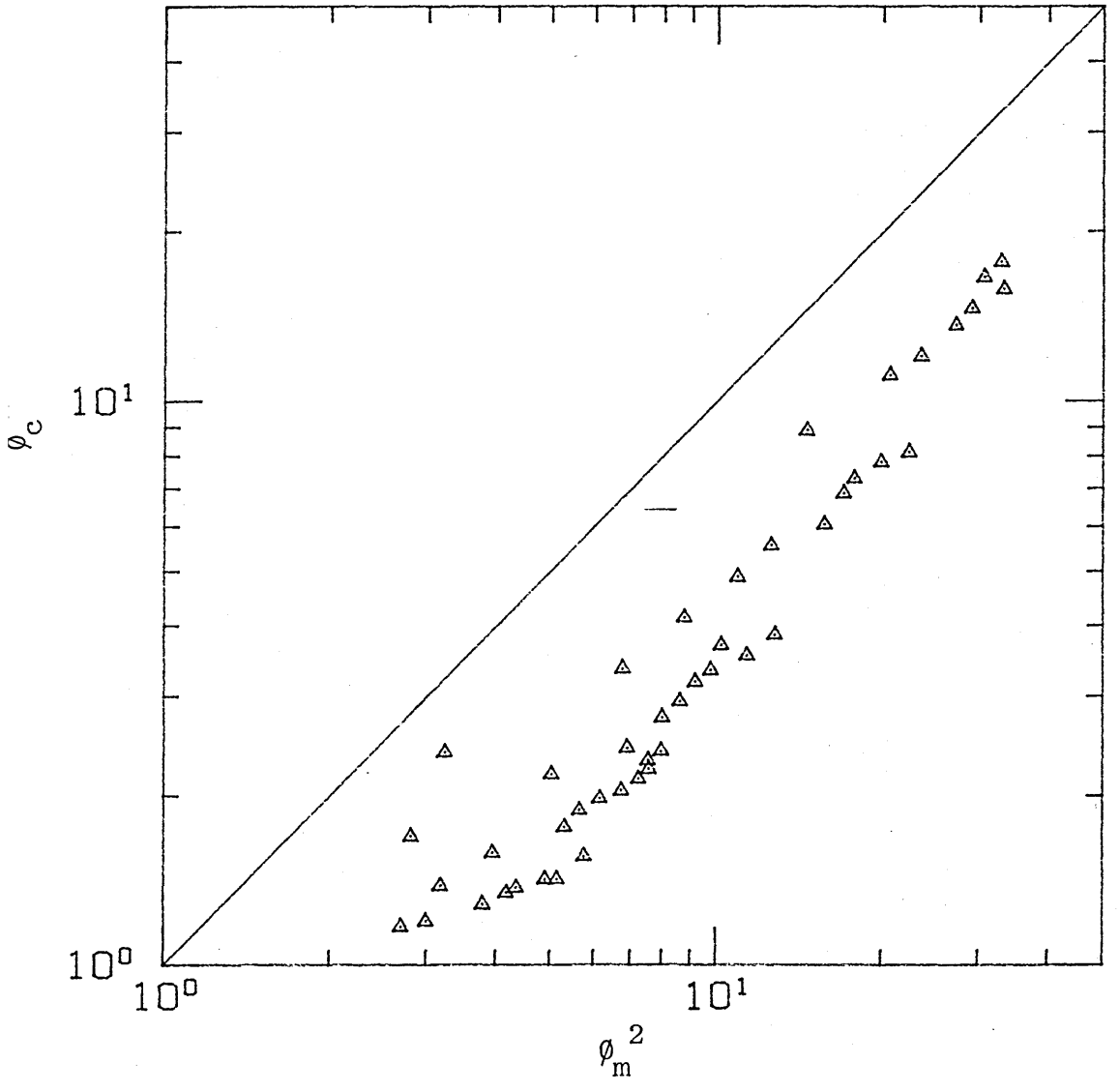

SINGLE-PHASE EQUATION FROM TEST USED
TWO-PHASE MULTIPLIER COMPARISON FOR $\frac{1}{4}$" STRAIGHT TUBE

FIG. 5.15

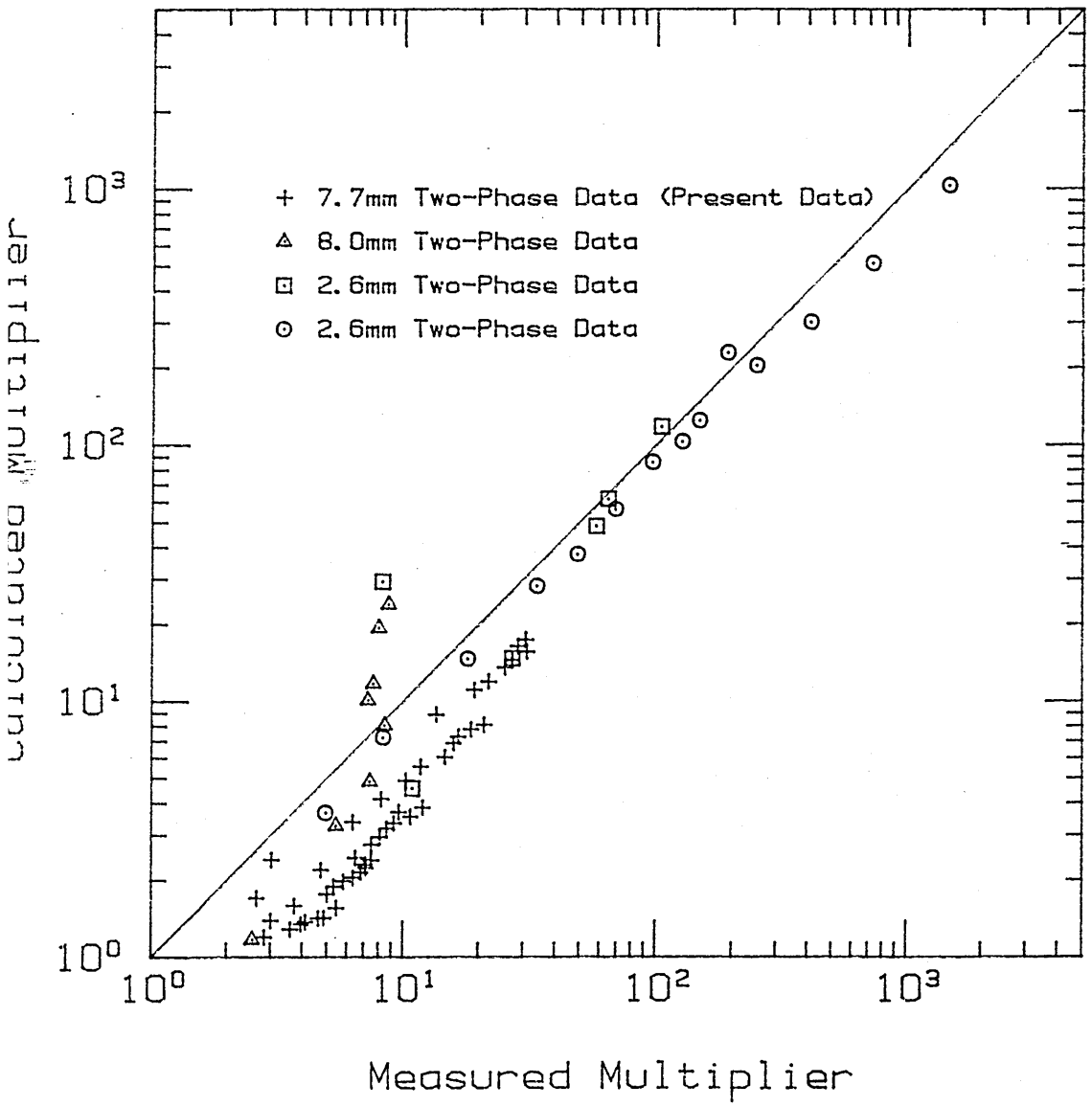

Two-Phase Multiplier Comparison
With Other Small Bore Data

FIG. 5.16

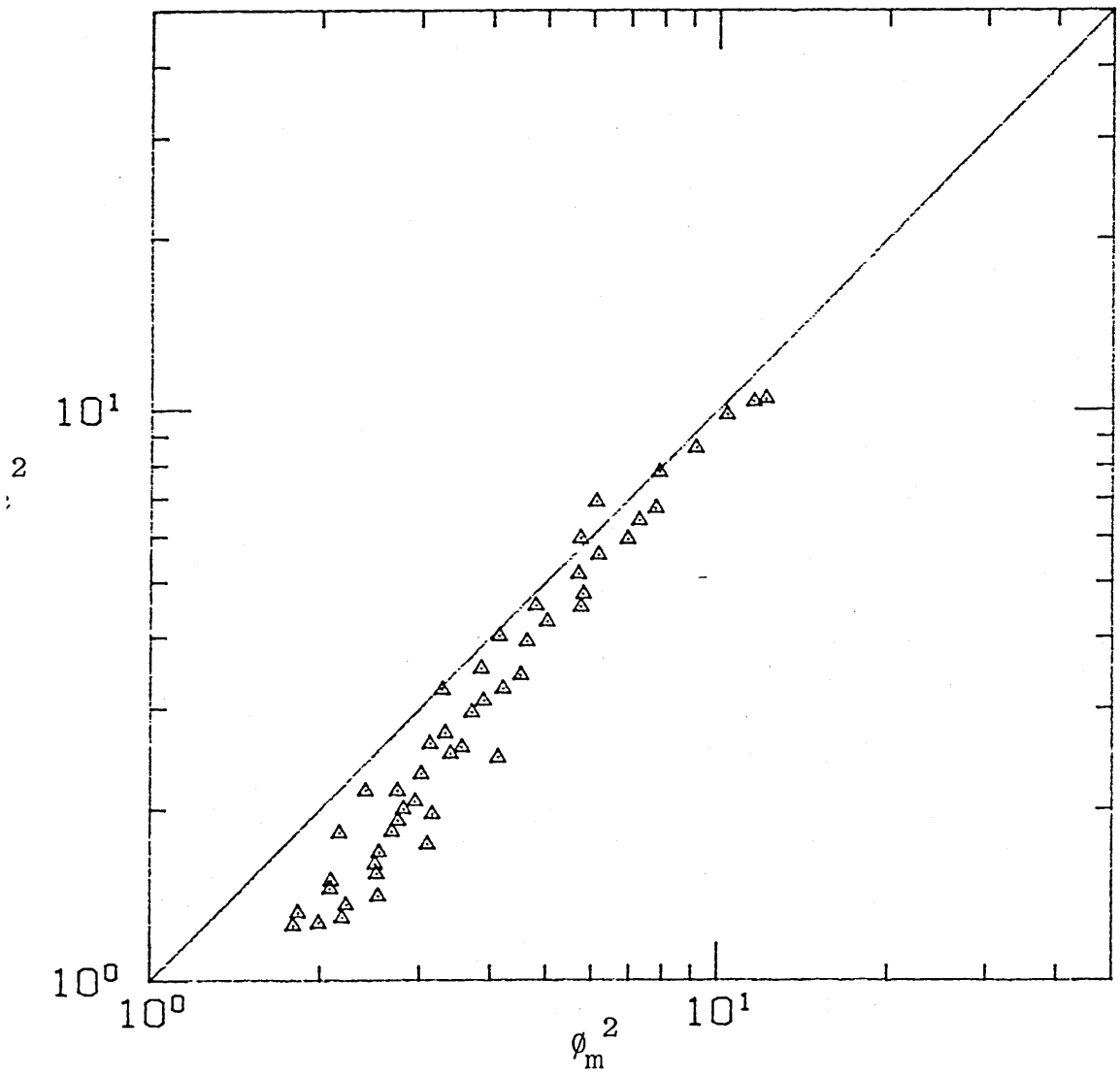

SMALL BORE COIL TWO-PHASE MULTIPLIERS USING SRINIVASAN CORRELATION FOR SINGLE PHASE FRICTION FACTOR

FIG. 5.17

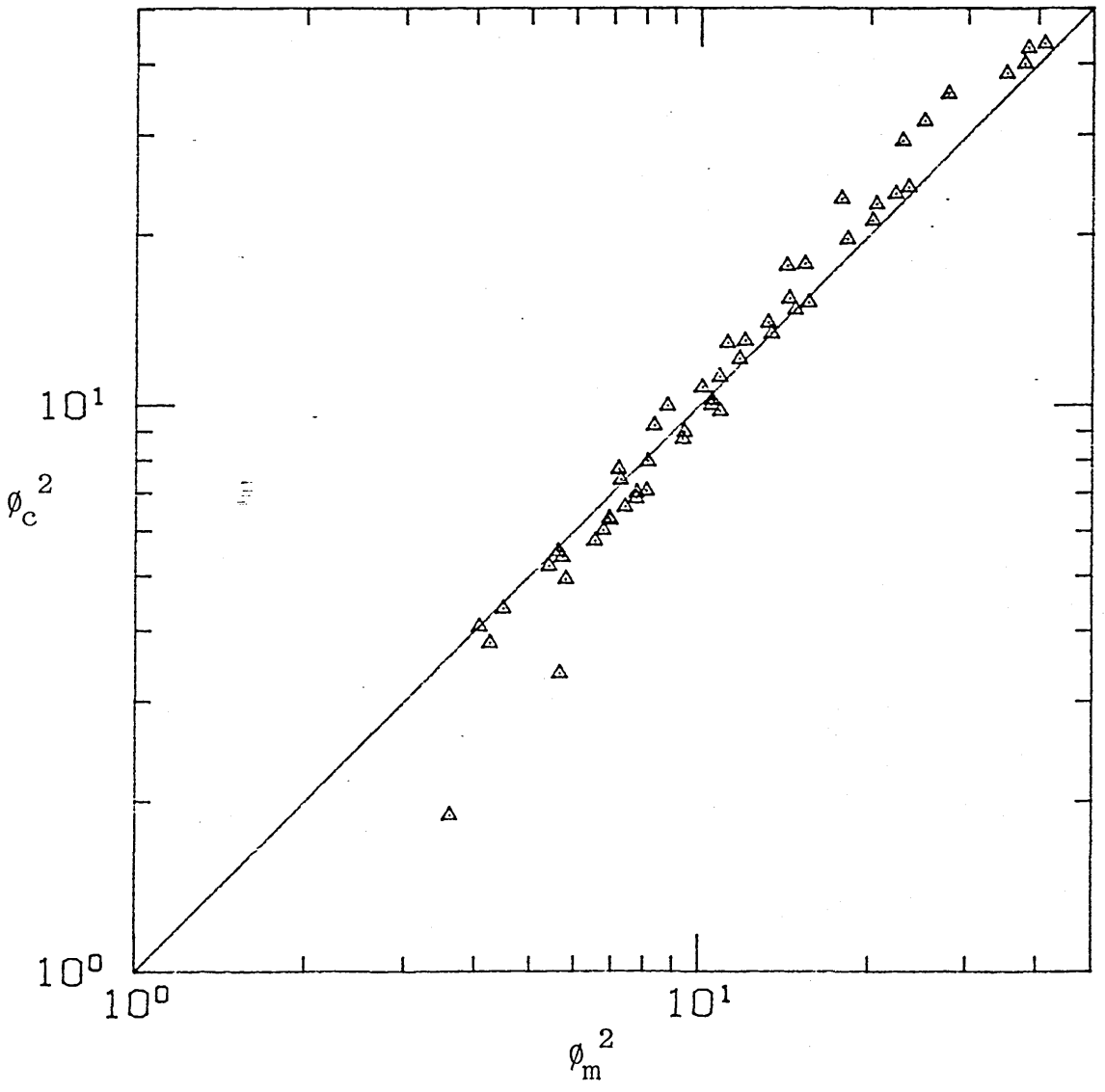

LARGE BORE COIL TWO-PHASE MULTIPLIERS USING SRINIVASAN CORRELATION FOR SINGLE PHASE FRICTION FACTOR

FIG. 5.18

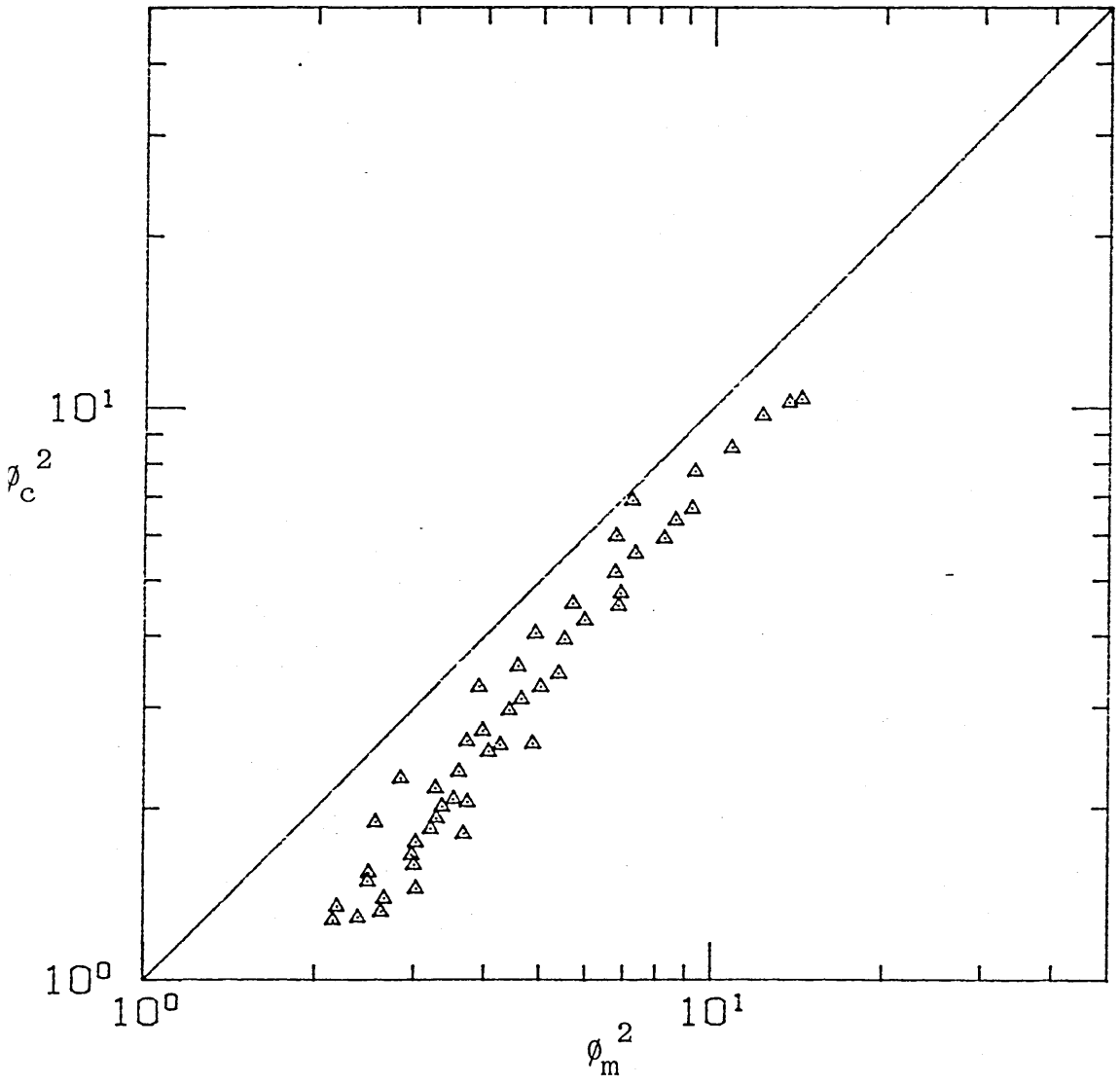

SMALL BORE COIL TWO-PHASE MULTIPLIERS USING TEST CORRELATION FOR SINGLE-PHASE FRICTION FACTOR

FIG. 5.19

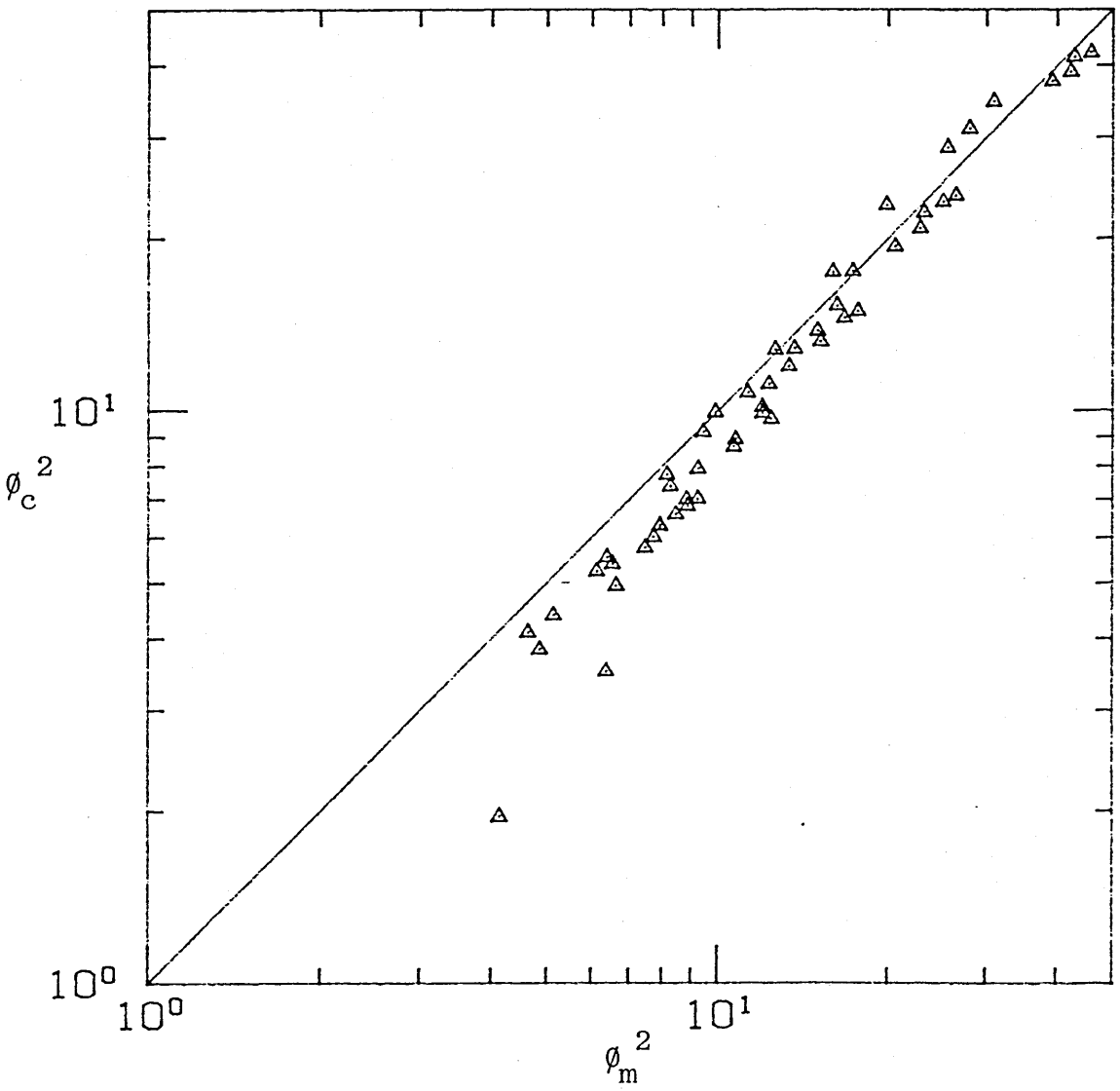

LARGE BORE COIL TWO-PHASE MULTIPLIERS USING TEST CORRELATION FOR SINGLE PHASE FRICTION FACTOR

FIG. 5.20

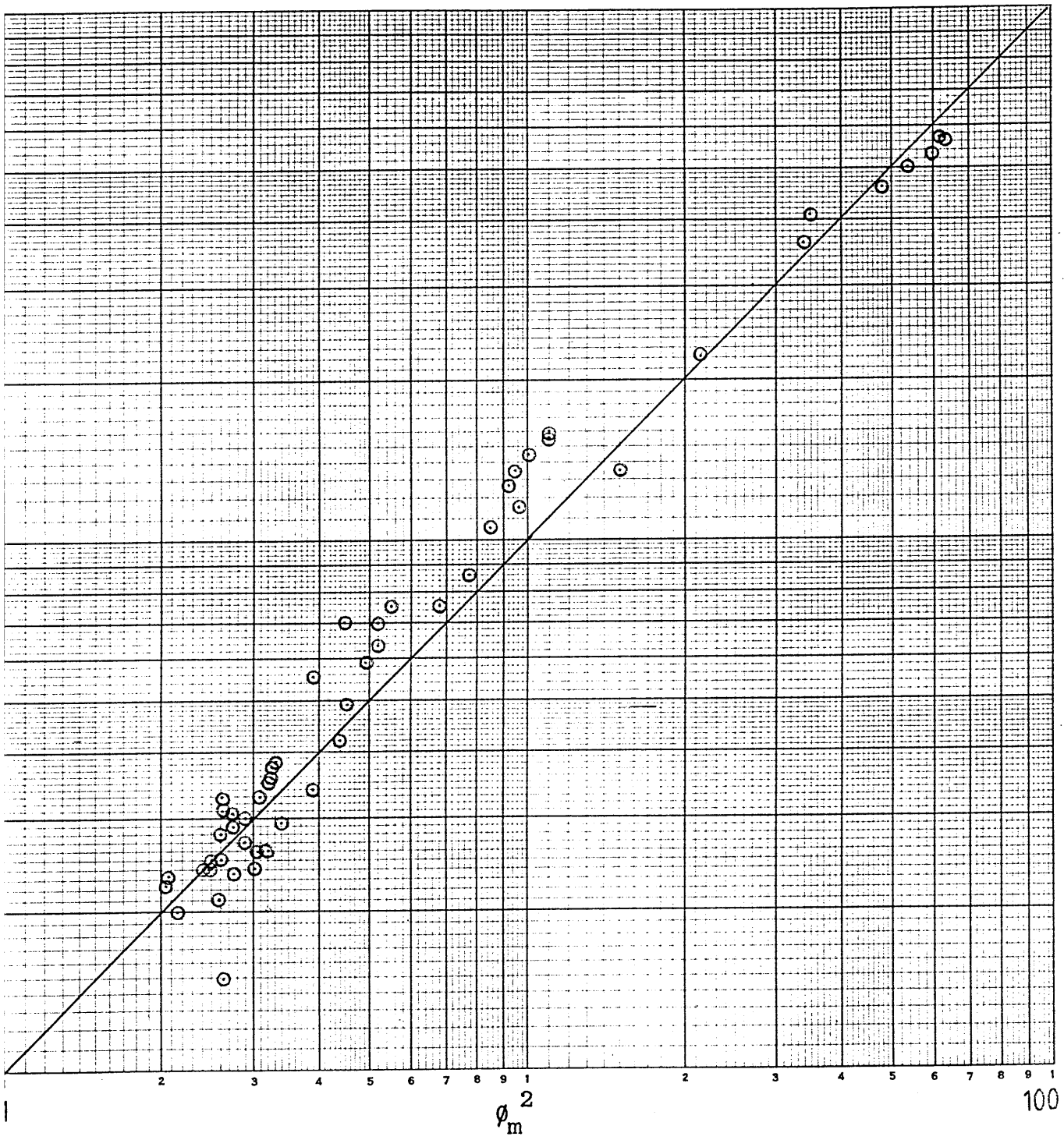

LARGE BORE STRAIGHT TUBE BY TEST CORRELATION

FIG. 5.21

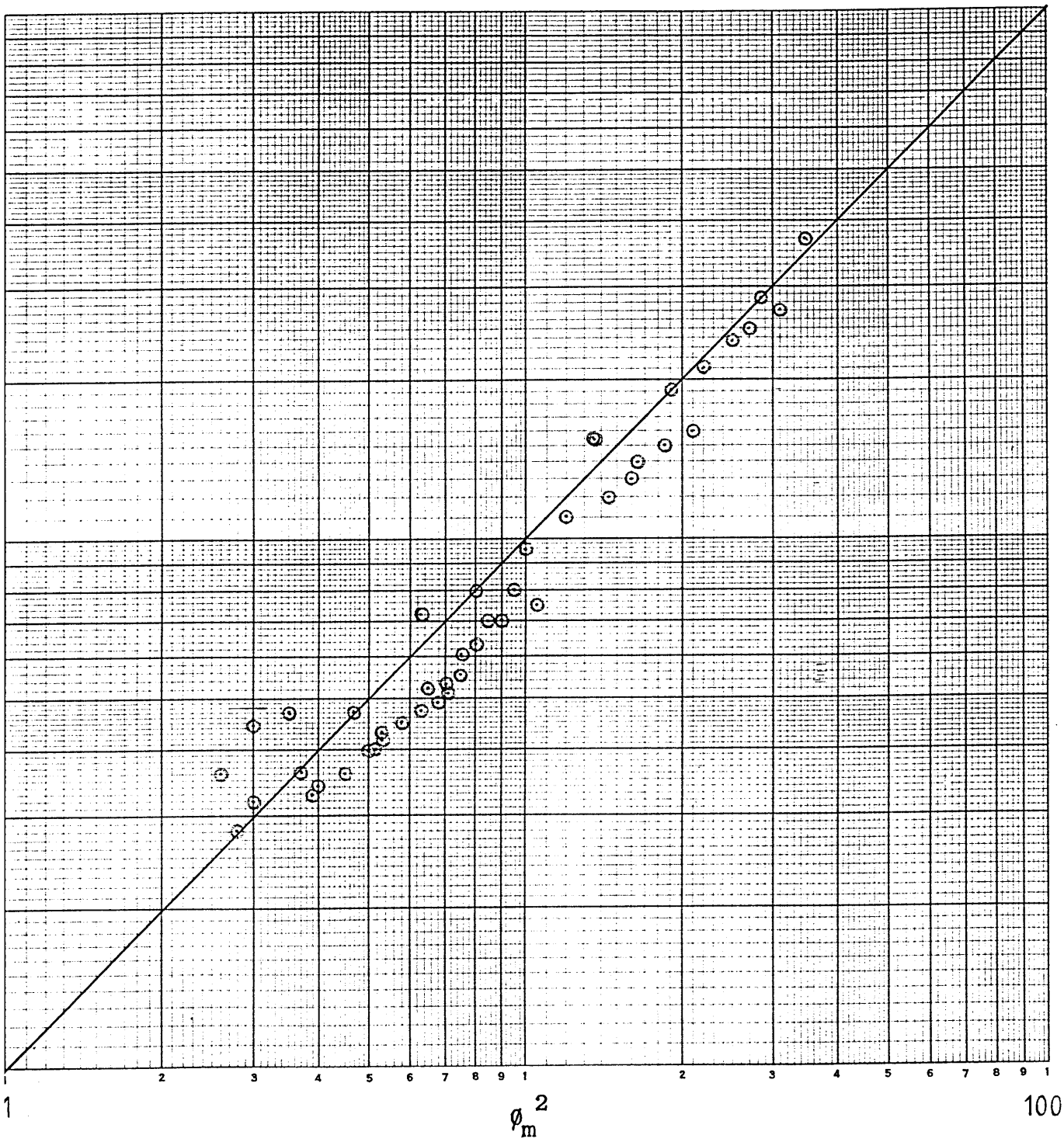

SMALL BORE STRAIGHT TUBE BY TEST CORRELATION

FIG. 5.22

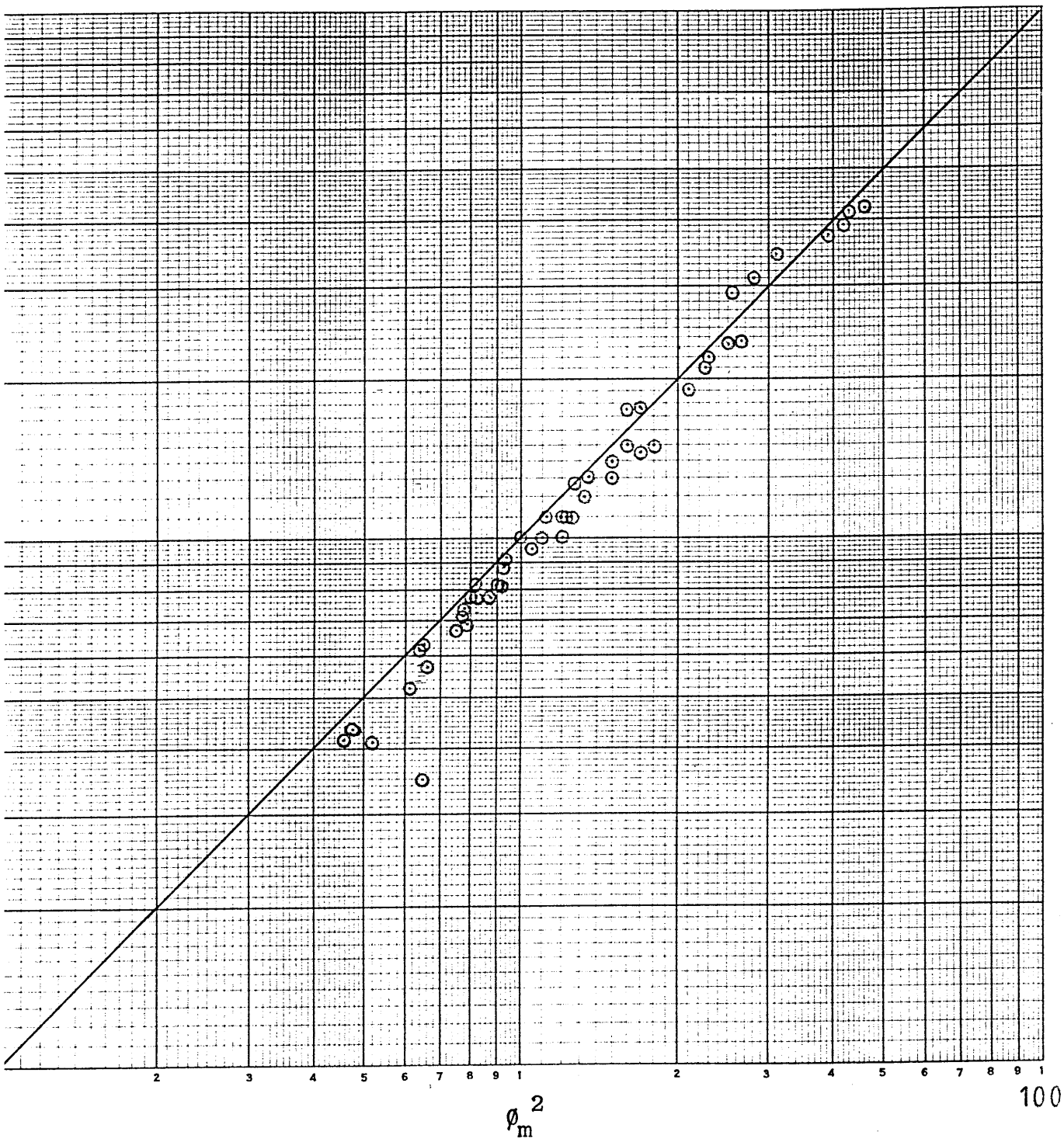

LARGE BORE COIL BY TEST CORRELATION

FIG. 5.23

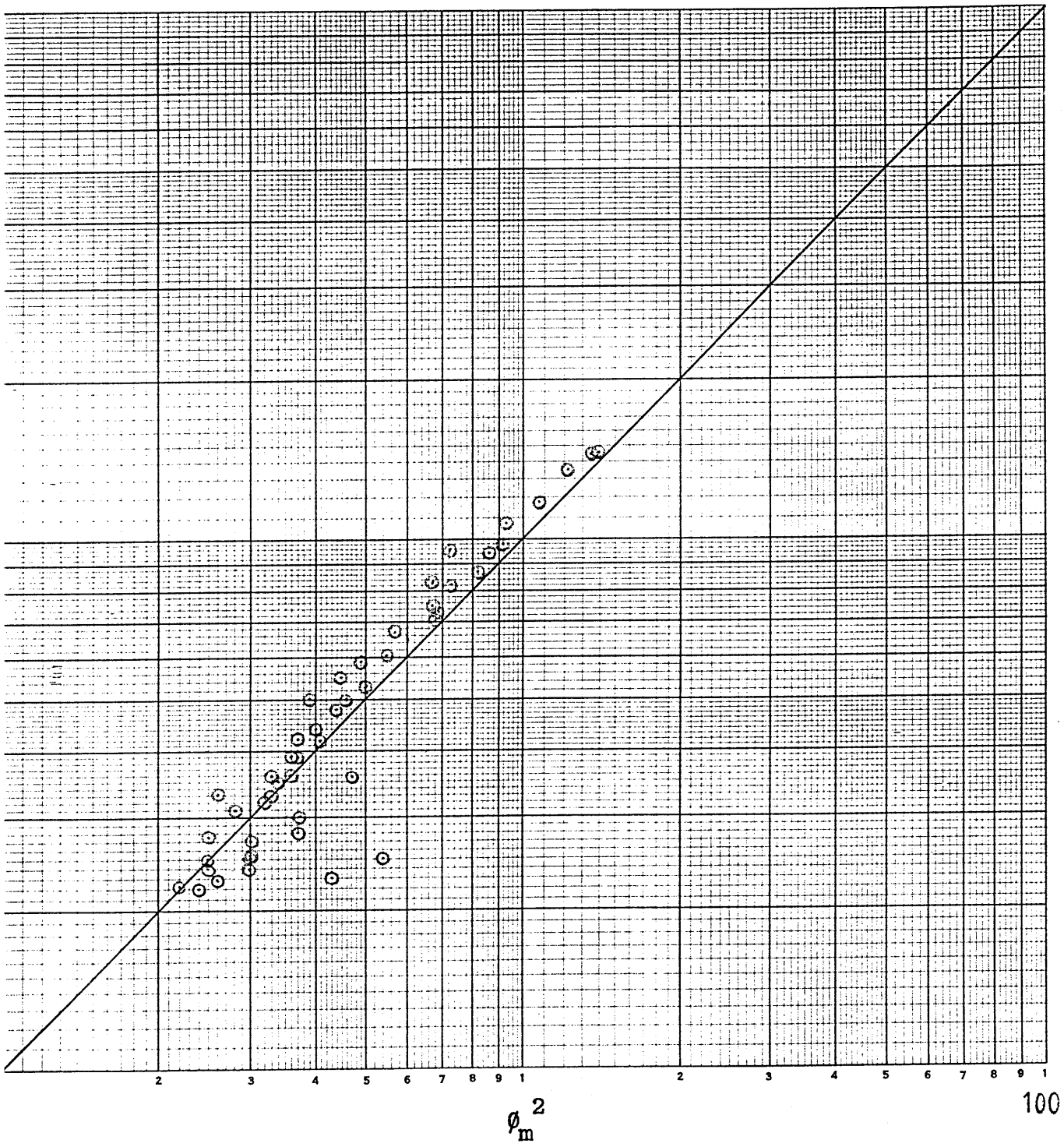

SMALL BORE COIL BY TEST CORRELATION

FIG. 5.24

SINGLE-PHASE AIR TESTS - RAW DATA

T in °C	T out °C	$\hat{M}$ kg/sec	P1 Bar	P2 -	P3 -	P4 -	P5 -	P6 -	P7 -	P8 -	P9 -	P10 -
7.8	7.0	0.0313	1.98	1.95	1.93	1.89	1.91	1.86	1.84	1.82	1.80	1.77
8.0	7.1	0.0295	1.90	1.87	1.86	1.82	1.85	1.79	1.77	1.75	1.73	1.70
8.2	7.5	0.0278	1.78	1.76	1.74	1.71	1.73	1.68	1.66	1.64	1.62	1.60
8.4	7.8	0.0255	1.65	1.63	1.61	1.58	1.60	1.56	1.54	1.53	1.51	1.48
8.6	8.1	0.0236	1.53	1.52	1.50	1.47	1.49	1.45	1.43	1.41	1.40	1.38
9.2	8.3	0.0205	1.38	1.37	1.36	1.33	1.34	1.31	1.30	1.28	1.27	1.25
10.2	10.3	0.0173	1.28	1.28	1.27	1.24	1.25	1.23	1.22	1.21	1.19	1.18
11.4	12.1	0.0147	1.21	1.20	1.19	1.18	1.19	1.17	1.16	1.15	1.14	1.13
12.9	13.6	0.0115	1.15	1.15	1.14	1.13	1.14	1.13	1.12	1.11	1.11	1.10
14.7	14.9	0.0074	1.09	1.10	1.10	1.09	1.10	1.09	1.08	1.08	1.08	1.076

Ambient temp , 17°C Barometric Press 0.9956 Bar.

Tube Diameter 0.0124 m. - Straight Tube.

TWO-PHASE TESTS - RAW DATA

in °C	T out °C	$\hat{M}$ H_2O kg/sec	$\hat{M}$ AIR kg/sec	P1 Bar	P2 -	P3 -	P4 -	P5 -	P6 -	P7 -	P8 -	P9 -	P10 -
0.1	19.9	0.1125	0.0183	1.82	1.81	1.78	1.74	1.69	1.62	1.56	1.49	1.42	1.35
0.2	20.0	0.1100	0.0172	1.72	1.71	1.68	1.63	1.58	1.52	1.46	1.39	1.33	1.27
0.3	20.0	0.1104	0.0152	1.49	1.48	1.45	1.41	1.36	1.31	1.26	1.19	1.13	1.07
0.2	20.0	0.1109	0.0133	1.29	1.28	1.25	1.22	1.18	1.13	1.08	1.03	0.97	0.92
0.1	19.9	0.1098	0.0114	1.08	1.07	1.05	1.02	0.98	0.94	0.90	0.85	0.80	0.75
0.0	19.9	0.1122	0.0095	0.89	0.88	0.85	0.83	0.79	0.76	0.72	0.69	0.64	0.60
0.2	20.1	0.1109	0.0076	0.70	0.69	0.67	0.65	0.62	0.59	0.56	0.52	0.49	0.45
0.3	20.2	0.1089	0.0057	0.50	0.49	0.48	0.46	0.43	0.41	0.39	0.36	0.33	0.31
0.3	20.4	0.1107	0.0038	0.35	0.34	0.33	0.31	0.29	0.27	0.26	0.23	0.21	0.19
0.5	20.6	0.1109	0.0020	0.15	0.15	0.14	0.13	0.12	0.11	0.10	0.08	0.07	0.05

Ambient Temp , 18.2°C Barometric Press 0.9678 Bar.

Tube Diameter , 0.0124 m. - Coiled Tube.

FIG 5.25

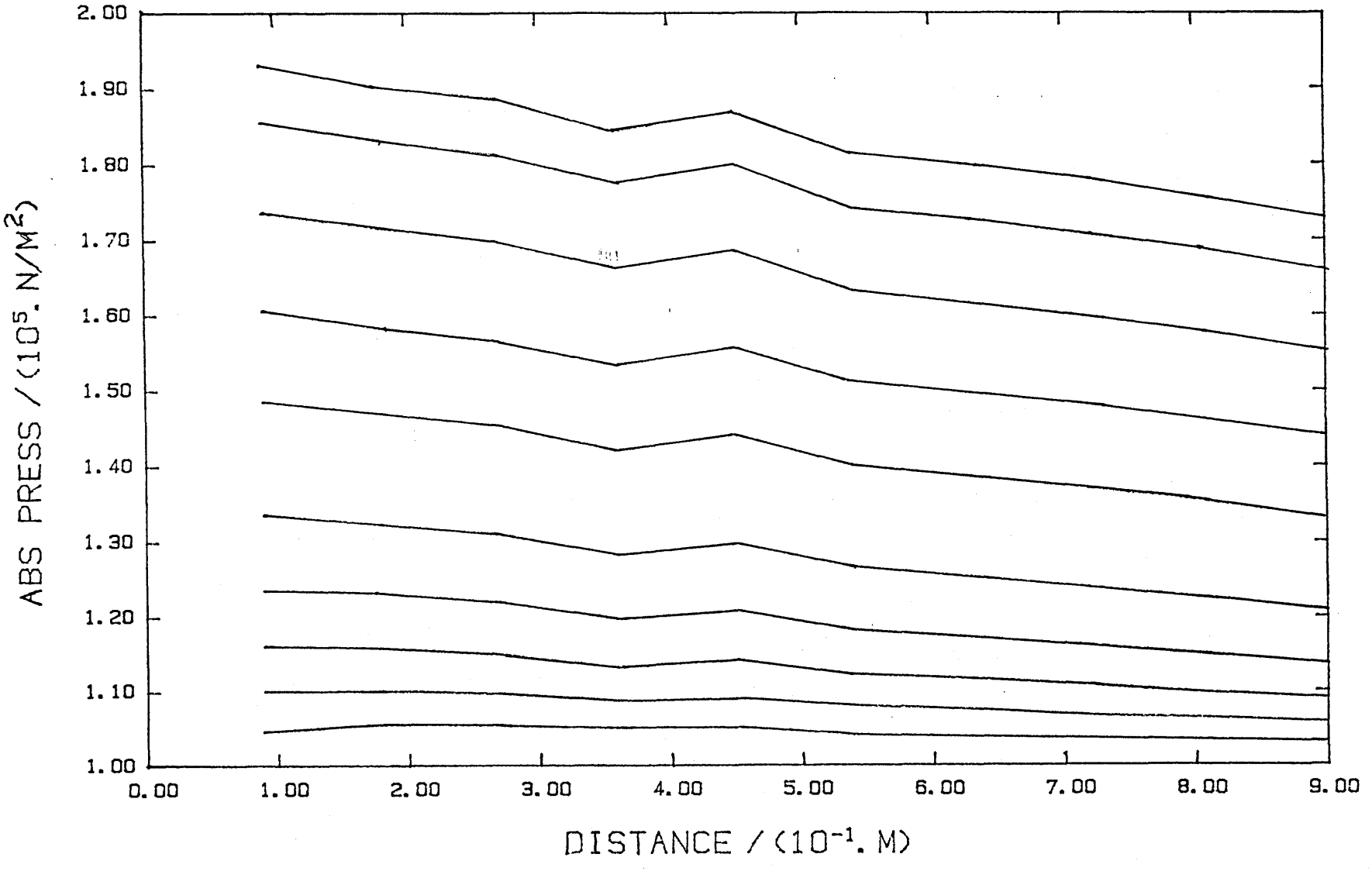

FIG. 6.1 LARGE BORE TUBE (STRAIGHT)
SINGLE PHASE AIR

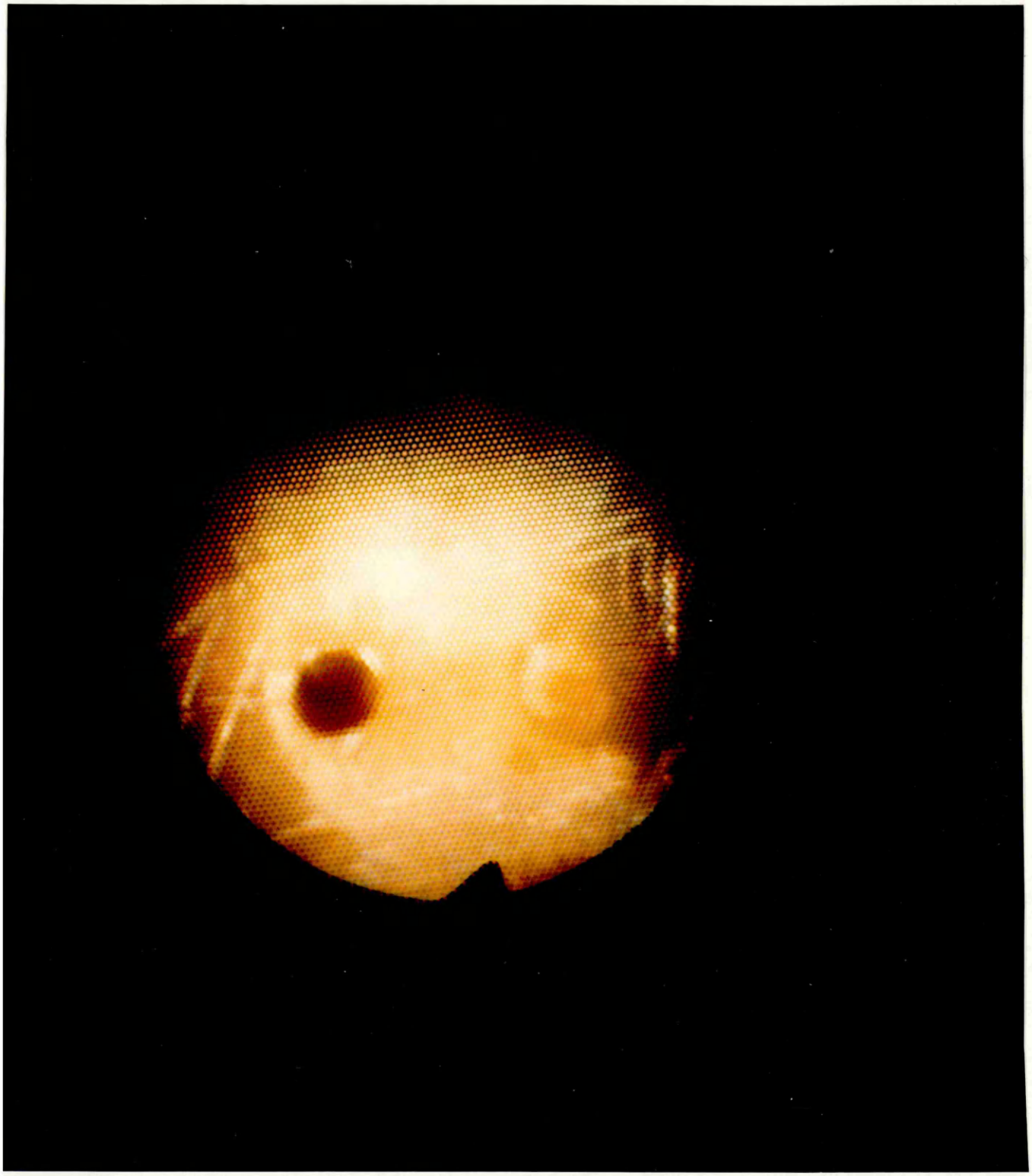

FIG. 6.2 GRINDING MARKS AROUND A TAPPING

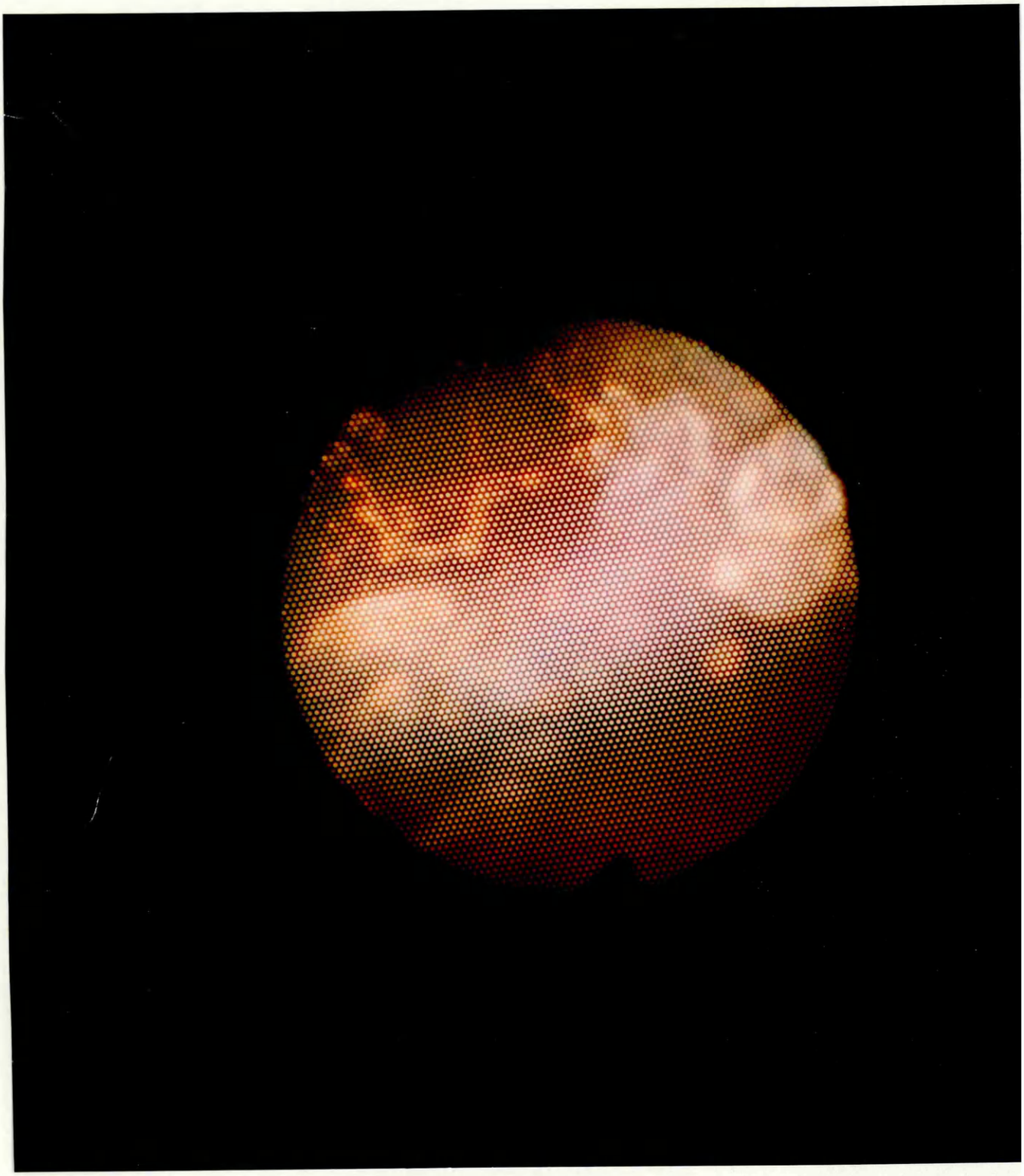

FIG. 6.3 WELD BURN THROUGH AT TAPPING

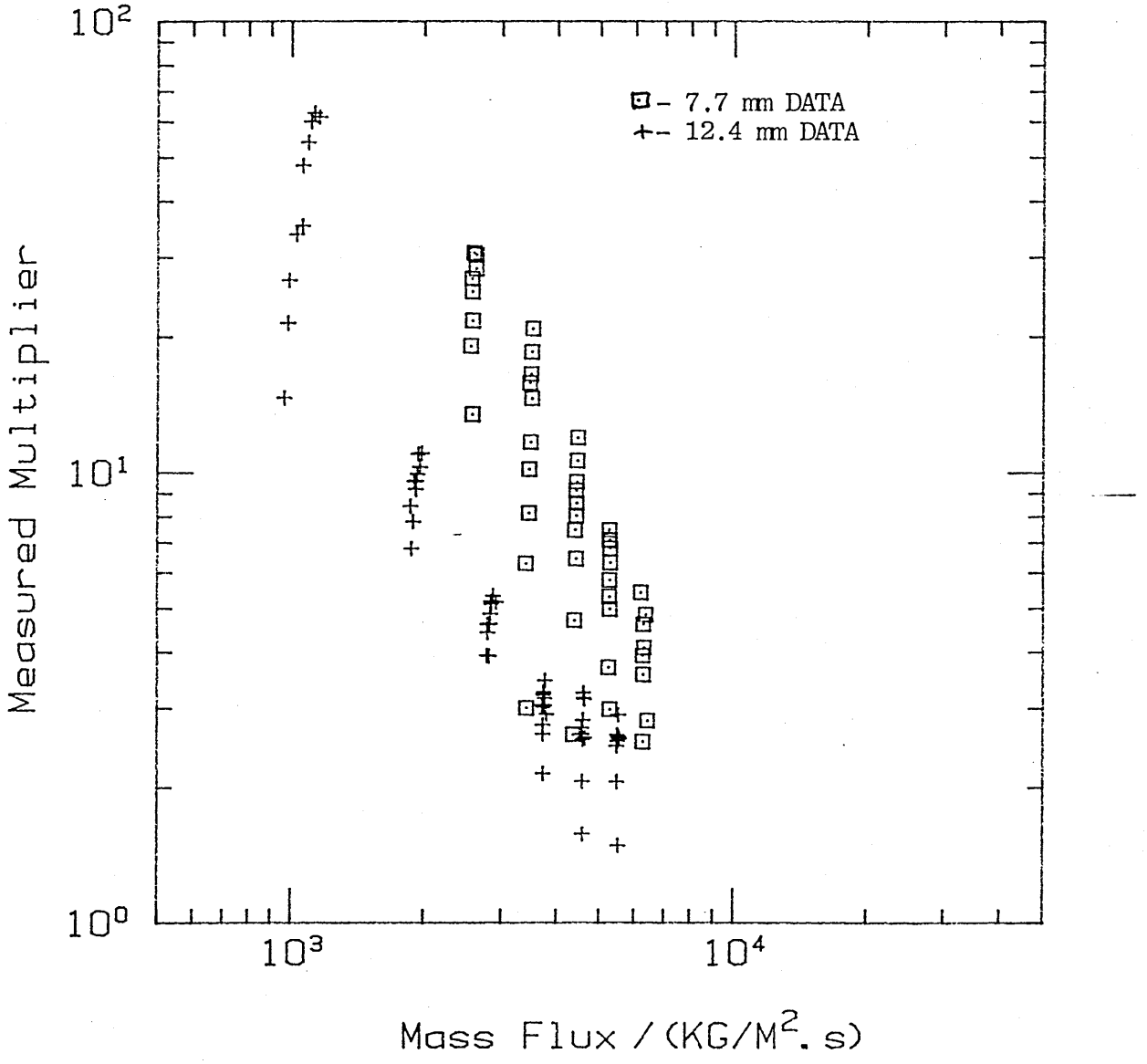

Large and Small Bore Data Comparison
Of Mass Flux To Measured Multiplier

FIG. 6.4

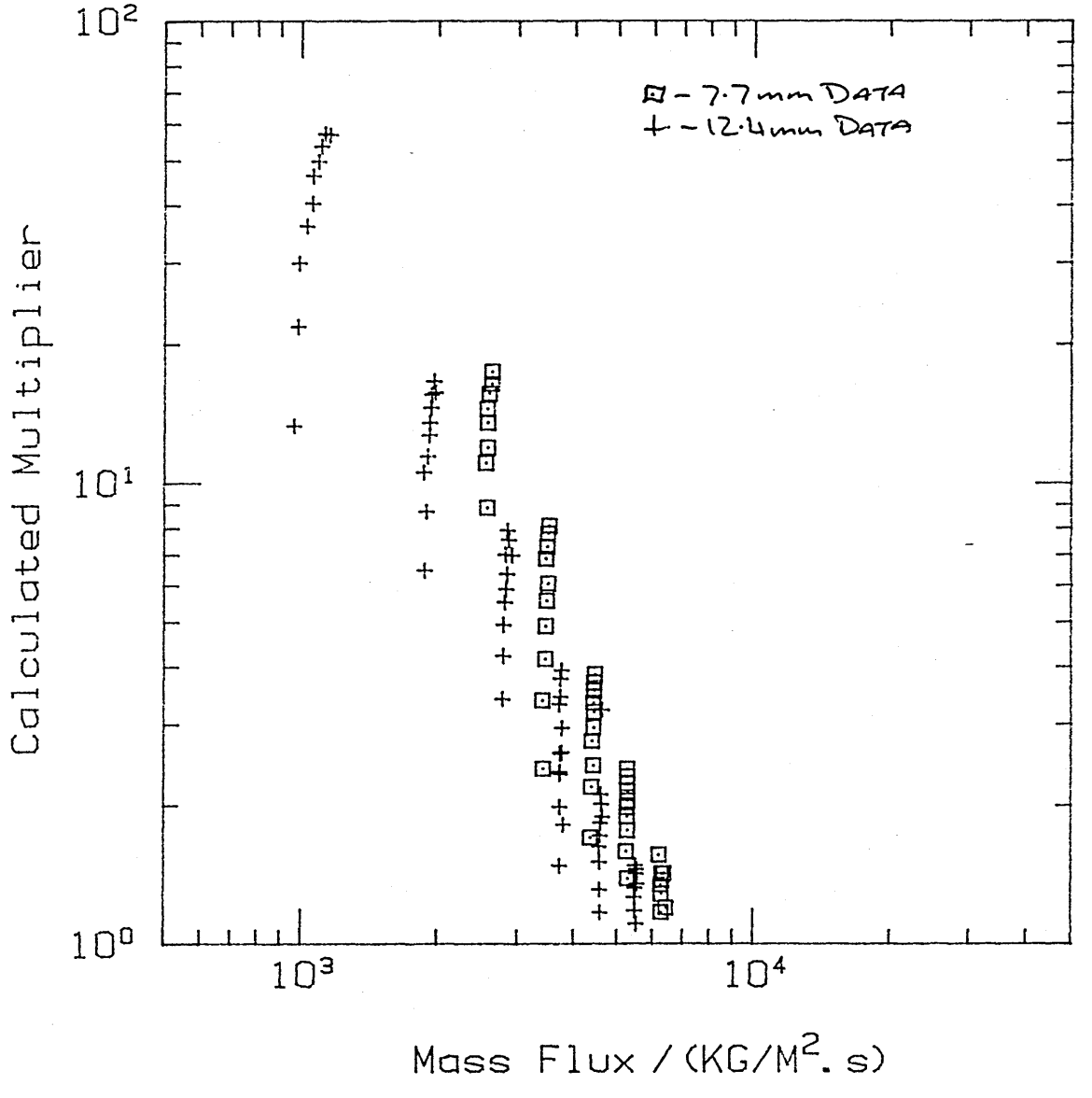

Large and Small Bore Data Comparison
Of Mass Flux To Calculated Multiplier

FIG. 6.5

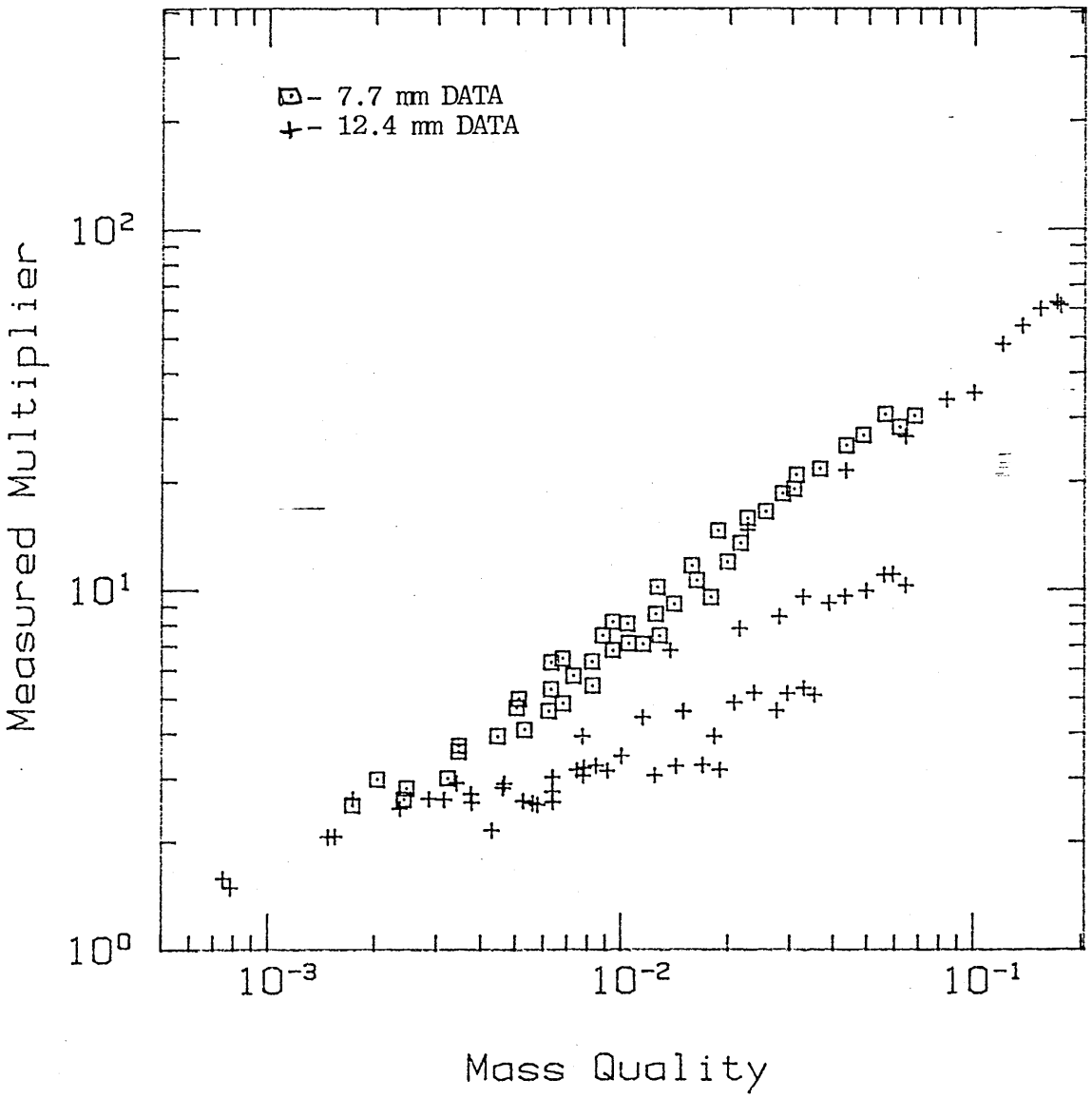

Large and Small Bore Data Comparison
Of Mass Quality To Measured Multiplier

FIG. 6.6

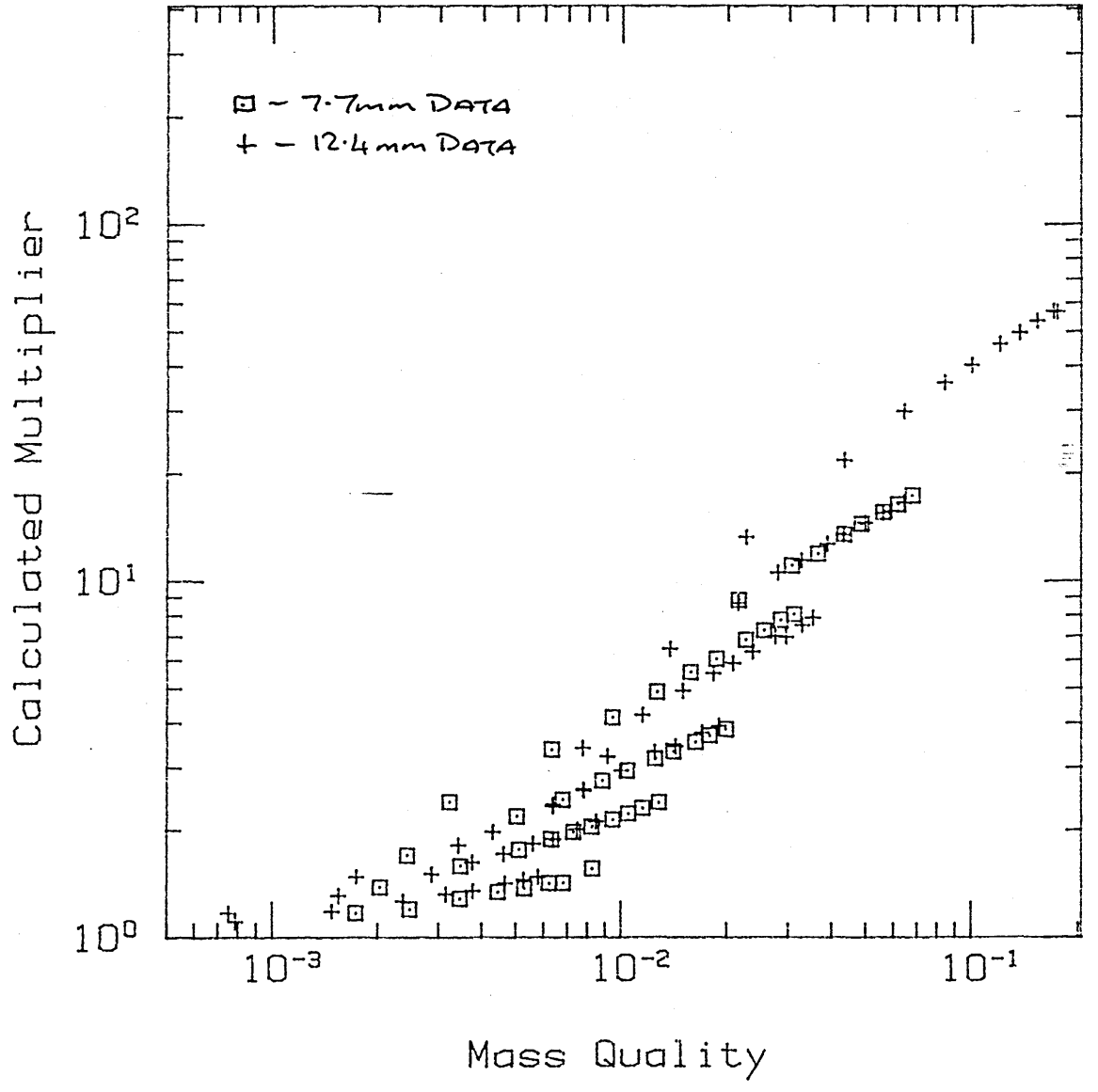

Large and Small Bore Data Comparison
)f Mass Quality To Calculated Multiplier

FIG. 6.7

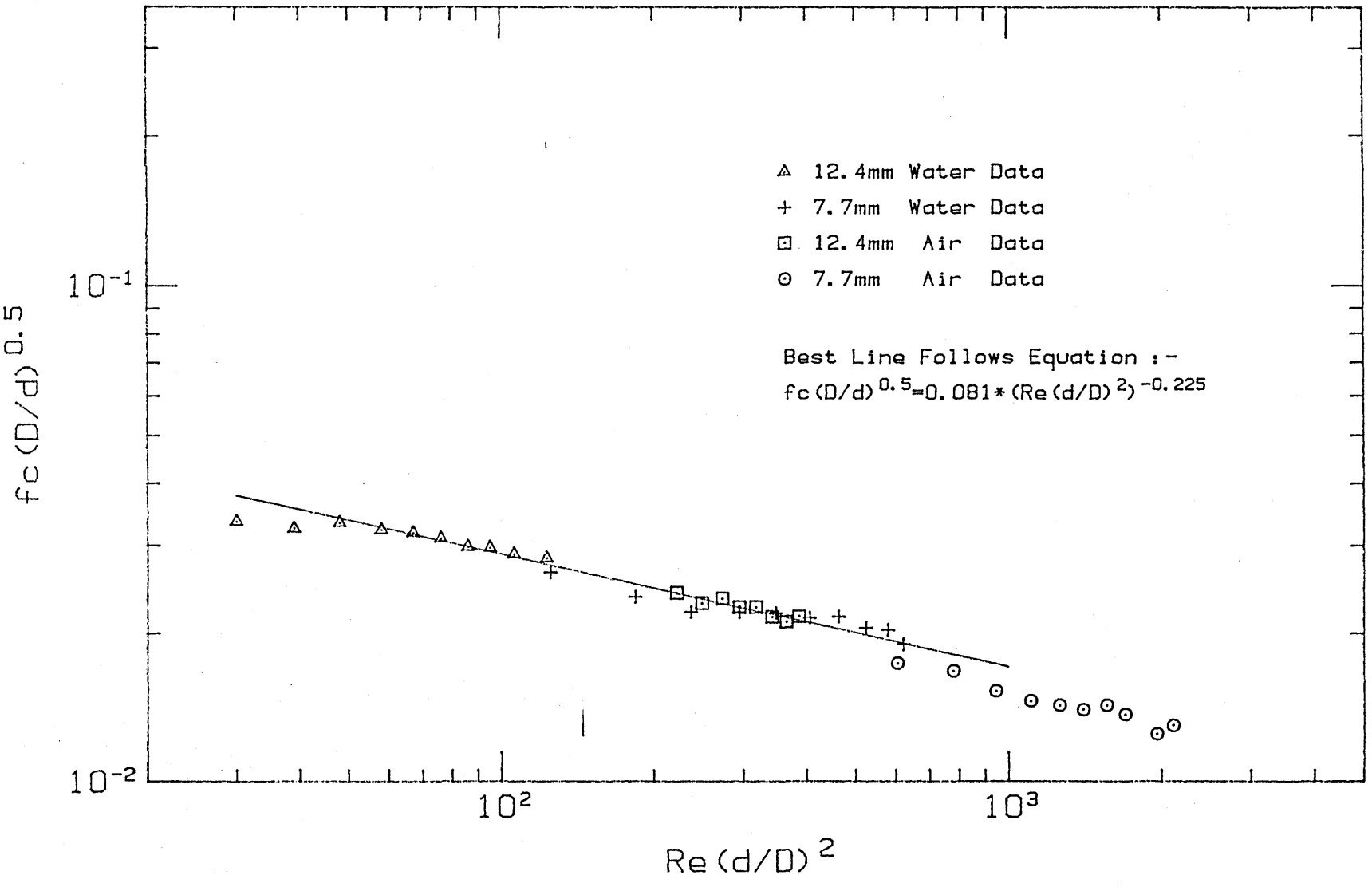

Best Line Fit Through All Collected Coil Single Phase Data (Air And Water)

FIG. 6.8

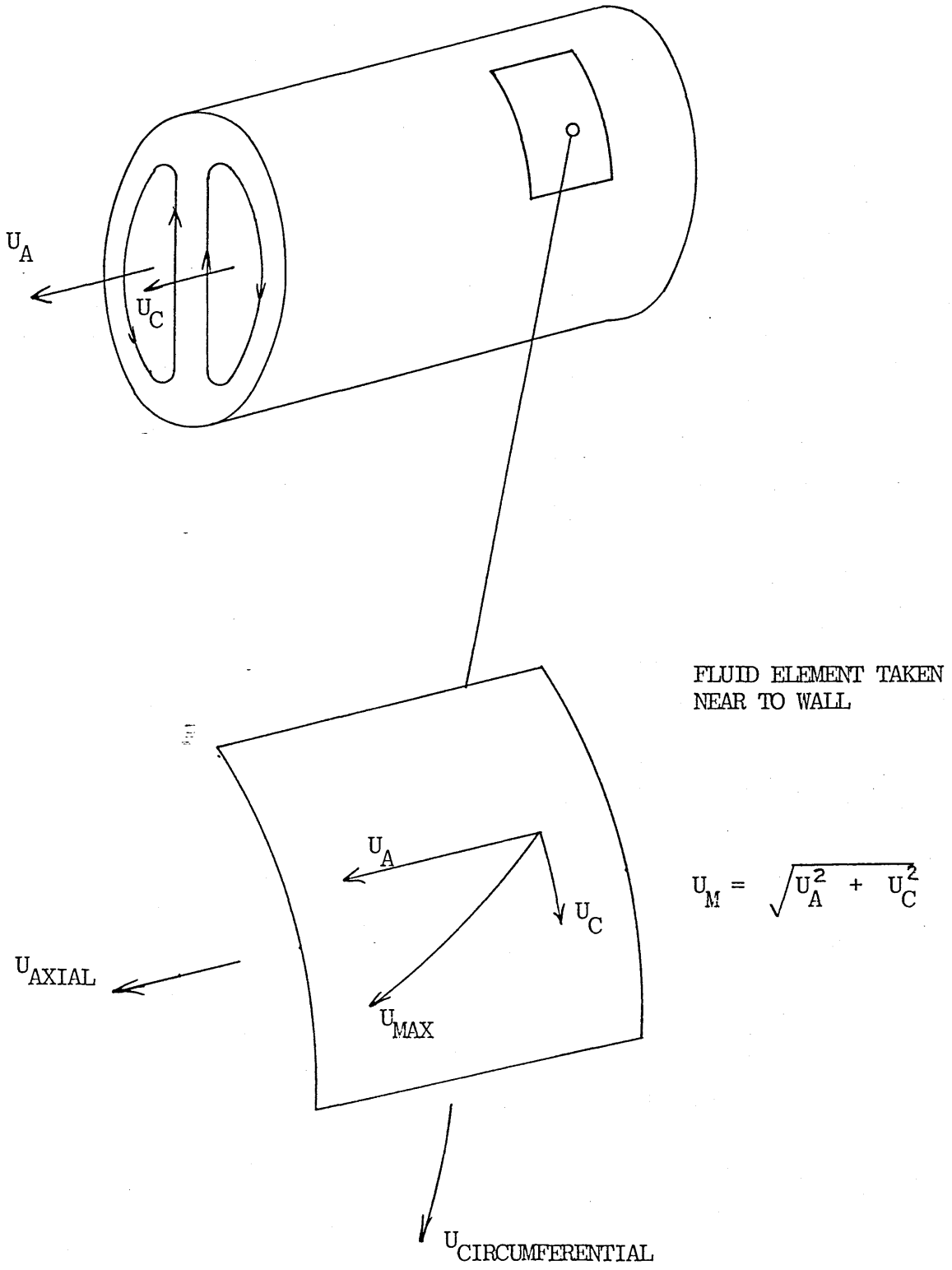
U_A
U_C
FLUID ELEMENT TAKEN NEAR TO WALL
U_A
U_C
$U_M = \sqrt{U_A^2 + U_C^2}$
U_{AXIAL}
U_{MAX}
$U_{CIRCUMFERENTIAL}$

FIG. 6.9

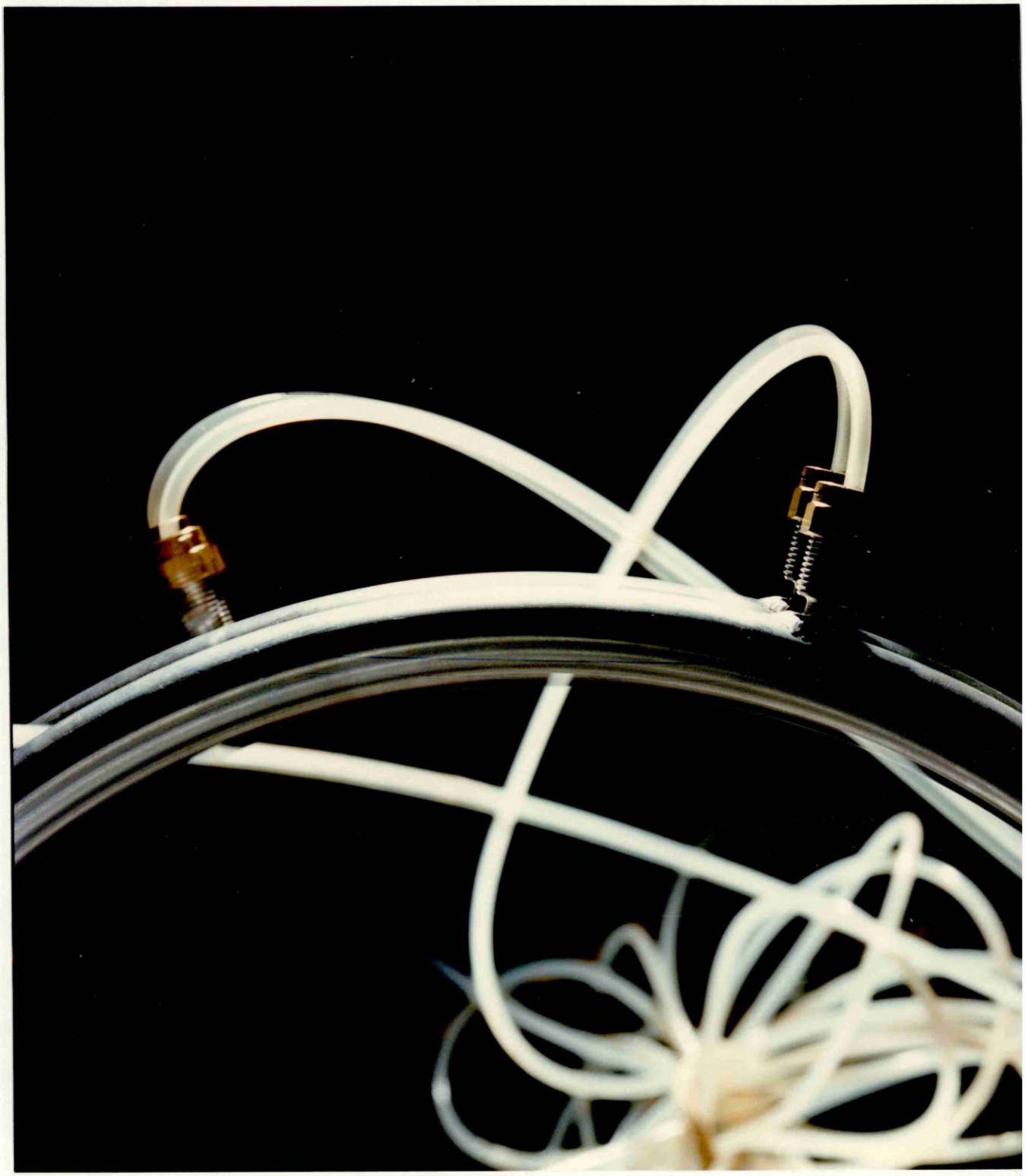

FIG. 6.10 COIL VIBRATION

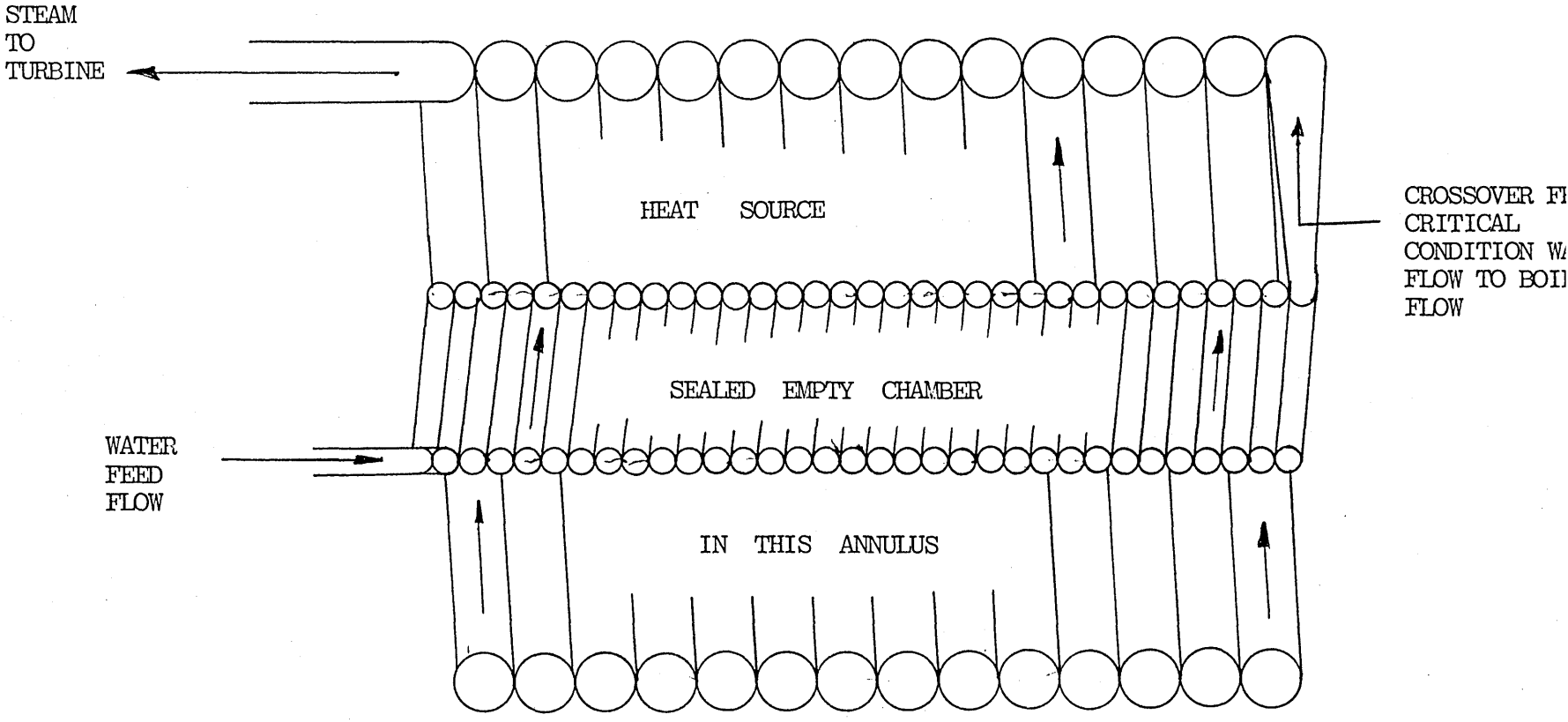

FIG. 6.11 POSSIBLE BOILER TUBE ARRANGEMENT

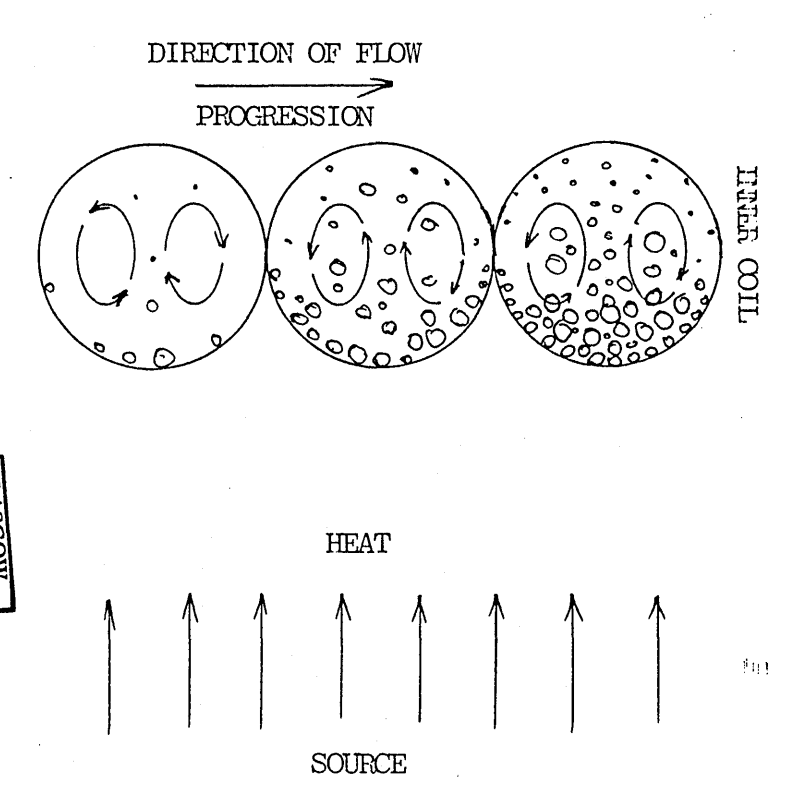

FIG. 6.12

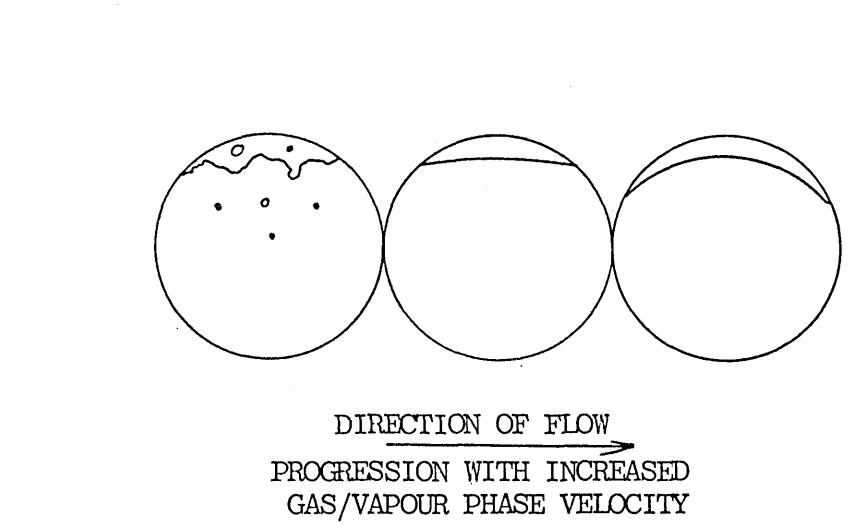

FIG. 6.13